INSTRUMENTATION OF A SENSOR FOR SMALL PART INSPECTION USING LASER FLUORESCENCE

by

ERIC A. ASK

B.S. Mechanical Engineering, Massachusetts Institute of Technology (1993)

SUBMITTED TO THE DEPARTMENT OF
MECHANICAL ENGINEERING
IN PARTIAL FULFILLMENT OF THE REQUIREMENTS
FOR THE DEGREE OF
MASTER OF SCIENCE AS RECOMMENDED BY THE DEPARTMENT OF
MECHANICAL ENGINEERING

at the

MASSACHUSETTS INSTITUTE OF TECHNOLOGY
May, 1994

Signature of the Author_____
Department of Mechanical Engineering
May 1994

Certified by _____
Dr. Andre Sharon
Thesis Supervisor

Accepted by _____
Prof. Ain A. Sonin
Departmental Committee on Graduate Studies
Department of Mechanical Engineering

INSTRUMENTATION OF A SENSOR FOR SMALL PART INSPECTION USING LASER FLUORESCENCE

by

ERIC A. ASK

Submitted to the Department of Mechanical Engineering on May 6, 1994 in partial fulfillment of the requirements for the degree of Master of Science as Recommended by the Department of Mechanical Engineering.

ABSTRACT

On-line part inspection is often hampered by the lack of availability of suitable sensors. This is especially true for small, non-rigid parts that must be manufactured within micron-range tolerances but are not sufficiently stiff to measure using mechanical means. Laser Induced Fluorescence (LIF), a technique based on the excitation and detection of fluorescent molecules, can provide a potentially high-resolution method for non-contact, non-destructive part measurement. It is the objective of the research presented in this document to investigate the feasibility of using LIF as an on-line sensor for the inspection of a class of small, non-rigid parts.

An LIF system optimized for this application was developed, designed and fabricated. Extensive experimentation and testing with the system yielded measurement resolution levels of 0.5% (.5 microns) and accuracy levels of 5%. The accuracy was further improved to 1% using an on-line calibration strategy. The achieved system performance supports the suitability of LIF as an on-line sensor for the measurement of small, high precision parts.

Thesis supervisor: Andre Sharon
Title: Executive Officer, The Manufacturing Institute
Research Scientist, Dept. of Mechanical Engineering

ACKNOWLEDGMENTS

My primary reason for attending graduate school was to meet and work with MIT faculty, staff and graduate students. I wanted the opportunity to learn from these people while working with them on common projects. To this end, my graduate work has been successful, and I still believe this facet to be the most important part of the experience. For this reason I would like to take this space and time to make mention of several of the people that have made the completion of my work possible.

Foremost, Dr. Andre Sharon and Dr. David Hoult provided me with both the opportunity to work on an exciting project and the technical leadership to see it through to its completion. Without them, this project would not have been possible. I would also like to thank Prof. Mary Boyce and Prof. David Hardt for supplying diversity and balance to my faculty interactions

With all those things that no one else ever knows the answer to, Dan Alvarado and Ann Seman always came through. Down in the shop Fred Coté and Jerry Wentworth provided the expertise and "patience" that only truly skilled and experience people could offer. All these folks made the difference between my work being bearable and being enjoyable. They are friends that I feel lucky to have. Dan, I hope to be seeing you in a few years at school.

Considering the number of hours that were necessary in lab, I believe myself to be truly fortunate to have a mix of labmates that made time in and out of lab fun, interesting, and bearable. Susie Ward provided the familiarity and comfort of a long time friend from my undergraduate work. Dave Phillips proved to be one of the nicest guys I have been lucky enough to meet in my life. Many times his mere presence was enough to give me a lift and keep me going on those occasional bad days. Frank Pennisi had the unfortunate pleasure of probably having to spend the most time with me in lab as we worked down that home stretch. With him I shared the broadest set of experiences: class, the job search, and the thesis.

Eric Deutsch and Jim Ryan were the two folks kind enough to explain to me this thing called LIF. They were always there to answer a question or two or three. You guys put up with a lot of pestering and hassles. I thank you. Goro, it takes a certain amount of tolerance to not be disturbed by an individual who sets your preamp a smokin'. It was a pleasure to work with you. It was also great hanging out with the other folks in the lab: Janice, Norm, Serge, Jon, Alan, and Doug.

I would also like to thank the other students that helped me when I had a question about something that I did not know about: Dave Albagli, Upe, and Lisa Tegeler.

TABLE OF CONTENTS

LIST OF FIGURES

LIST OF TABLES

NOMENCLATURE

Prefixes:

n	nano-	($x10^{-9}$)
μ	micro-	($x10^{-6}$)
m	milli-	($x10^{-3}$)
c	centi-	($x10^{-2}$)

Symbols:

λ	wavelength of light, measured in nanometers (nm)
c	constant speed of light (2.998×10^{10} cm/sec)
ν	frequency of light in Hz
Hz	Hertz (1/s)
E	energy measured in ergs
h	Planck's constant (6.624×10^{-27} erg sec)
I_a	rate of light absorption, (Einstein $liter^{-1}$ sec^{-1})
I_o	rate of light emitted, (Einstein cm^{-2} sec^{-1})
m	meter
f	focal length
D	Initial diameter of laser beam
d	smallest possible focused diameter of laser beam

Abbreviations

PMT	Photomultiplier Tube
SMA	A standard terminal for fiber optics [9]

INTRODUCTION

The past has seen products manufactured in groups or batches and later tested in quality-control rooms. If these products were acceptable, they became part of the inventory. Unacceptable parts were scrapped, sent back for rework, or sold as substandard products. Kalpakjian [1] explains that such a system ". . . lacks flexibility, requires maintaining an inventory, and inevitably results in some defective parts going through the system." This "post process inspection" merely counts mistakes that have already been made and does little to prevent their repetition.

Modern manufacturing facilities benefit from the use of on-line inspection. This method makes use of the theory that manufacturing processes often move slowly out of specification. Factors such as tool wear and thermal effects account for this gradual shift. By monitoring variances during production, adjustments can be made to avoid defective parts. Another benefit of this system involves the detection of defective components before they become part of a larger assembly or have further work completed on them. This eliminates the propagation of a mistake leading to further financial loss. "On-line inspection" may also eliminate the need for a final inspection at a separate facility in a plant.

The technology which has made this shift in inspection theory possible evolved from automated measurement devices. Accurate sensors integrated with microprocessors provide the equipment necessary to inspect parts without interrupting the flow of materials. Sensors currently are based on developments in ultrasonics,

acoustics, infrared radiation, optics, lasers, and many other technologies. These different sensors can be used to measure qualities from dimensional accuracy to surface finish. Computers can then take the data from the sensors and produce a graphical display which can easily be read by an operator. Assuming the process is also automated, the operator or control system can easily make adjustments in the production line to prevent any shifts in quality from moving outside of specifications.

Having automated measurement devices gives the additional benefit of abundant information about the process. This data can be studied to increase the understanding of what is happening during the manufacturing of products. Currently this information is mostly used to implement a series of statistical process controls. A variety of control charts can be plotted in real time. The most common control charts used today are Shewhart Control Charts and Cusum (Cumulative Sum) Charts [2]. Shewhart charts consist of the sequential plotting of batch averages. These plots have upper and lower bounds which correlate to specification ranges and indicate a process's level of stability. Cusum charts plot the sum of all deviations from a reference value. These charts are helpful in indicating a slight shift in the process away from this reference value. This is a feature that the Shewhart method does not possess. Both these methods ultimately improve quality and simplify the task of observing a process.

These benefits make it clear that an on-line inspection system is desirable if it is feasible. Problems occur, however, when a manufacturer is unable to find a system that will measure accurately

a particular critical attribute. Such a problem serves as the stimulus for researching a new sensor.

A new challenge has surfaced in non-destructively measuring small, non-rigid parts which need to be held to close tolerances. The shortcomings of current technology are varied and multiple. Simple tools, such as calipers or micrometers do not have part to instrument interfaces which allow for quick measurement of soft parts. Also, these methods are not capable of measuring curved surfaces. Coordinate measurement devices use hard probes which work well for hardened or stiff products, but they would indent or puncture soft surfaces. Other methods such as photographing cross-sections provide the accuracy, but they often involve destroying the part and are only capable of taking an outline image. In addition to these drawbacks, most of these methods are time consuming and offer little possibility of on-line detection during a manufacturing process. In order to bypass these restrictions, it was proposed to use a pre-existing technology in a new way.

The solution involves the use of Laser Induced Fluorescence (LIF) technology. LIF has been used to assist in research, but it has not yet been implemented in large scale uses. It is now used to measure oil film thicknesses in combustion engines with micron resolution. [3] The method makes use of the principle that fluorescent molecules emit a unique bandwidth of light when their electrons are excited by an appropriate light source. Researchers currently dissolve a fluorescent dye in a solution which is then exposed to laser light. The intensity of the fluorescence is measured

and calibrated against the depth of the solution. Varying depths of the solution can then be measured by measurement of the light intensity.

The technique designed for this sensor requires submerging the parts in a fluorescein solution and measuring their "imprints." A reading is taken of a specimen holder with only a dye and water solution in it. These results are then calibrated against data obtained using a Coordinate Measuring Machine. The part is then submerged and inspected. By subtracting these results from the known profile, the dimensions of the part can be determined. This process has yielded 0.5% resolution, and the testing can potentially be done in a matter of seconds. The advantages of the system allow for the prospect of an on-line sensor in a manufacturing process where it had not been previously possible.

The following chapters discuss the research that was completed on this project. A theory chapter gives background information on luminescence and the physics of fluorescence. The understanding of these ideas is important since they explain how light forms a connection between system components. This is followed by a design chapter that outlines the design constraints and the decision process used to select all components of the system. Included there are details of all system components. The experimental results and analysis are provided in the fourth chapter. Signal to noise levels, resolution, accuracy, and repeatability of the system are quantified there to provide a basis for analyzing the feasibility of the system. This feasibility analysis is provided in the last chapter. It is accompanied by detailed recommendations for further work.

2. LASER FLUORESCENCE THEORY

2.1 LUMINESCENCE

Sources of light emission can be broken down into two separate categories. Incandescence deals with heated bodies which are able to emit light due to their raised energy levels. All other forms are considered luminescent. These forms lose energy as they emit light. It follows that maintaining luminescence requires an influx of energy. It is the source of energy which differentiates the kinds of luminescence. The numerous categories include thermo-luminescence, bioluminescence, and photoluminescence to name a few. Photoluminescence, which concerns our study, receives energy from light.

A brief discussion of the nature of light is necessary to explain the phenomenon of photoluminescence. Light is characterized through the use of two models, the wave and particle theories. Frequency (ν) and wavelength (λ) define light as it relates to the wave theory and are correlated by:

$$\lambda (\nu) = \mathbf{c} \qquad \text{(eq. 1)}$$

c in this equation represents the constant speed of light in a vacuum (3×10^{10} cm/sec). The wave model is used to explain reflection, refraction, and diffraction. None of these phenomena describe the absorption or emission of light.

Describing these last two phenomena requires the Quantum Theory of light. This theory maintains that radiant energy can be

absorbed in finite units; these units are referred to as photons. Photons are emitted from electrons falling from higher energy levels to lower energy levels. When an electron absorbs a photon, the reverse occurs. The difference in energy levels effects the energy, **E**, carried by the photon. This amount of energy effects the wavelength and frequency of the particle. The relationship can be expressed by:

$$\mathbf{E} = h\nu = hc/(\lambda) \text{ ergs} \qquad \text{(eq. 2)}$$

where h is Planck's constant (6.624 x 10^{-27} erg sec).

2.2 PHYSICS OF FLUORESCENCE

Figure 1 illustrates an example of fluorescence. The different quantum levels proceed vertically representing the different shells of an atom. The energy increases incrementally at each different level. Molecules at room temperature tend to remain in the lowest level of the ground electronic state (level 0 of S_0 in Fig. 1). As an electron absorbs photons of sufficient energy, it elevates to a higher state, S_1. When the electron returns to its original level, it emits a photon of a particular frequency.

An excited molecule quickly looses excess vibrational energy due to collisions with neighboring molecules. This is the case for all excited states above the first. Internal conversion also assists in the loss of excess energy. During this process, molecules pass from the lower vibrational levels of higher excited states to the higher vibrational levels of the lower excited states. These transitions do

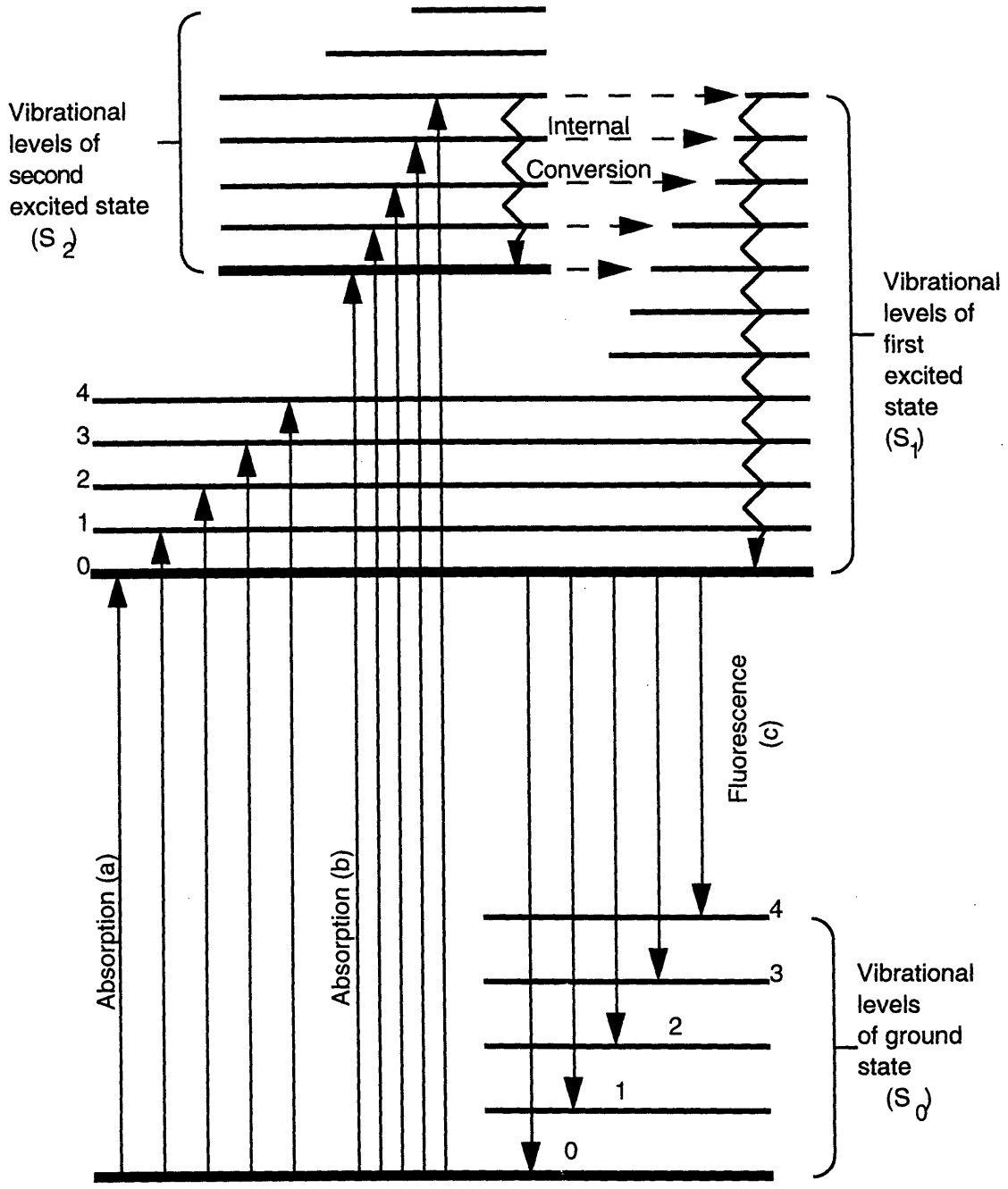

Figure 1. Transitions giving rise to absorption and Fluorescence emission spectra. Parker [2].

not actually cause a reduction in energy; however, subsequent to this transition, molecules are reduced to lower vibrational levels by collisions with solvent molecules. The final result is that molecules which are raised to excited levels above the first vibrational level of the first excited state quickly,within 10^{-12} s, fall to the level 0 of State 1. From this L_0 of S_1 the electrons of the molecule fall to the ground state, L_0 of S_0. This final process occurs in the relatively slow tme of 10^{-9} seconds. Because of the time differential between the two processes, the slower process dominates the emission spectrum seen. The absorption and emission spectrums of fluorescein are shown in Figures 2 and 3.

Figure 4 displays a solution that is illuminated by a constant intensity laser beam. Assuming that the optical density is small, one can conclude that the rate of light absorption, I_a, throughout the solution is constant. The light absorption is described by:

$$I_a = 2300EI_o \qquad \text{(eq. 3)}$$

Where I_a is measured in Einstein $litre^{-1}sec^{-1}$ and I_O is measured in Einstein $cm^{-2}sec^{-1}$. After a relatively long period, 10^{-5} seconds, a steady state is achieved where the number of excited molecules is constant. During this steady state, the light emitted, I_O, will be linear with the depth of the solution. This holds true as long as the solution does not become quenched.

Fluorescence quenching, or bleaching, refers to the physical phenomenon where the emitted fluorescence of a solution decreases with increasing temperature. The increase in temperature is

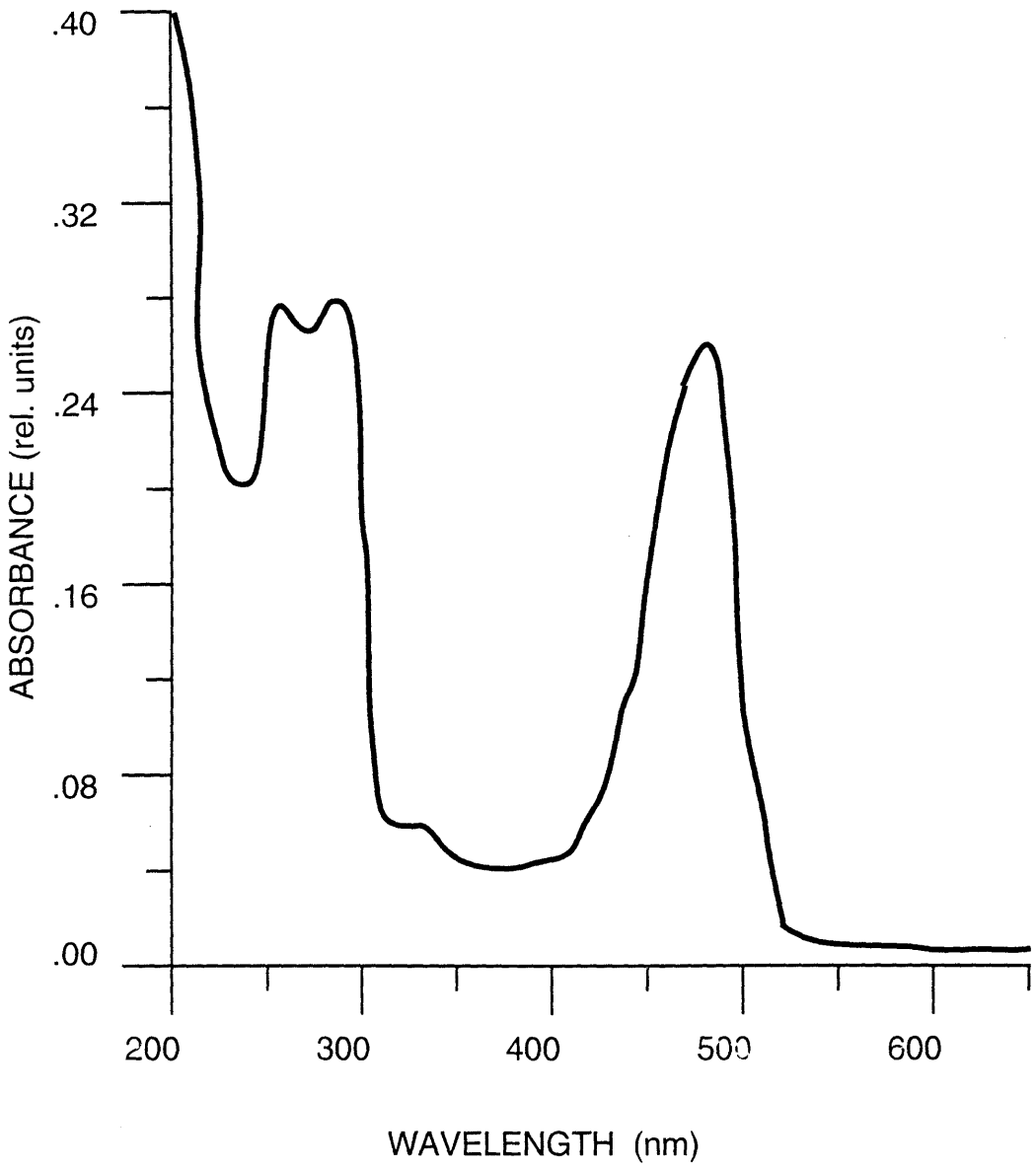

Figure 2. Absorption spectrum for fluorescein in distilled water.

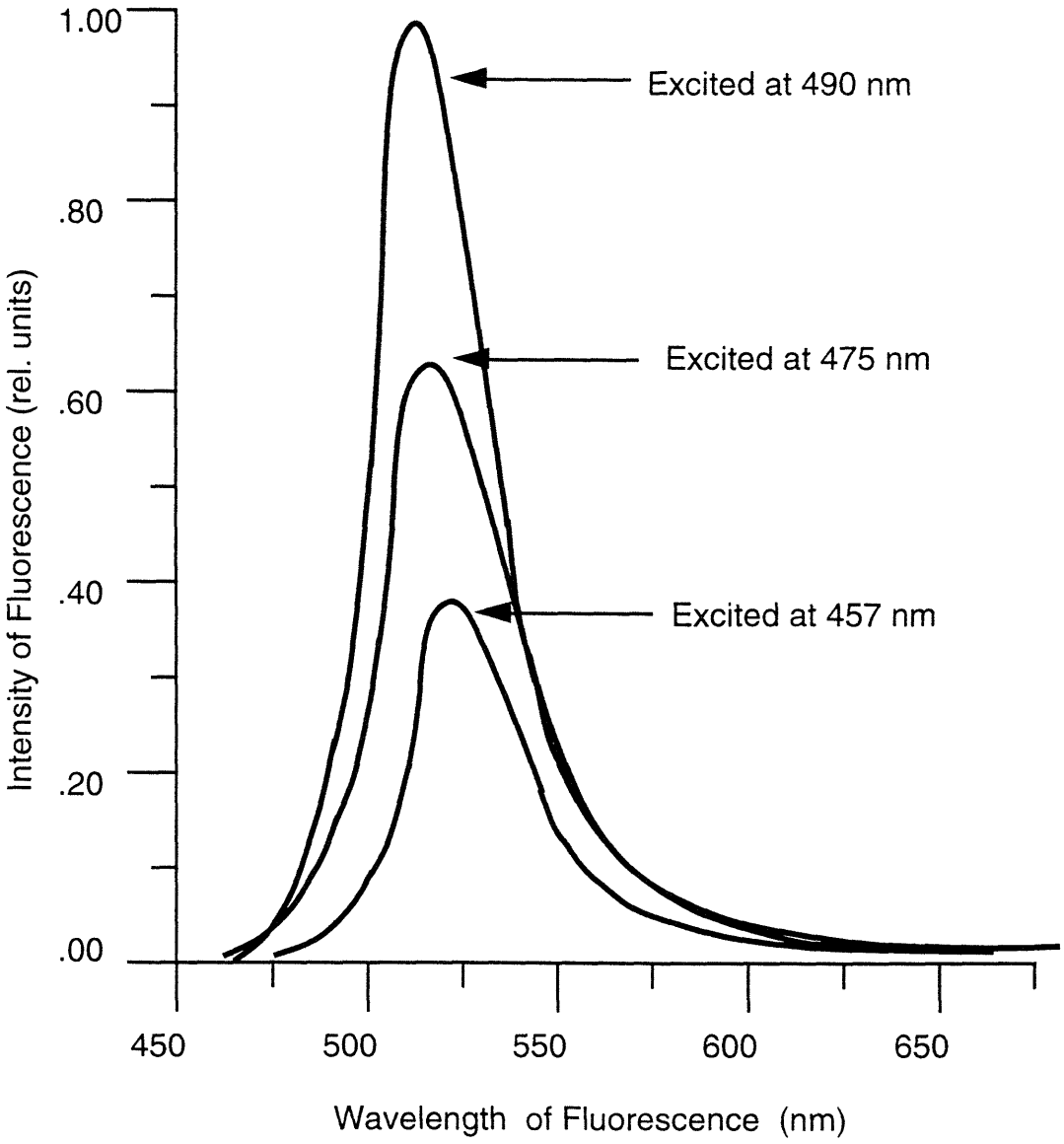

Figure 3. Emission spectrum for fluorescein dye and distilled water.

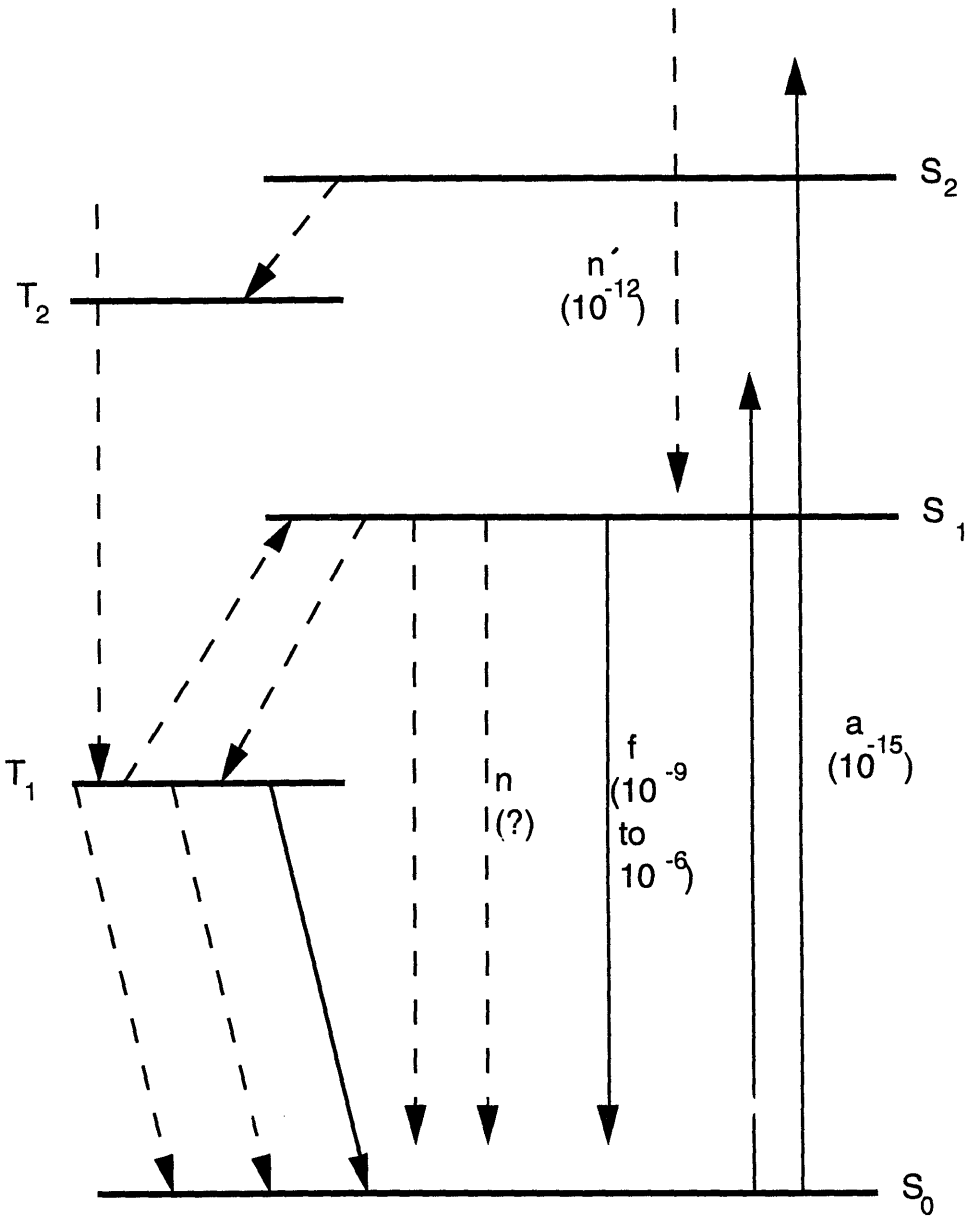

Figure 4. Typical reciprocal rates of transitions.

Principle transitions:
"a" is absorption
"f" is fluorescence
"n" and "n'" are radiationless internal transitions
Parker [2].

localized and results from the energy influx from the laser beam. Hoult and Takaguchi [4] studied this effect in detail. Their research mentions several methods for reducing this effect. The fluorescent solution can be maintained at a constant temperature by: using a cooling system, circulating the solution to prevent localized heating, allowing the solution to cool between measurements, or using a chopper wheel to limit the solution's exposure to the laser beam. For these experiments both a chopper wheel and shutter were used to limit exposure time to the laser. Figures 5a and 5b illustrate the difference between using and not using these techniques. Figure 5a shows an unchopped signal which is clearly decaying while the chopped signal in Figure 5b is maintaining a constant output. A more detailed explanation of this effect and the other theories discussed in this section can be found in Parker's Photoluminescence of Solutions[5] and General Chemistry [6].

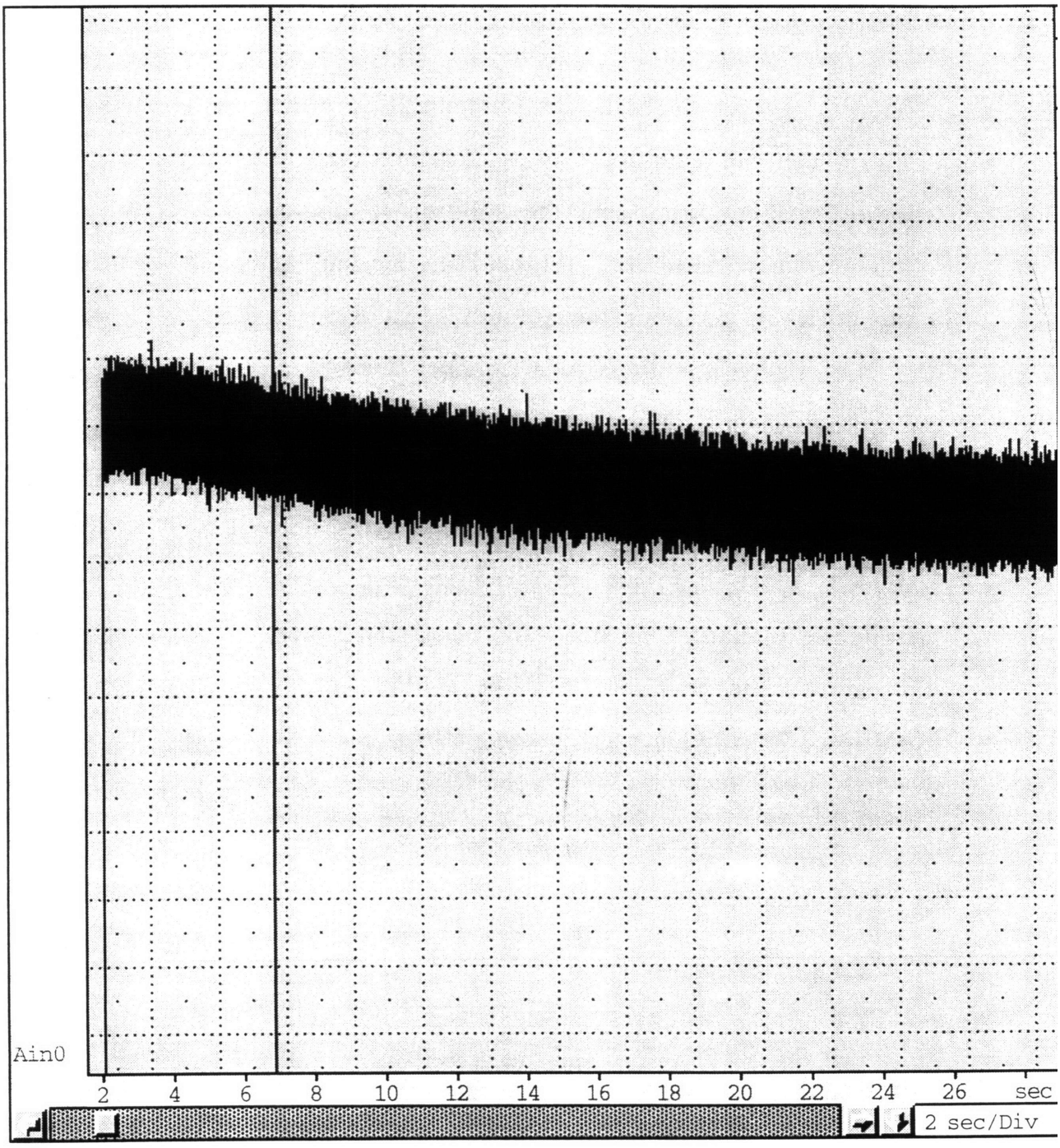

Figure 5a. **Bleach effect caused by local heating in the solution.**

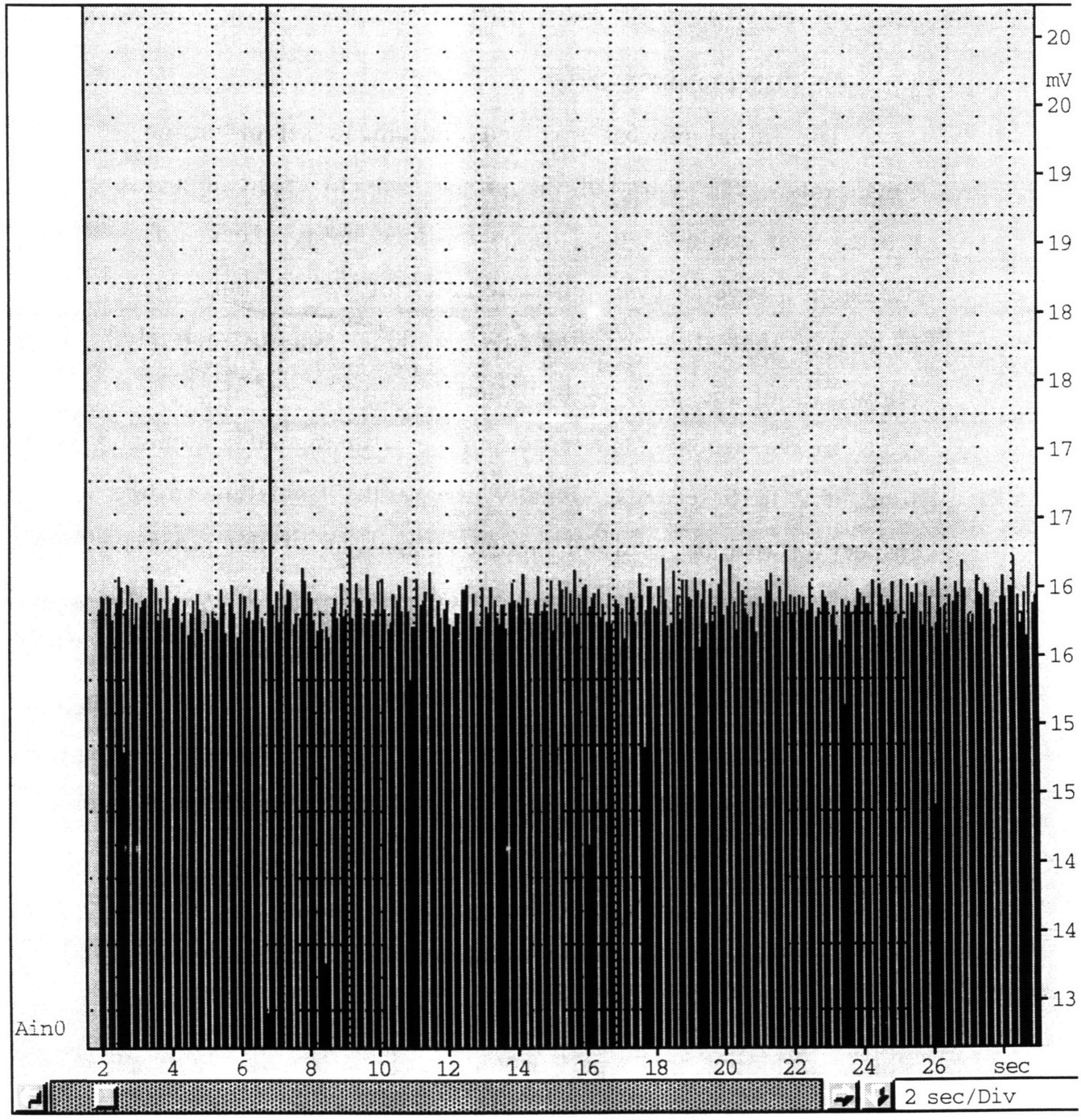

Figure 5b. Chopped signal showing no decay due to bleaching.

3. DESIGN OF APPARATUS

3.1 DESIGN CONSTRAINTS

The initial process involved outlining a set of design constraints. The focus of the project was to create a measurement process that could be used as an on-line quality check. This use determines several basic characteristics of the system. It is necessary that the measurements be done non-destructively. This allows all of the parts to be tested. Testing large quantities of parts leads to the second main criteria of a scanning and processing cycle time of 2 to 6 seconds. Finally, the results from this on-line inspection will be used for statistical analysis of the process. Such analysis requires a sensor with analog or digital output This output would allow for the inspection data to be easily accessible for computer processing. These are the three main criteria arising from the on-line inspection restriction.

The other design constraints evolved from the part geometry and the tolerances required. The design goal was to accommodate non-rigid parts with sloping and slanted surfaces. This moves the sensor selection away from a physical contact method. The tolerances required are on the order of 1%. This means that a one-hundred micron thick part would need to be manufactured within one micron of specification. The combined effect of these issues pushed the equipment selection toward a Laser Induced Fluorescence system.

3.2 OVERVIEW

Figure 6 displays a typical LIF system. This system contains the basic elements required: a laser, focusing optics, reception optics, a light sensor, and signal collection equipment. This general setup served as an outline for the system. Each component was then designed for this unique application. A schematic of the final design can be seen in Figure 7. Details of the system components can be referenced from Table 1.

3.3 SELECTION OF LASER AND DYE COMBINATION

Selection of a laser began with researching commercial lasers. Cost, wavelength, and power ratings were used to narrow the different laser choices. This analysis yielded three possible lasers: Helium-Cadmium, Argon, and solid state. An Argon-Ion laser from Omnichrome was selected as the best option. It was more stable and less expensive than the He-Cd laser, and it operated in a better wavelength range than the solid state laser. The wavelength range was considered better because more commercial dyes were available to work with the Argon laser emitting at 488 nm. This laser also has a longer predicted life.

A commercially available dye which had peak absorbency near or above 488 nm was then located. Fluorescein sodium is produced by several companies making it readily available. The absorption and emission characteristics of the dye are shown in Figures 2 and 3. The additional benefit of fluorescein was its solubility in water. This fact added to the flexibility of the system by eliminating concern for damage to the part from caustic solvents. These solvents are

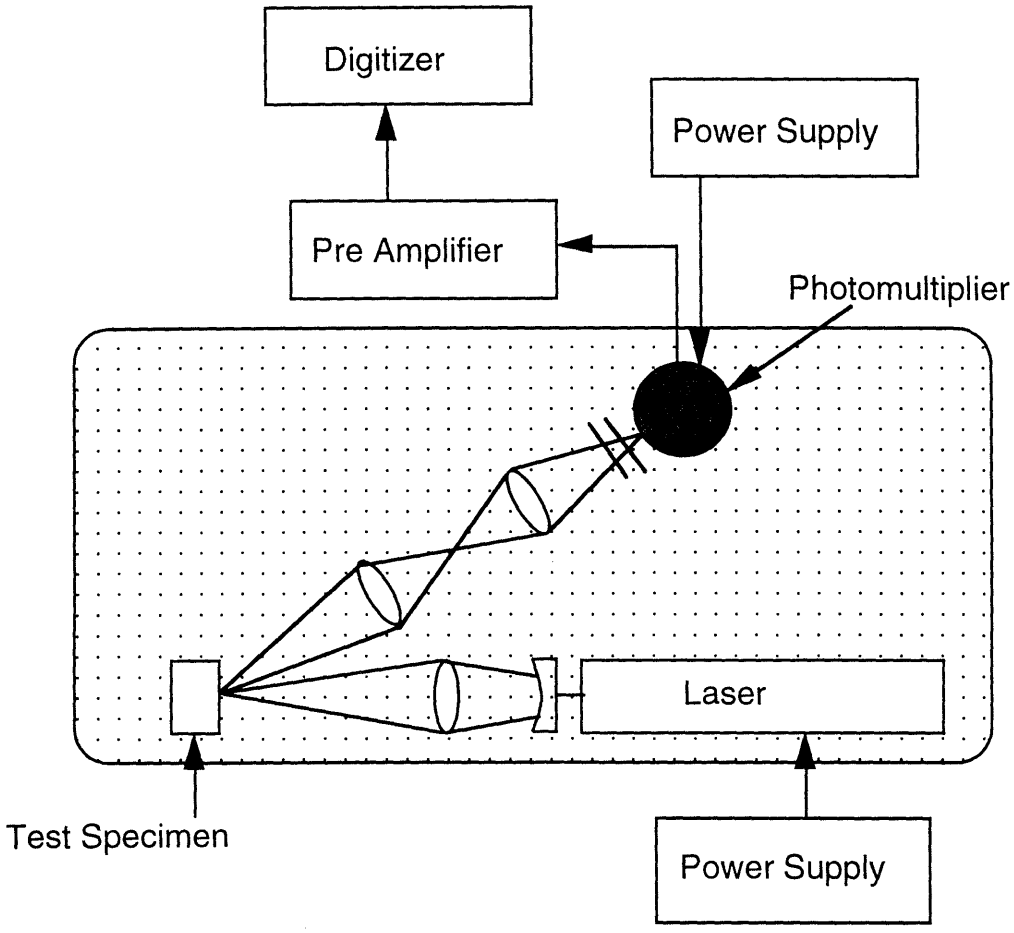

Figure 6: Typical laser induced fluorescence apparatus setup.

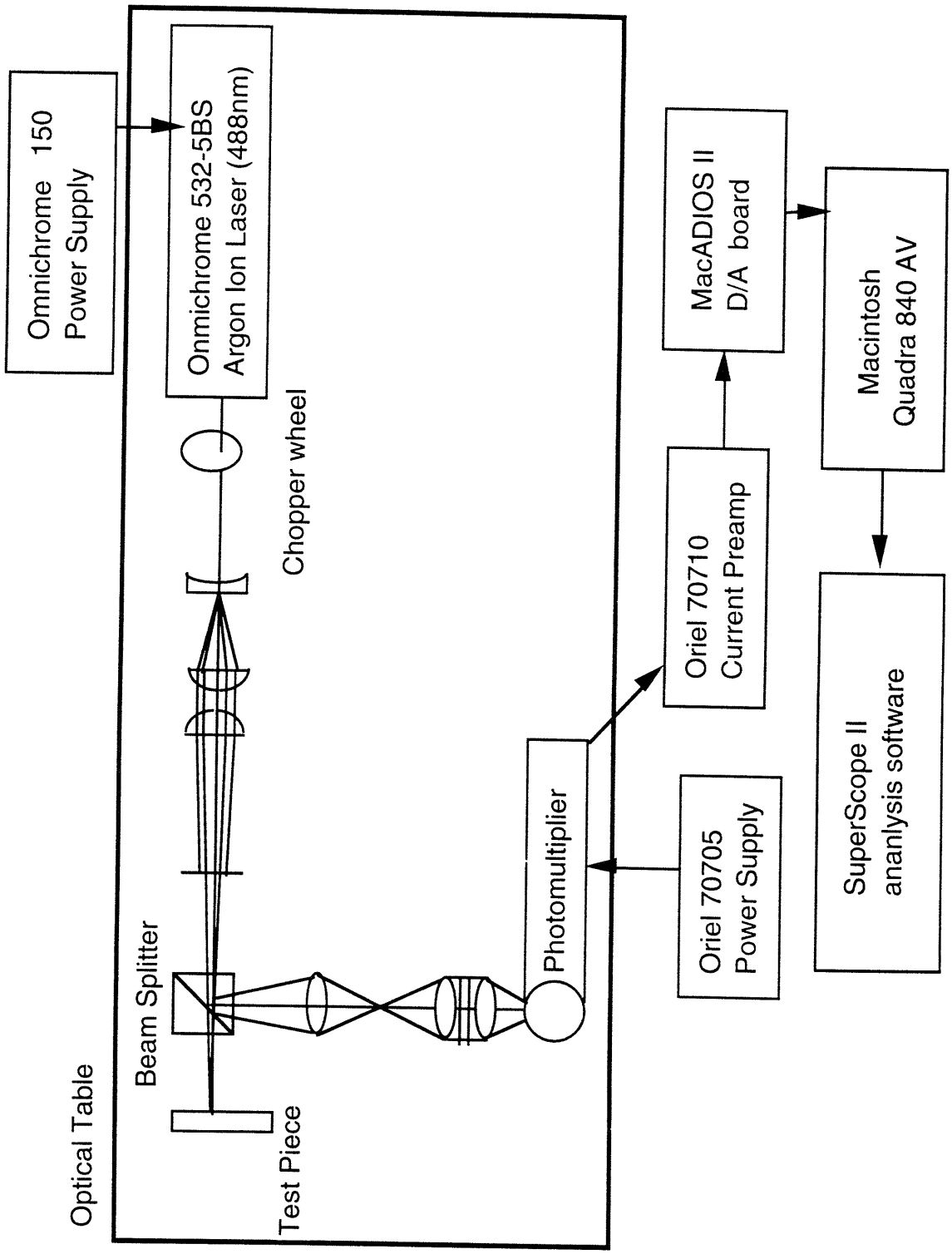

Figure 7. Schematic diagram of the final design.

TABLE 1

Equipment	Company Specifications
General	
Argon Ion Laser 20 mW	Omnichrome
Laser Power Supply	Omnichrome
Optics	
Diverging Lens	Oriel # 15640
Collimating Lens	Oriel # 41365
Narrow Pass Filter (488 nm)	Oriel # 52650
Focusing Lens	Oriel # 41390
Lens and Filter Holders	Oriel # 7123
12" Alignment Rail	Oriel # 11502 (2x)
Carriers w/ Rod Mount	Oriel # 11670 (6x)
Beam Splitter	Previously owned prisms
Rotary Table	Oriel # 11771
Lens and Filter Holders	Oriel # 7123 (5 x)
Collimating Lens	Oriel # 41350
Narrow Pass Filters	Oriel # 53874 (2x)
Focusing Lens	Oriel # 41390
Spacer Tube	Oriel # 7132
Aperture and Holder	Oriel # 49165 & 77660
Sensor Equipment	
Photo Multiplier Tube (PMT)	Oriel # 77430
PMT High Voltage Power Supply	Oriel # 70705
PMT Housing	Oriel # 70680
PMT Amplifier	Oriel # 70710
Amplifier Power Supply +/- 12V	Servo Systems Dynage 800-196A
Analog/Digital Converter	GWI Instruments, MacADIOS II/16
Data Analysis Software	GWI Instruments, SuperScope II

Table 1. Equipment specification for design of the LIF system.

commonly needed to dissolve other fluorescent dies. Having found the appropriate dye and laser combination, it was necessary to design the optics and select a sensor for the system so that the necessary laser power could be determined. Subsequent design of these components yielded a power rating for the laser equal to 5 to 20 mW.

3.4 OPTICAL DESIGN

The LIF system calls for both a focusing and receiving set of optics. The emitting optics are defined by the need to focus the beam onto the specimen. The design of the specimen holder is discussed later in the chapter. The smallest identifiable detail is determined by the beam diameter. The smallest possible diameter is determined by the equation [7]:

$$d = 1.27(\lambda)f / D \qquad \text{(eq. 3.1)}$$

"D" represents the initial beam diameter, and "d" is the smallest theoretical diameter of the output beam. The focal length of the lens and the wavelength of the light are signified by "f" and "λ" respectively. The traditional way to minimize the final beam diameter is to maximize the incoming diameter of the beam. This is done by using a beam expander. The optics for a generic expander are shown in Figure 8. This system has a theoretical limit of 9 microns for "d" and an actual value of 1 mm. The final design of the emitting optics is shown in Figure 9.

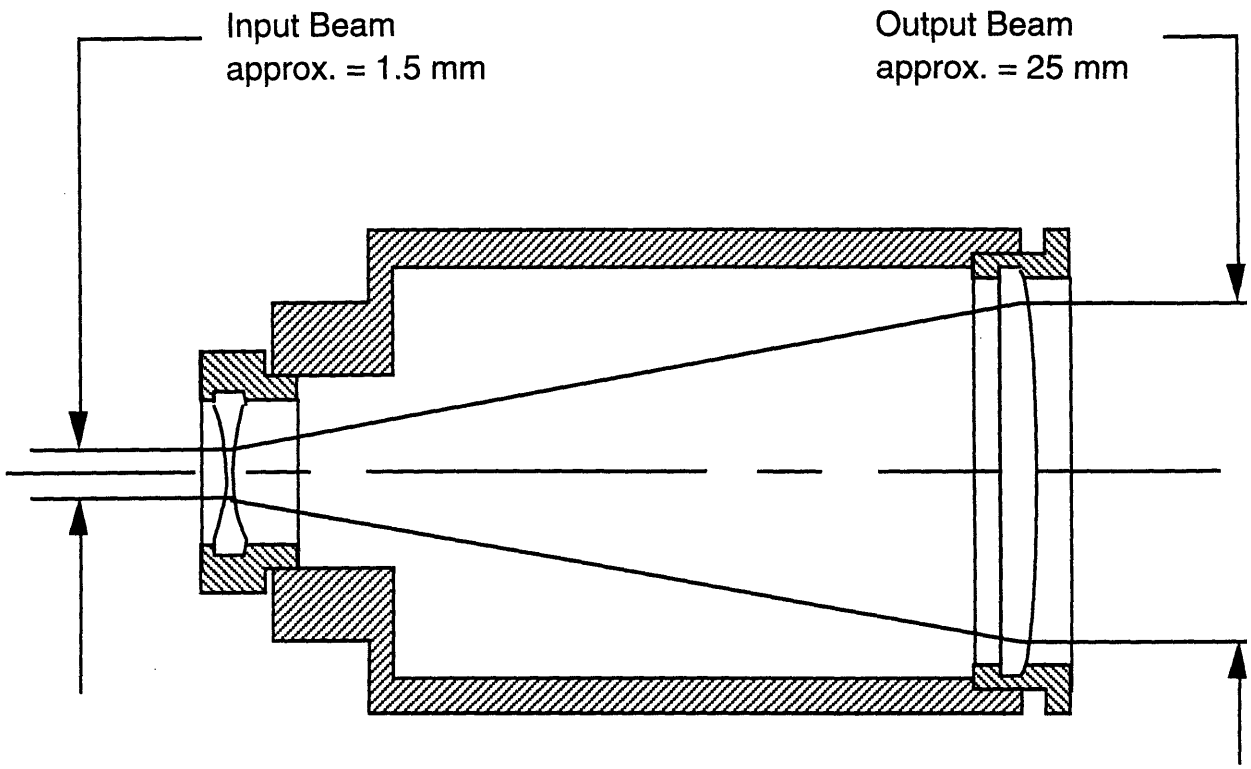

Figure 8. A generic beam expander.
The incoming beam diameter is enlarged so that a smaller final diameter can be achieved.

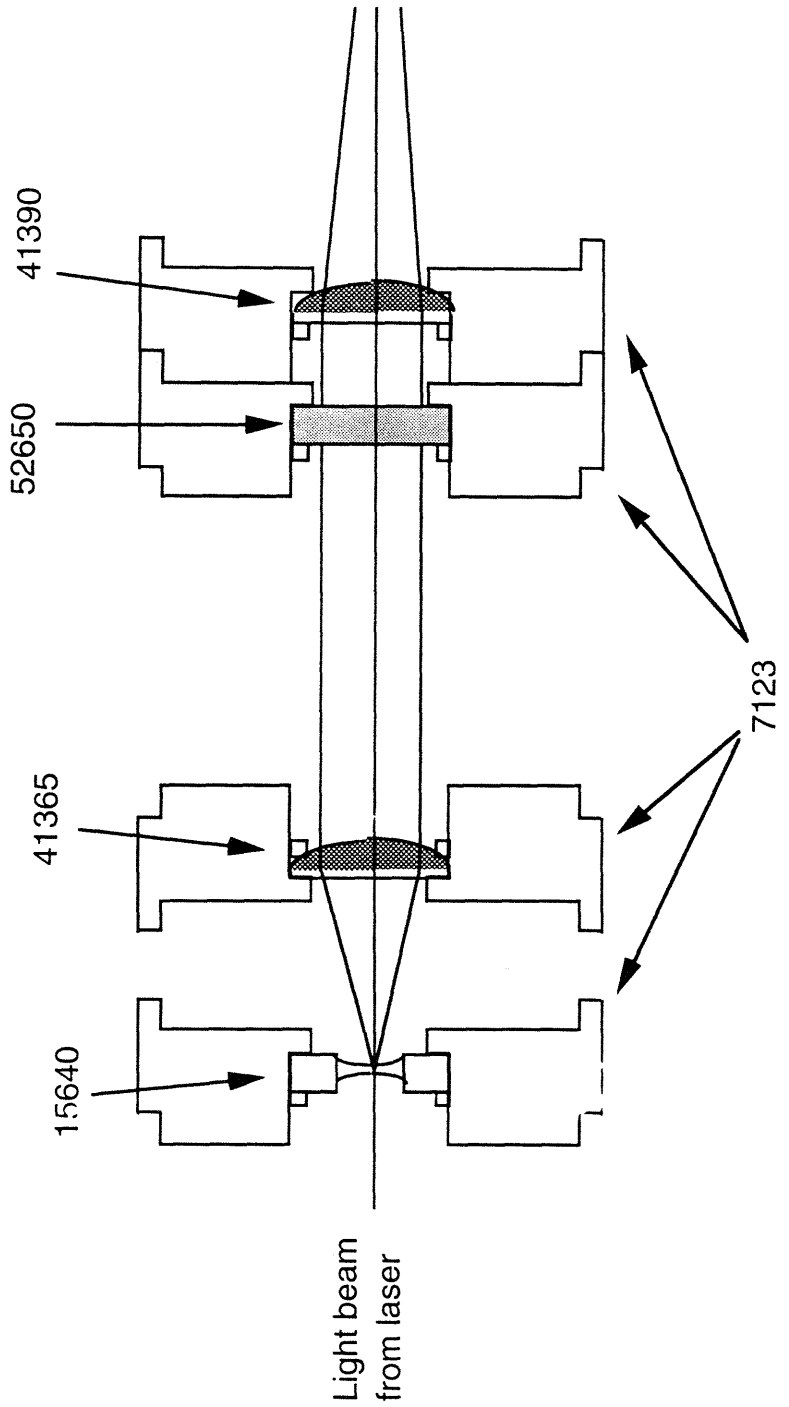

Figure 9. Diagram of focusing optics.
Numbers refer to Oriel Corp part numbers. Parts 4xxxx and 15640 are fused silica lenses. #52560 is a filter. #7123 refers to lens and filter holders.

The reception optics of Figure 10 must filter the fluorescent light from the specimen and then focus it onto the Photomultiplier Tube (PMT), a light sensitive sensor. The first lens and aperture create a spatial filter. The method of spatial filtering is commonly used in many optical applications. The concept follows that the light is focused by a first lens through an aperture onto a second lens. Then, only these properly focused light rays will approach the second lens at the correct angle and subsequently be focused onto the light sensitive area of the PMT. This spatial filter, the first lens and aperture, was ultimately removed from the final sensor because it did not noticeably improve the signal to noise ratio.

The midsection of the reception system collimates the light to pass it through two narrow pass filters centered at 530 nm. The transmittance ranges of these filters can be seen in Figure 11. This use of two filters follows the recommendations of Ingles [8]. The combination of these two filters guarantees that only the fluorescent light from the specimen holder is transmitted to the PMT. The final lens of the system actually focuses the light. The last aperture eliminates fringe light rays, making a cleaner signal on the PMT.

A cube beam splitter is used to direct the laser light onto the specimen and then transmit the fluorescent signal to the reception optics. Positioning of the components and the need to eliminate noise from scattering in the specimen dictate that a beam splitter should be used. The splitter allows the specimen to be isolated from the rest of the system excepting a small aperture which allows for incoming and outgoing rays. The aperture blocks most of the light

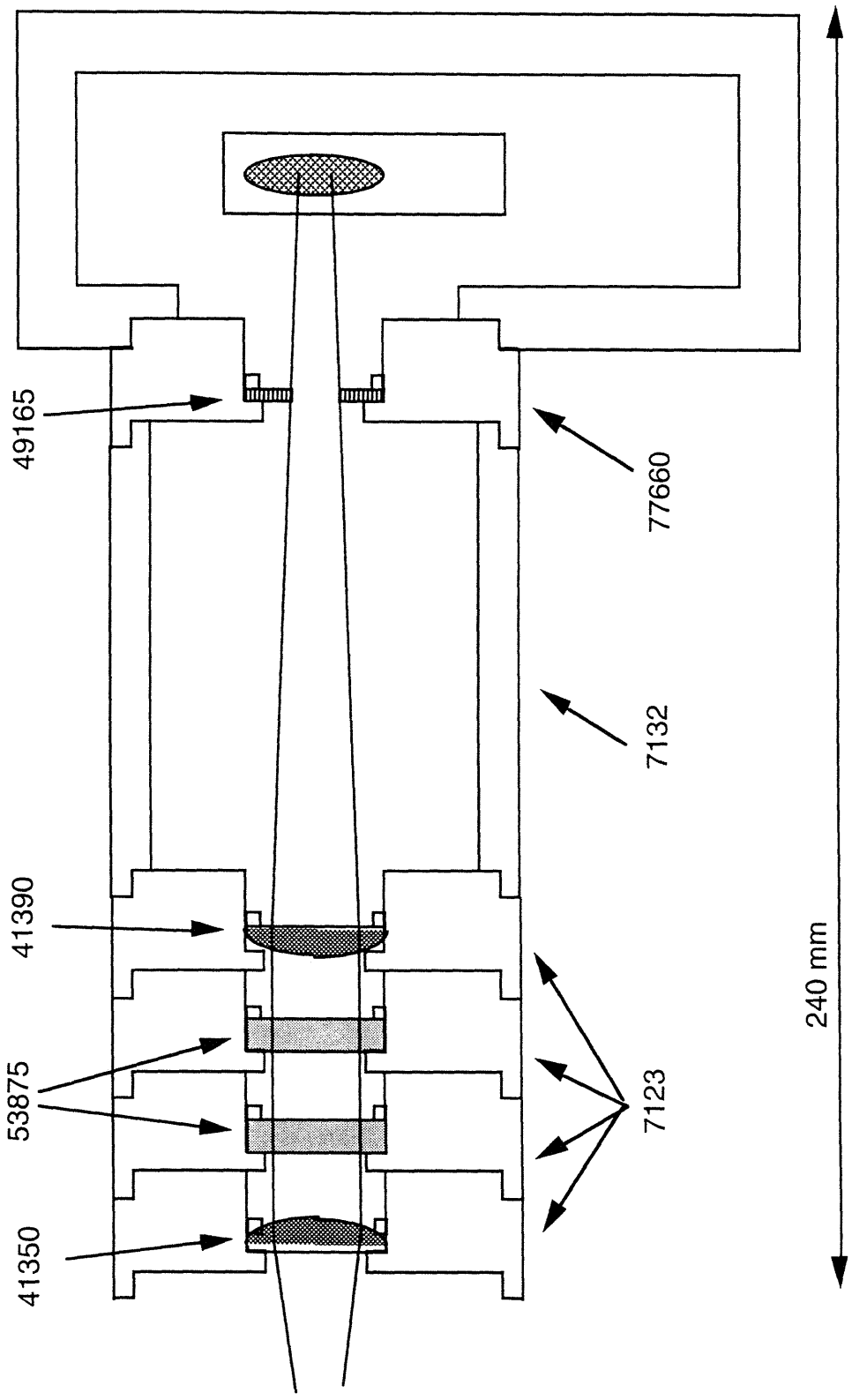

Figure 10. Diagram of reception optics.
Numbers refer to Oriel Corp. part numbers. Referencing catalog descriptions will give specific details.

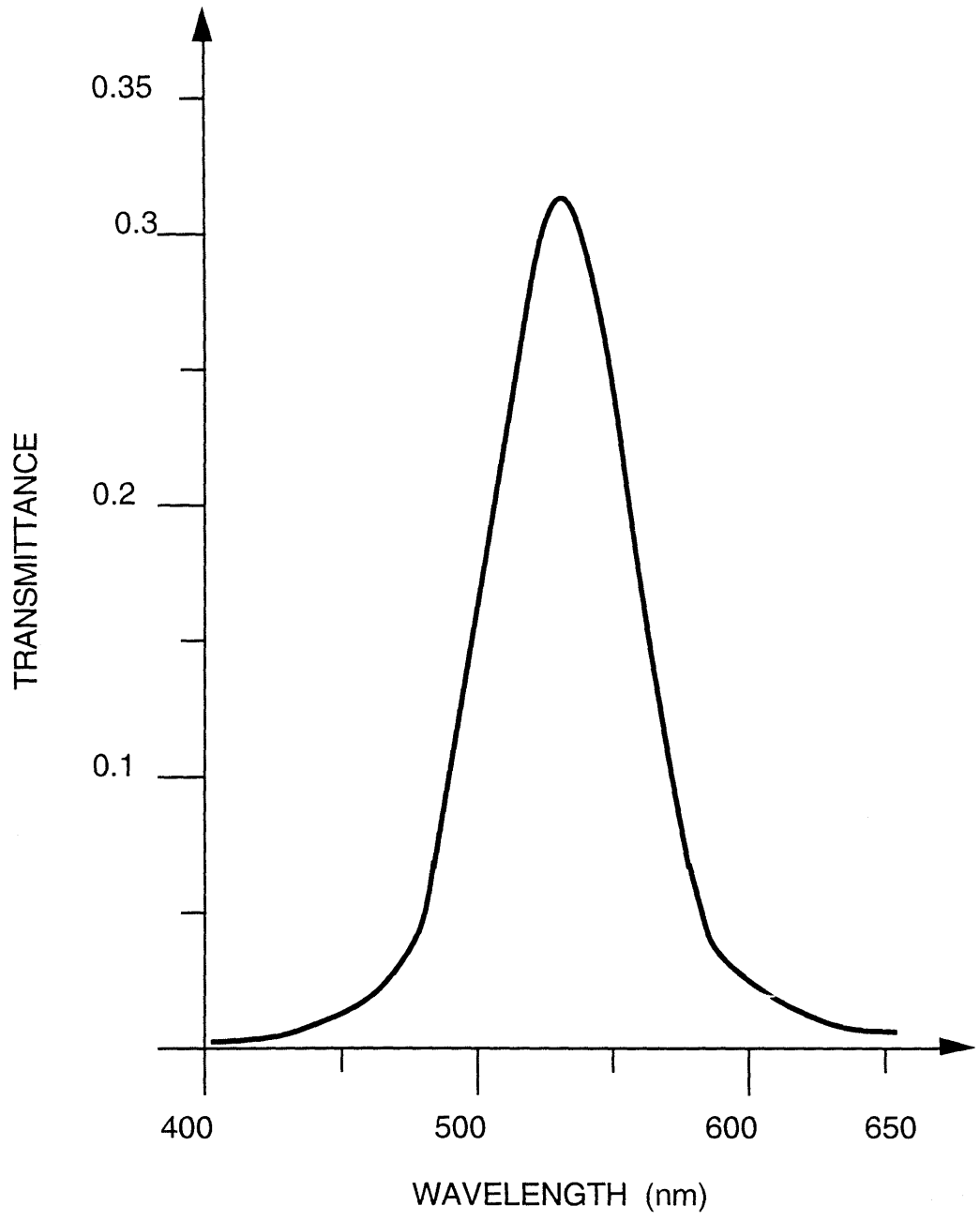

Figure 11. Transmittance of 530 nm filters.

caused by scatter effects. Without the beam splitter, two apertures would be required, presenting difficult mounting problems. Examining small parts allows little room to locate the apparatus within the desired distance. A beam splitter helps eliminate the problem. The second generation sensor will overcome this problem with fiber optics that emit and receive light with one probe.

A calculation of the system's efficiencies indicates how much of the original laser beam reaches the specimen and subsequently how much fluorescent light reaches the PMT. Table 2 lists the efficiencies of all the components. These values are multiplied to obtain the actual efficiency of the system. This and the sensitivity of the sensor help determine the laser power required and the potential resolution. Appendix B explains the procedure used to align the optics.

3.5 SENSOR SELECTION

The first of several criteria to be considered when choosing a detector is the wavelength at which the tests will be operating. This application requires a sensor that will work well in the 530 nm range. The next consideration is the detectivity of the device. The efficiency calculations suggest that a detectivity range of 10^{-6} to 10^{-11}mW will be required. These two criteria reduce the choice of main stream sensors to Photomultiplier Tubes and Silicon Photo Diodes. PMT's were chosen for this application because of their greater sensitivity. This is approximately two orders of magnitude better than the Silicon Photo Diodes.

TABLE 2

Theoretical Transmittance

Item	Transmittance
Light hitting lens	0.90
Diverging Lens	0.84
Light hitting lens	0.45
Collimating Lens	0.84
488 nm Filter (not used)	1.00
Focusing Lens	0.84
Beam Splitter (emitting)	0.25
Aperture (2,5 mm)	0.40
Fluorescent Efficiency	0.01
Aperture (.13/50)	0.002
Beam Splitter (receiving)	0.25
Collimating Lens	0.84
530 nm Filter (2 X)	0.09
Focusing Lens	0.84
Aperture	0.25
Resulting Emission	1.91 E-09
Energy to PMT (W)	3.81 E-11
Signal from PMT (A)	2.86 E-05
Preamp Signal (V)	0.143
Actual Readings (V)	.001 to 1.0

Table 2. Theoretical transmittance of the system.

PMT's are based on the concept of light interacting directly with electrons on a detector material. The material absorbs photons and releases electrons from it's surface. By applying a high voltage (-1000 V) across the PMT, the electrons are forced to flow toward an anode. An electron multiplier using dynodes amplifies this photo current as it moves toward the anode. The end result is a current proportional to the incoming light intensity increased by 6 to 8 orders of magnitude. A typical PMT and this process are shown in Figure 12. This current signal is then increased another 4 orders of magnitude and converted into a voltage signal by a preamplifier.

After deciding on Photomultiplier Tubes, several other issues needed to be resolved. It was decided that a cooled housing for the PMT was unnecessary. The major advantage of a cooled housing is a more level signal over a variety of wavelengths. Since this application requires readings at a single wavelength, the added cost for performance could not be justified. Various tubes also have different peak wavelength and signal responsivity across the spectrum. Tubes with more level responses over wider ranges have higher prices. The single wavelength application allows a PMT to be purchase for only $130 where others might cost more than a thousand dollars. Detailed descriptions of the components used in the setup can be found in reference [9].

3.6 DATA ACQUISITION

To obtain data from the system efficiently, data acquisition hardware and software needed to be selected. Due to laboratory logistics where this work was conducted, it was desirable to have a

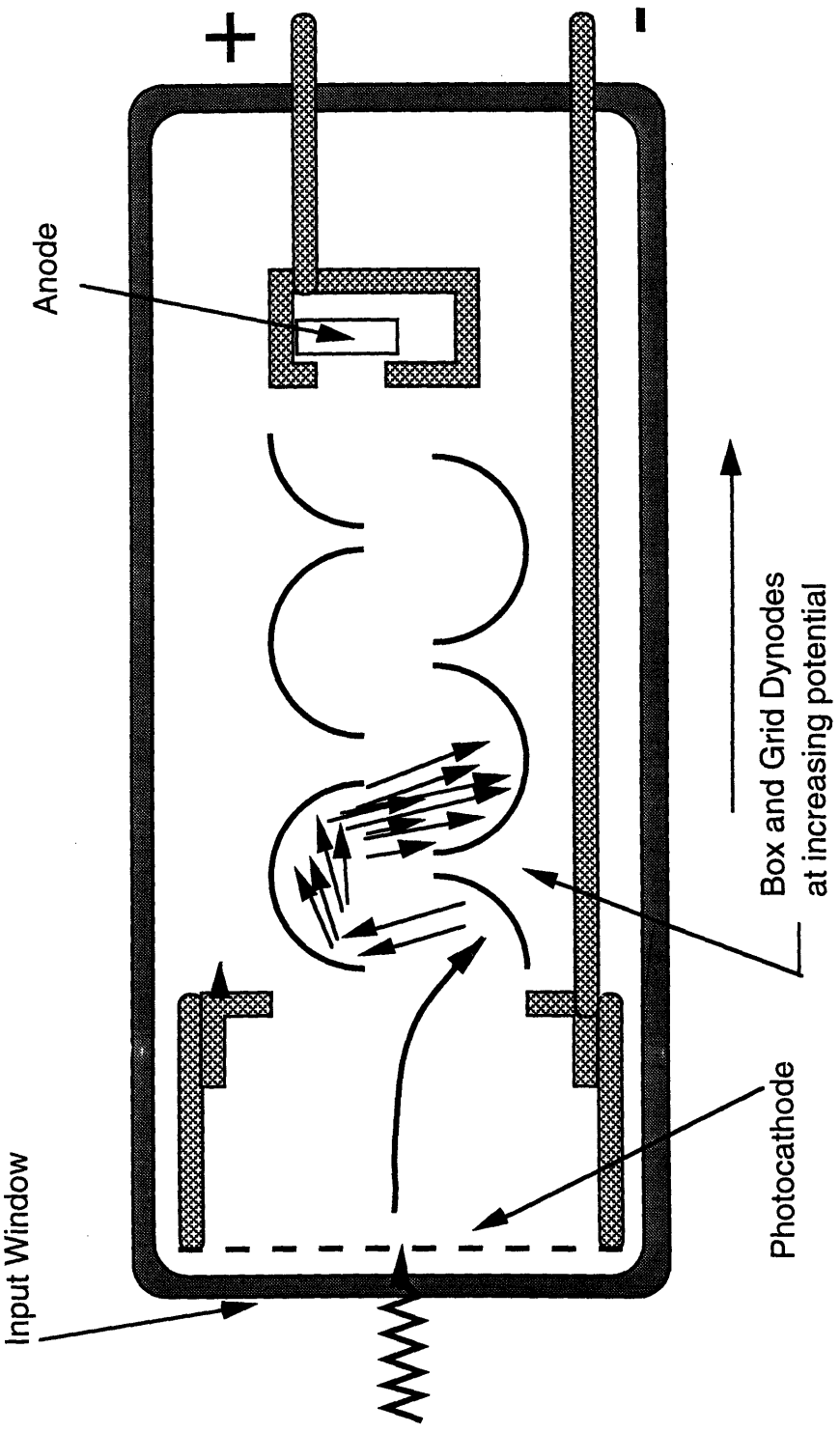

Figure 12. Schematic of a photomultiplier tube.

Macintosh compatible system. A local company GW Instruments™ proved to have a product line that offered a wide range of performance and a simple user interface.

A high resolution analog to digital conversion board was selected. This board took the voltage signal from the preamp and digitized it with 16 bit resolution. This allowed for readings ranging from -5 to +5 volts with 0.15 mV accuracy. The maximum conversion rate of the board was 55 kHz, translating to one point taken every 20 milliseconds. This board was installed in a Macintosh Quadra 840AV to allow for full use of its capabilities.

The software used a package called "SuperScope II™." This program allowed users to design instrument panels customized to their own needs. In a generic application the computer was used as an oscilloscope. By modifying the system, an end user can reduce data acquisition to a single push-button function. An example of a custom front panel is shown in Figure 13. One button activated the acquisition of data, and a second button initiated analysis of the data and transfered the results to an on-screen journal. From the journal the results can be moved into a spreadsheet for further analysis.

3.7 SPECIMEN HOLDER

The physical design of the specimen holders established the details for what had been left as a black box this far in the design. All other components were selected previous to the final design of the system. This was difficult since the holders had to simulate parts being submerged and positioned. Also, they had to allow for light

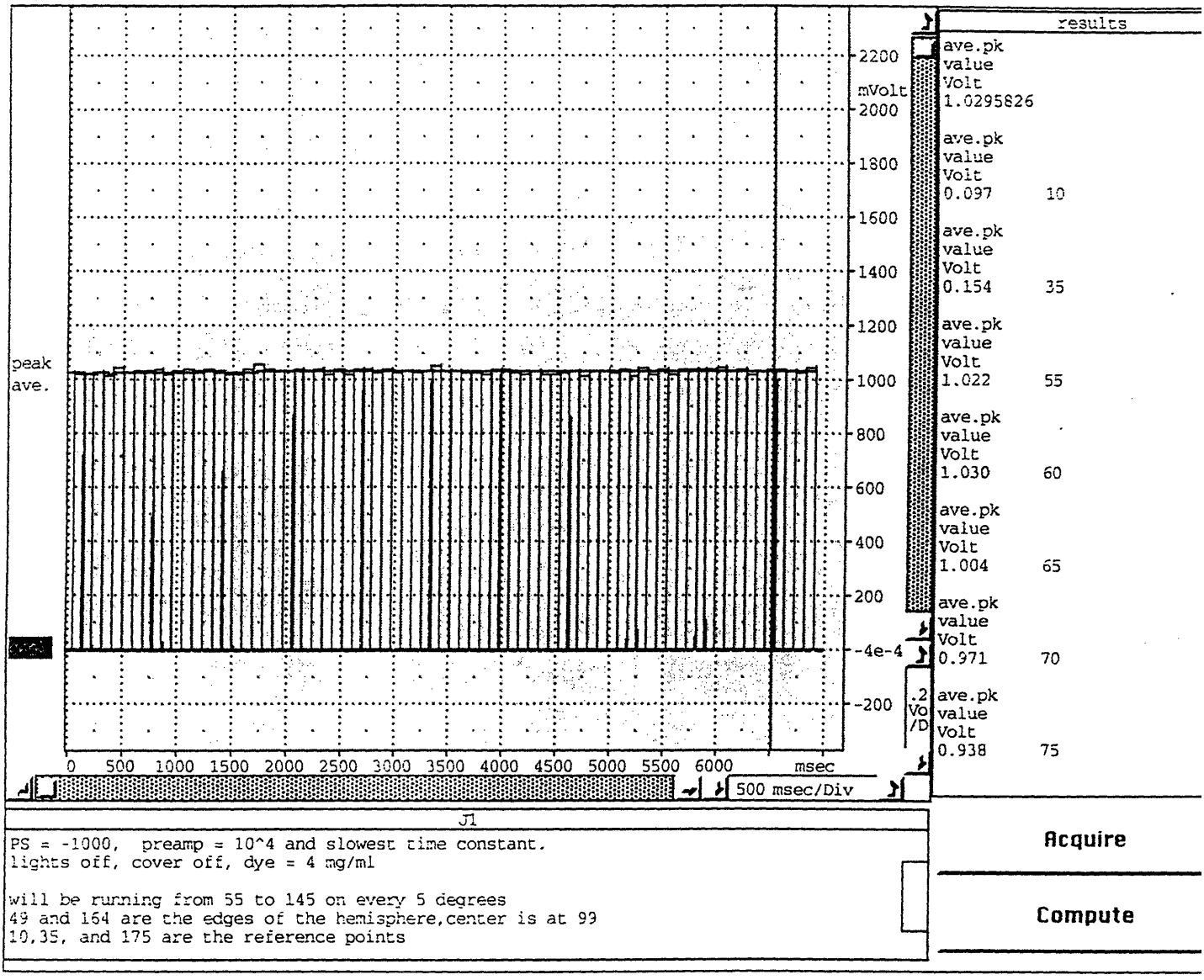

Figure 13. **Instrument panel used to acquire and process data for the chopped scans.**

entering and leaving unimpeded across the entire part. Resolution requirements demanded that the water and dye solution be kept at a depth equal to the small parts which were to be measured. This meant accommodating for differences in part thickness.

The solution to these problems came in different forms. Several holders were designed, but only three were actually built. The first two pieces were simple step models that moved linearly across the path of the laser beam. They provided the test data necessary to determine the resolution, linearity, and stability of the system. The data used to correlate light intensity and solution depth were also obtained from tests conducted with these specimens. These models, shown in Figure 14, were made from Plexiglas and had microscope slides clamped to them forming the top boundary.

The final holder illustrated a few principles of how a small, complex part might be positioned. The generic solution implies that a custom holder should be made for different parts. A unique backing locates the part and eliminates the opportunity for any solution to seep behind it. Having any solution behind the part could complicate calibration problems if the part is not entirely opaque. The part is held firmly by drawing a vacuum through the back, guaranteeing positive location. The top surface of the holder then conforms to the part profile allowing for a relatively constant solution depth. This outer surface is constructed from Plexiglas™ or quartz to allow for transmittance of the light.

The actual specimen holder and insert designs are shown in Figures 15a, 15b, and 16. A hemisphere was selected to simulate the

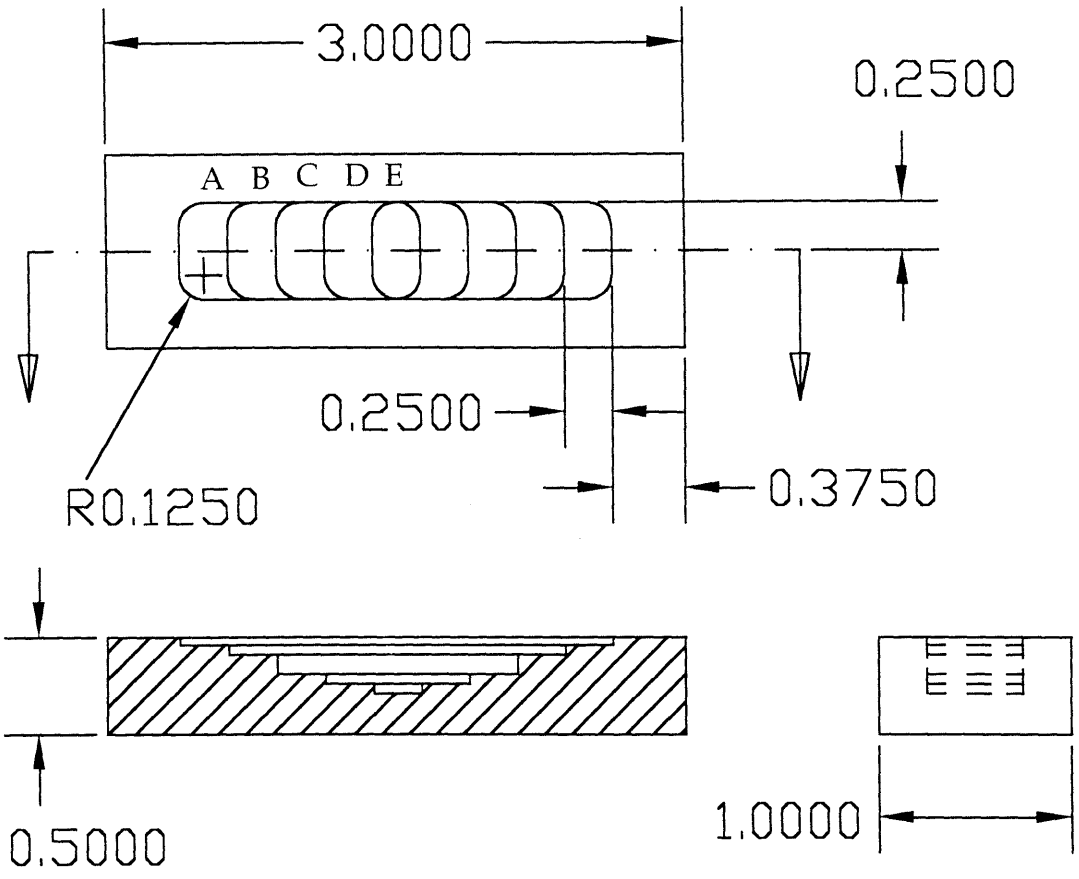

*The dimensions are in inches and the material is Plexiglas.

There are 5 symmetrically spaced steps with varying depths. These depths vary for the thin and deep step specimens.

Step / Specimen	Deep Step Specimen	Thin Step Specimen
Step A	.0400"	.0070"
Step B	.0895"	.0115"
Step C	.1880"	.0215"
Step D	.2380"	.0265"
Step E	.2880"	.0315"

Figure 14. Dimensions of the two step specimens.

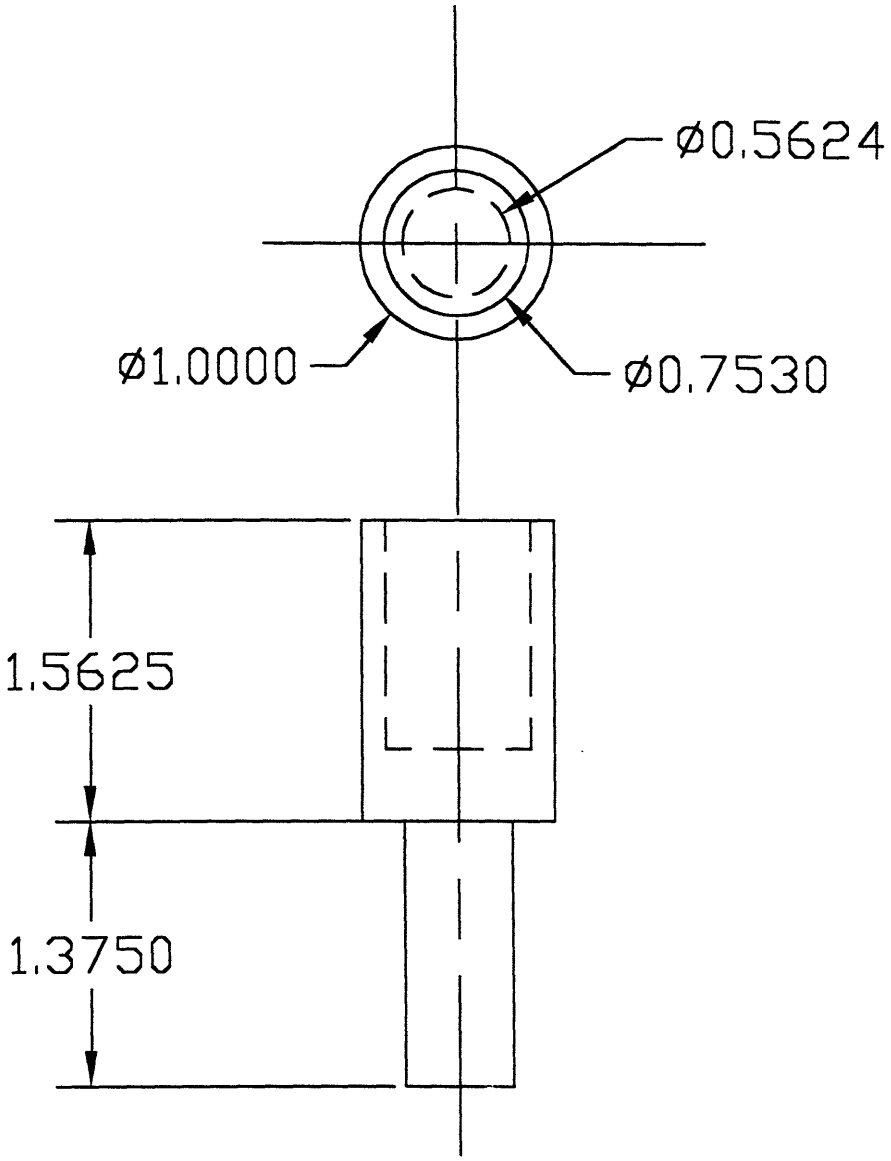

*The material is Plexiglas, and all dimensions are in inches.

Figure 15a. Insert holder used for the simulation of part measurement.

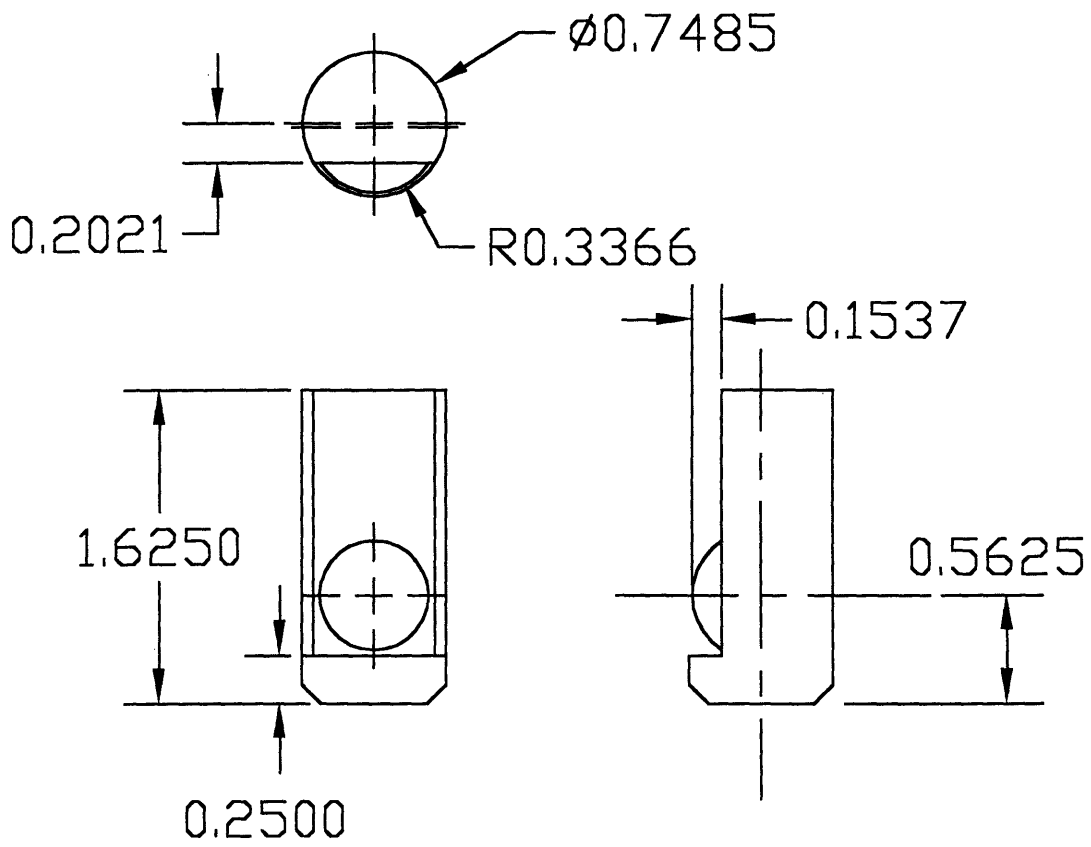

* The material is Plexiglas, and all dimensions are in inches.

Figure15b Insert used for the simulation of part measurement.

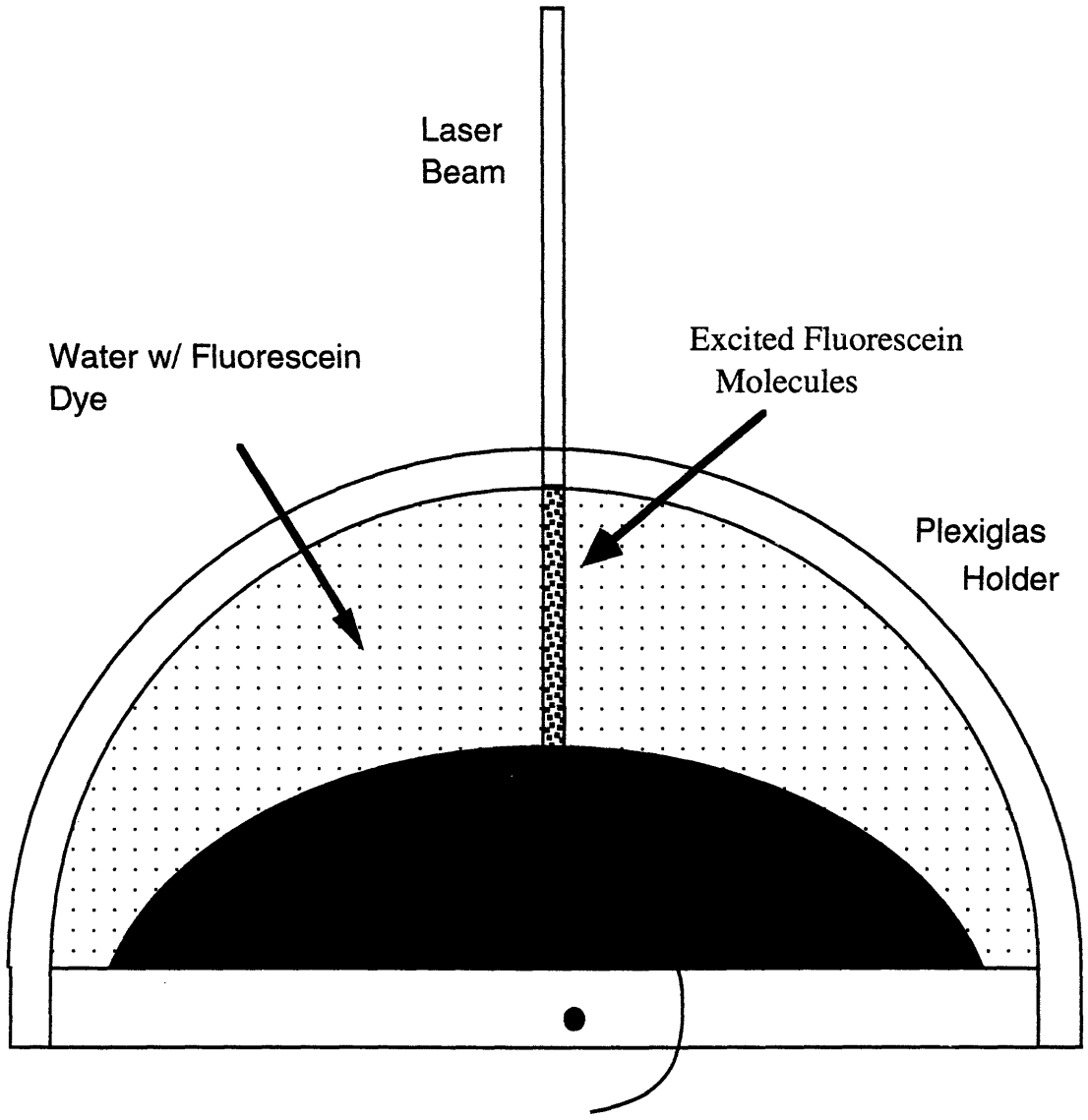

Figure 16. **Top view of the rotary holder and hemisphere insert.**
The laser beam enters the front of the holder and excites the fluorescein dye.

curves of a complex part. This holder had several key characteristics. First, the curved front conformed to the general profile of the hemisphere. This allowed for the solution to remain at a depth of 350 to 700 microns. Second, the holder rotated about an axis, keeping the laser beam constantly perpendicular to the part surface. Finally, the holder and insert were Plexiglas™ allowing unabsorbed laser light to pass through the back of the holder. This reduced scattering and reflectance problems that could reduce the linearity of the system.

4. EXPERIMENTAL RESULTS AND ANALYSIS

4.1 OVERVIEW

Extensive testing was done using the LIF system. This work was done to assist in identifying sources of noise, determining the transmitting efficiency of the system, refining the optical alignment, and characterizing the performance of the system. A series of tests was also performed to determine optimal chopper frequency, sample rate, and test duration. Although useful in refining the system, some of the tests offered little insight into the performance of the system. For this reason only the results of the tests that quantify the performance of the system will be presented in this chapter. Some additional information is provided in the appendices. Detailed instructions for testing are given in Appendix C to assist in replicating the experiments. Appendix D provides explanations of the data processing methods used.

4.2 CALIBRATION AND LINEARITY

A matrix of tests was completed using the two step specimens and three different dye concentrations: .001 mg/ml, .004 mg/ml, and .016 mg/ml. The solution was a mixture of distilled water and fluorescein sodium dye. Each specimen had four different depths; the first ranged from .0070 to .0215 inches, and the second ranged from .040 to .238 inches. Each level was scanned three times for each dye concentration. The end result was two 4x3 matrices with three data points for each combination of variables. The data for these tests is given in Table 3. Figures 17 through 19 and 20

TABLE 3

Fluorescent intensity results from the thin step tests

	Dye Concentration (mg/ml)								
Depth	.001	.001	.001	.004	.004	.004	.016	.016	.016
0.0070"	1.88*	1.99	1.85	10.91	11.11	10.81	29.72	29.92	30.66
0.0115"	4.16	4.19	4.28	17.33	17.10	17.29	55.40	55.44	56.11
0.0215"	8.78	8.99	9.10	30.39	31.96	32.77	78.05	82.82	81.11
0.0265"	11.01	10.86	11.00	38.30	36.40	36.48	89.52	85.99	89.28

*Intensity represented in mV

Fluorescent intensity results from the deep step tests

	Dye Concentration mg/ml								
Depth	.001	.001	.001	.004	.004	.004	.016	.016	.016
0.0400"	9.96*	11.18	12.98	35.00	30.16	33.08	60.36	60.65	65.31
0.0895"	17.8	18.45	18.78	55.36	56.90	56.60	104.68	107.54	108.43
0.1880"	36.46	38.16	38.27	94.86	98.95	98.67	150.68	151.95	151.80
0.2380"	46.46	49.01	47.99	114.00	116.75	116.87	164.45	164.90	164.21

*Intensity represented in mV

Table 3. Data from the step test scans.
The two different specimens have four steps of varying depths. These depths are referenced on the left side of the tables. The tests were conducted with three different dye concentrations. These concentrations are referenced across the tops of the tables. The values in the tables are fluorescent intensity values represented in mV.

through 22 show the results organized by shallow and deep holder respectively. Figures 23 to 25 display the data sorted by concentration of fluorescent dye. Regression data is given with each graph.

These tests prove that the system gives linear results for most combinations:

	Dye Concentration		
Depth of Solution	.001 mg/ml	.004 mg/ml	.016 mg/ml
.0070 - .0215 in.	.993	.994	.950
.040 - .238 in.	.992	.985	.916

Table 4. R^2 values from the linearity tests.

These results provided the basis for selecting the .004 mg/ml concentration for the remaining tests. This concentration's correlation coefficient is .714 inches/volt.

4.3 SIGNAL / NOISE RATIOS AND RESOLUTION

The inherent noise of a system often dictates resolution limits and cycle time because it creates the need for higher volumes of data. This system has a signal / noise, S/N, ratio on the order of 5 to 10. This number fluctuated with the absolute level of the readings which ranged from 5 to 200 mV. Previous studies [8] indicate that the noise component does not continue to increase beyond 20 to 30 mV. This implies that if signal readings could be raised to the 1.5 V range, the S/N ratio would improve to about 50. Improving the optical setup could feasibly yield a signal in this power range.

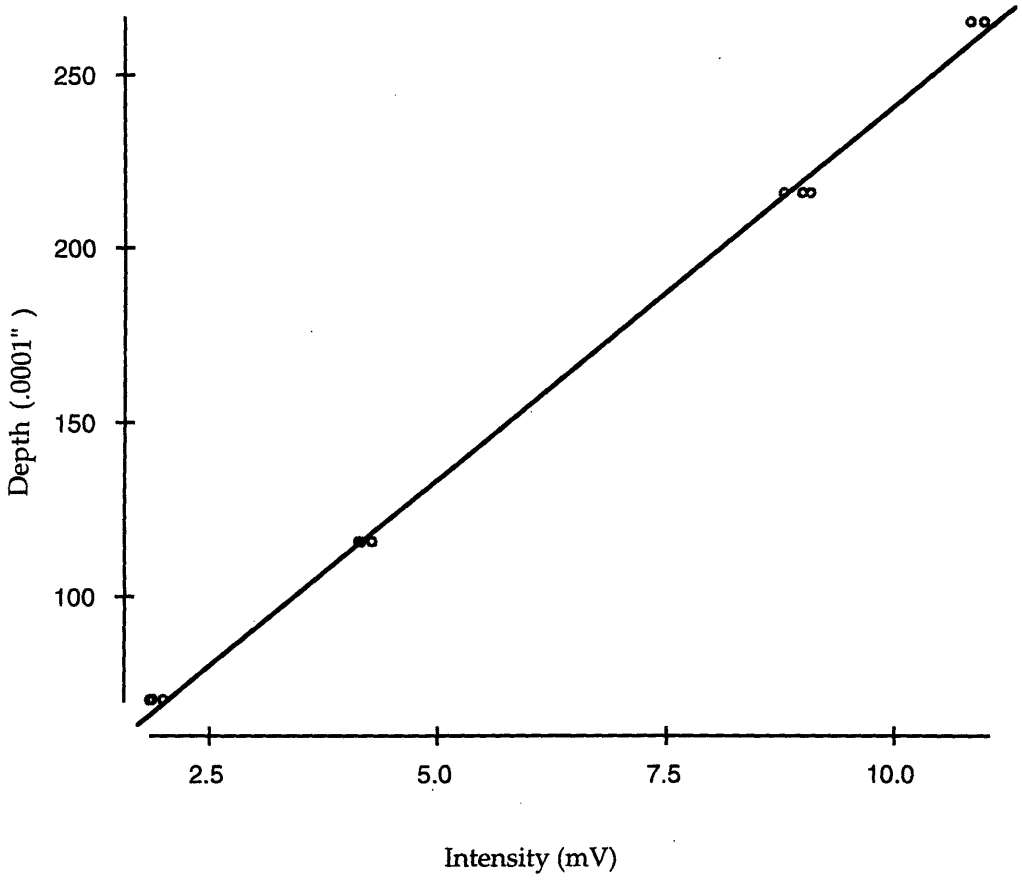

Dependent variable is: depth
R squared = 99.8% R squared (adjusted) = 99.8%
s = 3.803 with 12 - 2 = 10 degrees of freedom

Source	Sum of Squares	df	Mean Square	F-ratio
Regression	71911.7	1	71911.7	4973
Residual	144.595	10	14.4595	

Variable	Coefficient	s.e. of Coeff	t-ratio	prob
Constant	26.8912	2.261	11.9	≤0.0001
t011	21.4151	0.3037	70.5	≤0.0001

Figure 17. Line fit and regression data for thin steps and a dye concentration of .001 mg/ml

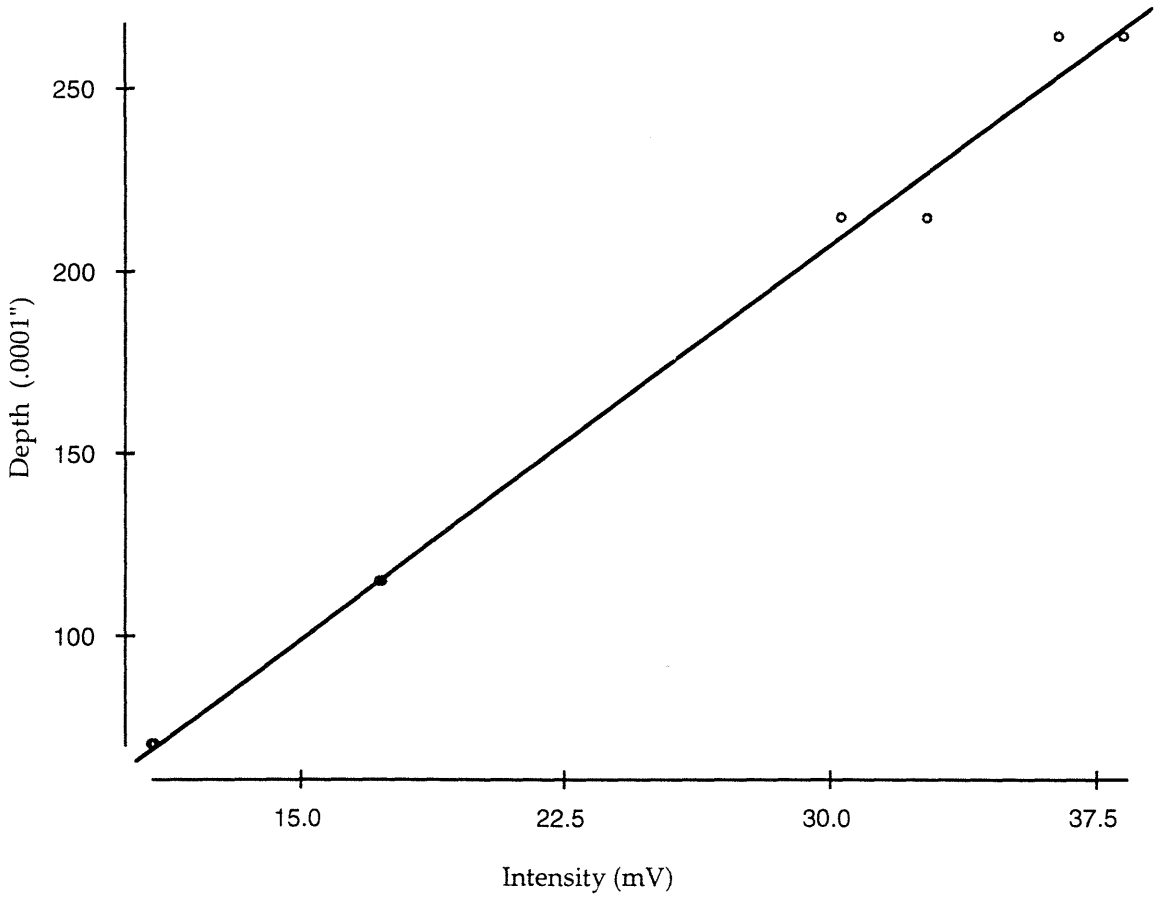

Dependent variable is: depth
R squared = 99.2% R squared (adjusted) = 99.1%
s = 7.574 with 12 - 2 = 10 degrees of freedom

Source	Sum of Squares	df	Mean Square	F-ratio
Regression	71482.7	1	71482.7	1246
Residual	573.588	10	57.3588	

Variable	Coefficient	s.e. of Coeff	t-ratio	prob
Constant	-9.72119	5.443	-1.79	0.1044
t041	7.24087	0.2051	35.3	≤0.0001

Figure 18. Line fit and regression data for thin steps and a dye concentration of .004 mg/ml.

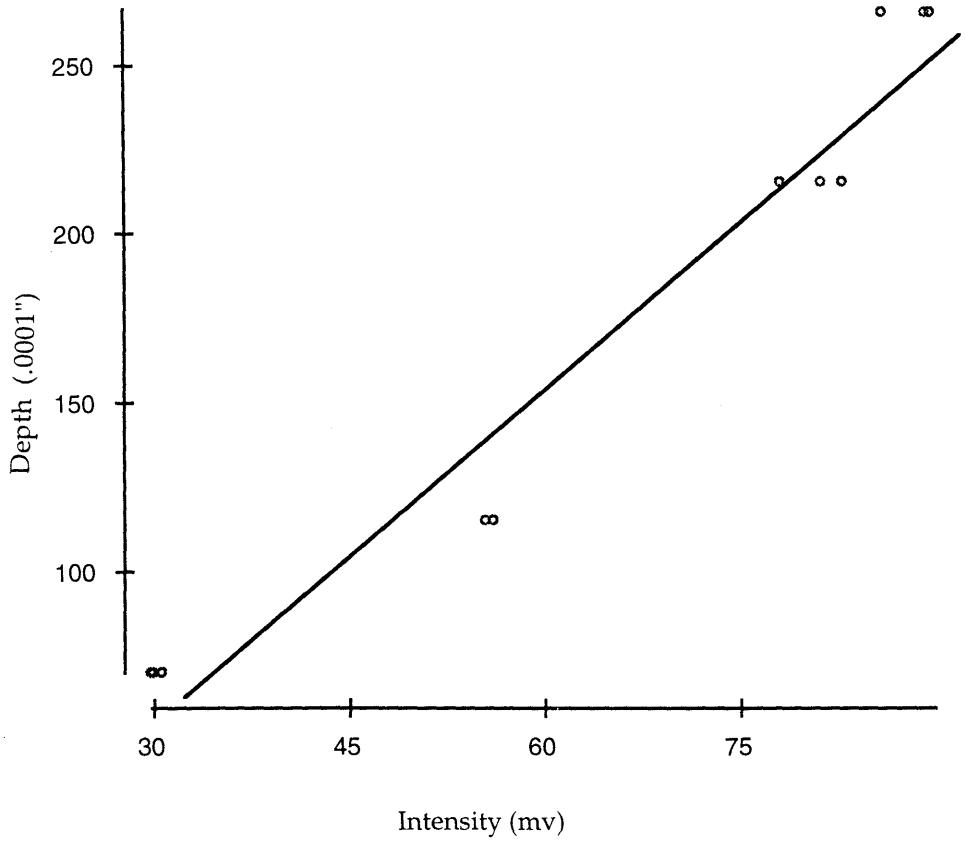

Dependent variable is: depth
R squared = 94.7% R squared (adjusted) = 94.2%
s = 19.46 with 12 - 2 = 10 degrees of freedom

Source	Sum of Squares	df	Mean Square	F-ratio
Regression	68270.3	1	68270.3	180
Residual	3785.96	10	378.596	

Variable	Coefficient	s.e. of Coeff	t-ratio	prob
Constant	-43.7640	16.62	-2.63	0.0250
t161	3.29856	0.2456	13.4	≤0.0001

Figure 19. Line fit and regression data for thin steps and a dye concentration of .016 mg/ml.

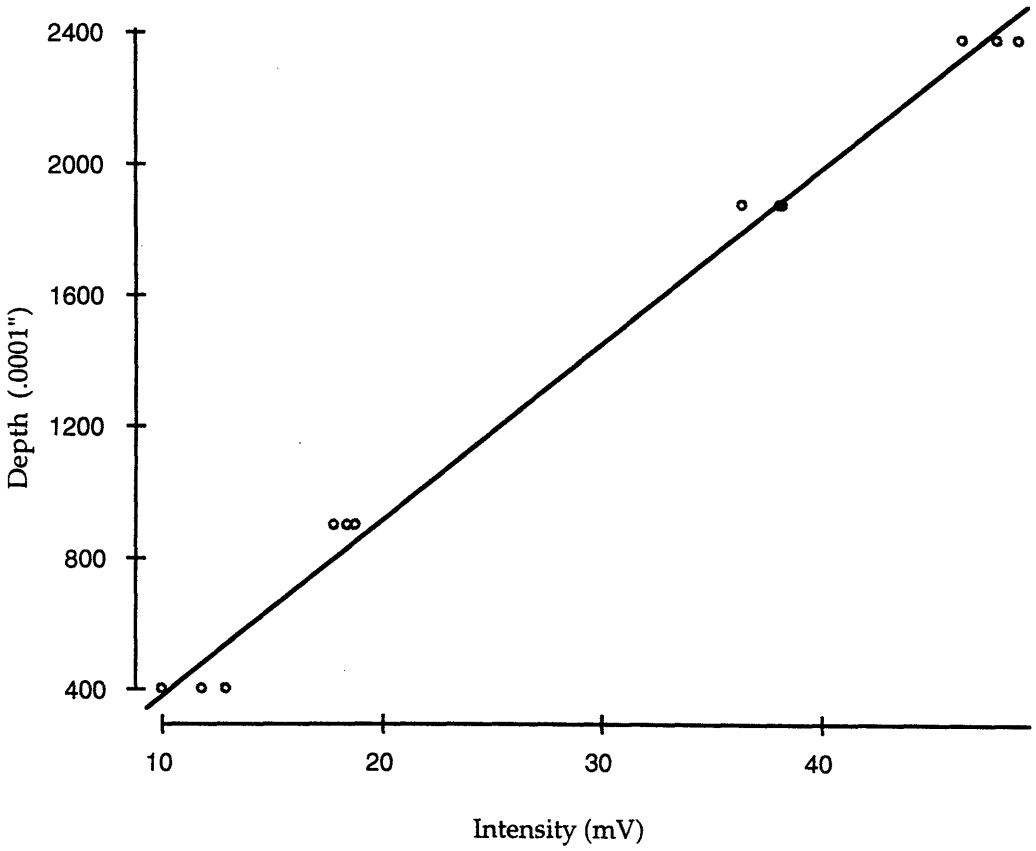

Dependent variable is: depth
R squared = 99.2% R squared (adjusted) = 99.1%
s = 77.58 with 12 - 2 = 10 degrees of freedom

Source	Sum of Squares	df	Mean Square	F-ratio
Regression	7275766	1	7275766	1209
Residual	60190.4	10	6019.04	

Variable	Coefficient	s.e. of Coeff	t-ratio	prob
Constant	-153.652	49.70	-3.09	0.0114
t011	53.4659	1.538	34.8	≤0.0001

Figure 20. Line fit and regression data for deep steps and a dye concentration of .001 mg/ml.

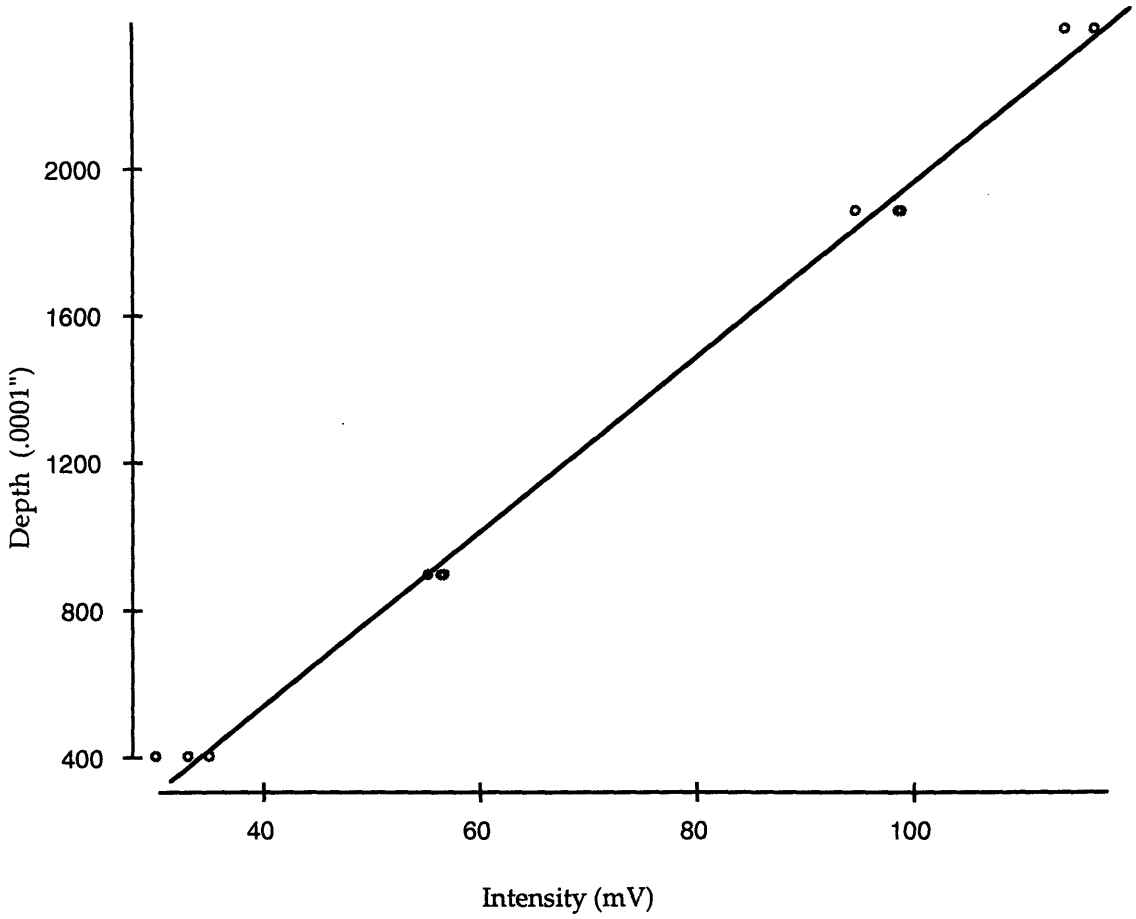

Dependent variable is: depth
R squared = 99.6% R squared (adjusted) = 99.6%
s = 53.50 with 12 - 2 = 10 degrees of freedom

Source	Sum of Squares	df	Mean Square	F-ratio
Regression	7307336	1	7307336	2553
Residual	28619.8	10	2861.98	

Variable	Coefficient	s.e. of Coeff	t-ratio	prob
Constant	-406.290	38.74	-10.5	≤0.0001
t041	23.7436	0.4699	50.5	≤0.0001

Figure 21. Line fit and regression data for deep steps and a dye concentration of .004 mg/ml.

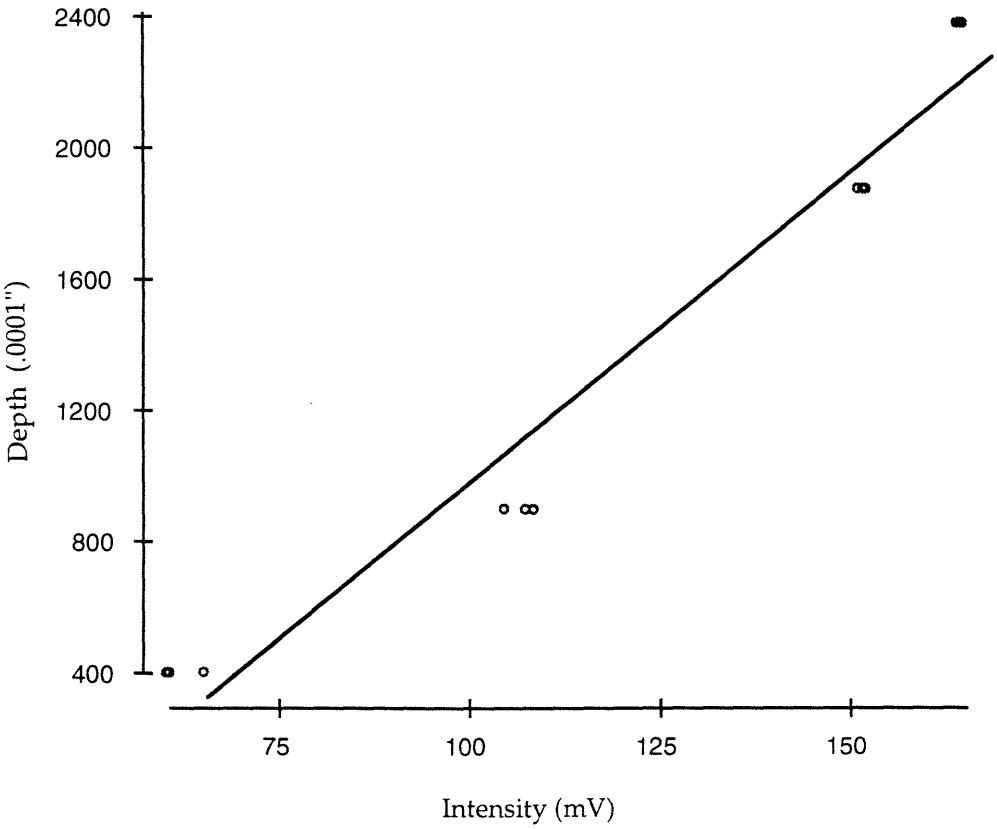

Dependent variable is: depth
R squared = 95.7% R squared (adjusted) = 95.2%
s = 178.0 with 12 - 2 = 10 degrees of freedom

Source	Sum of Squares	df	Mean Square	F-ratio
Regression	7019032	1	7019032	221
Residual	316924	10	31692.4	

Variable	Coefficient	s.e. of Coeff	t-ratio	prob
Constant	-911.318	162.9	-5.60	0.0002
t161	18.9664	1.274	14.9	≤0.0001

Figure 22. Line fit and regression data for deep steps and a dye concentration of .016 mg/ml.

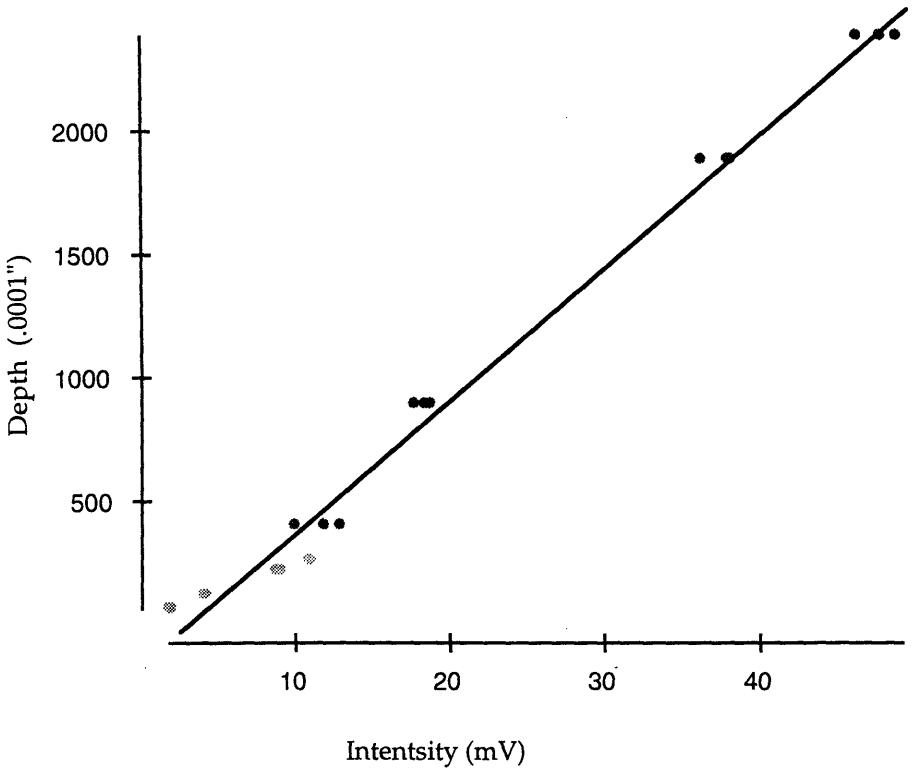

Dependent variable is: depth
R squared = 98.6% R squared (adjusted) = 98.6%
s = 101.3 with 24 - 2 = 22 degrees of freedom

Source	Sum of Squares	df	Mean Square	F-ratio
Regression	16149206	1	16149206	1573
Residual	225844	22	10265.6	

Variable	Coefficient	s.e. of Coeff	t-ratio	prob
Constant	-163.728	31.48	-5.20	≤0.0001
t011	53.2432	1.342	39.7	≤0.0001

Figure 23. Line fit and regression data for all steps and a dye concentration of .001 mg/ml.

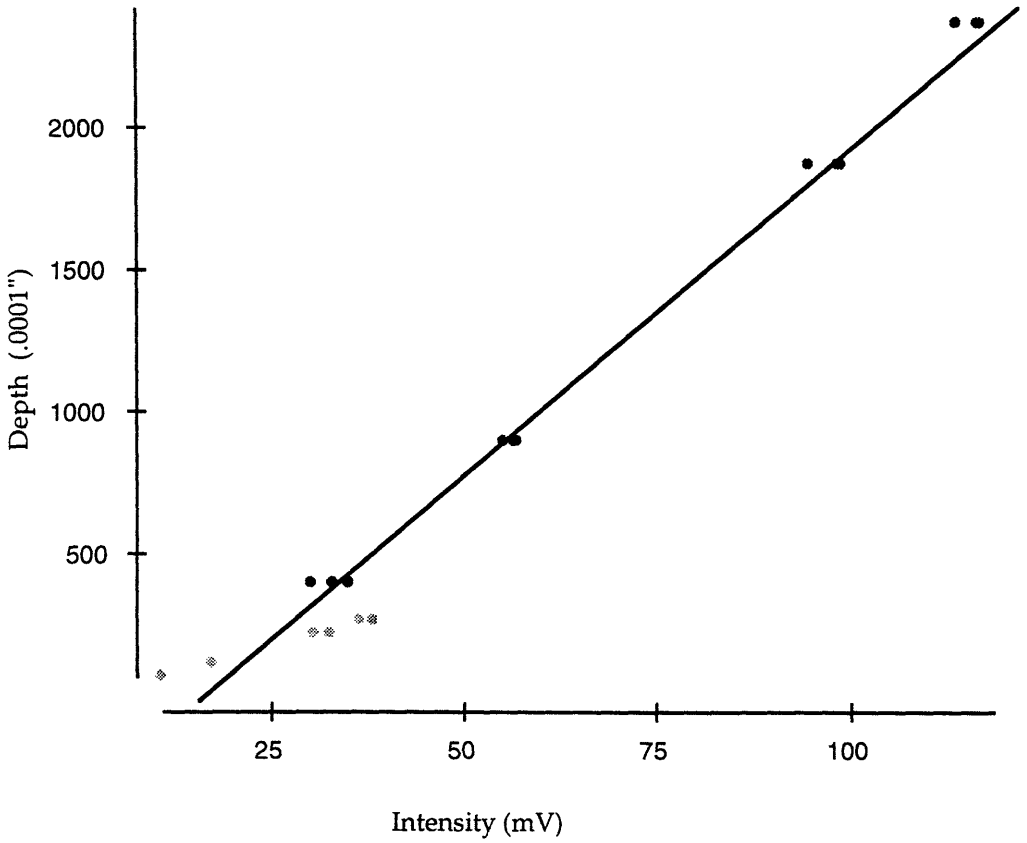

Dependent variable is: depth
R squared = 97.6% R squared (adjusted) = 97.5%
s = 132.4 with 24 - 2 = 22 degrees of freedom

Source	Sum of Squares	df	Mean Square	F-ratio
Regression	15989237	1	15989237	912
Residual	385813	22	17537.0	

Variable	Coefficient	s.e. of Coeff	t-ratio	prob
Constant	-373.506	46.73	-7.99	≤0.0001
t041	23.0424	0.7631	30.2	≤0.0001

Figure 24. Line fit and regression data for all steps and a dye concentration of .004 mg/ml.

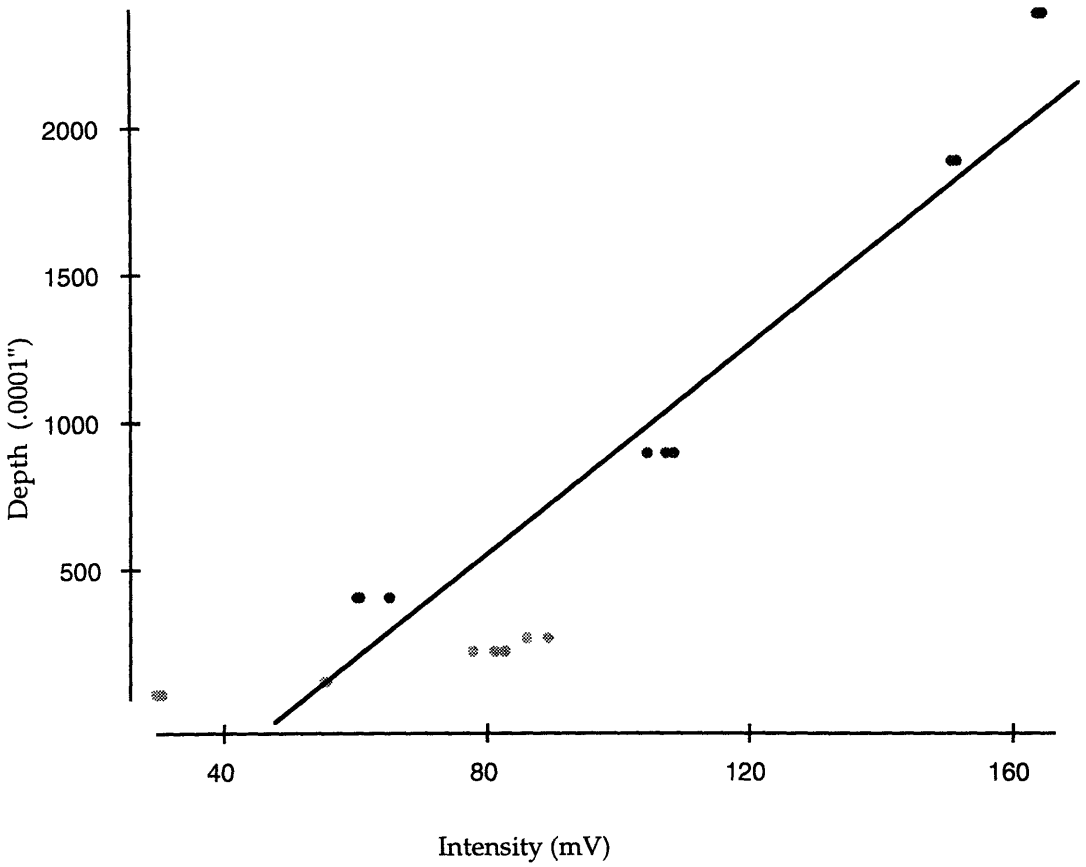

Dependent variable is: depth
R squared = 88.4% R squared (adjusted) = 87.9%
s = 293.9 with 24 - 2 = 22 degrees of freedom

Source	Sum of Squares	df	Mean Square	F-ratio
Regression	14475042	1	14475042	168
Residual	1900008	22	86364.0	

Variable	Coefficient	s.e. of Coeff	t-ratio	prob
Constant	-868.288	140.6	-6.18	≤0.0001
t161	17.7982	1.375	12.9	≤0.0001

Figure 25. Line fit and regression data for all steps and a dye concentration of .016 mg/ml.

Despite this low ratio of 5, a high degree of resolution has been obtained. The tests used to demonstrate repeatability had a resolution of 0.5 %. This percentage represents absolute resolutions of 0.3 mV or 3 microns. The accuracy of the system is not yet at this level. Primarily, positioning problems and the lack of precision specimen holders keeps the accuracy at 5% or 34 microns for a 680 micron part. Sources of error are listed in Table 5. As with the S/N ratio, it is expected that the percent resolution would increase with signal power since the absolute resolution will remain at a fraction of a millivolt.

4.4 REPEATABILITY AND STABILITY

It has been observed that day to day variations in the system are extremely difficult to eliminate. Primarily, the laser power drifts by 0.5 %, and dye concentrations fluctuate. For this reason calibration marks would be used on a production sensor. Areas of known depth would be part of the scan on a specimen holder. The readings from these scans would provide the information necessary to make minor adjustments in the calibration coefficient. To prove the feasibility of this concept, a series of tests were completed.

The tests involved taking readings from two steps sequentially. These two measurements were made with only a one second delay between them. These paired tests were then conducted every three minutes for a 90 minute period. The results are listed in Table 6 and shown graphically in Figures 26 through 28. The absolute data experienced a drift of 3.0% while the ratio between pairings never deviated by more than 0.4% from the group average.

TABLE 5

Equipment	Range of Operation	Error Possible	Error (%)
Laser Power Supply	0 to 115 V	+/- 1 Volt	0.10
20 mW Argon Laser	0 to 20 mW	.1 mW	0.50
Photomultiplier Tube	48 mA/W	.05 mA/W	0.10
PMT Power Supply	-1000 to 0 V	1 V	0.10
Pre - amplifier	+/- 5 V	1 mV	0.01
Pre-amp Power Supply	-12 to 12 V	24 mV	0.10
Analog to Digital Converter	-5.0 to 5.0 V	.2 mV	0.0015
Position of Insert Holder	10 degrees	1 degree	1.00
Position of Rotary Table	360 degrees	1 degree	1.00
Position of Part on Insert	10 degrees	1 degree	1.00
Cumulative Effect			**3.9**

Table 5. Different sources of error in the system.
This method estimates that the system error will be 3.9%. The actual error appears to be approximately 5%.

TABLE 6

Run #	Step 1	Step 2	Ratio 1/2
1	0.0560*	0.0650	0.8752
2	0.0570	0.0640	0.8781
3	0.0570	0.0650	0.8773
4	0.0569	0.0651	0.8741
5	0.0565	0.0648	0.8728
6	0.0570	0.0650	0.8766
7	0.0572	0.0655	0.8733
8	0.0563	0.0643	0.8743
9	0.0564	0.0644	0.8759
10	0.0562	0.0642	0.8753
11	0.0561	0.0640	0.8767
12	0.0559	0.0638	0.8749
13	0.0559	0.0637	0.8764
14	0.0559	0.0637	0.8785
15	0.0560	0.0638	0.8787
16	0.0559	0.0637	0.8789
17	0.0557	0.0635	0.8767
18	0.0559	0.0638	0.8797
Averages	0.0563	0.0642	0.8763

* Intensity represented in mV

Table 6. Data from repeatability tests.
18 tests were conducted and the results are recorded in the table above. Each test has two values. The fluorescent intensity values are represented in mV. These values represent the fluorescence emitted by the fluorescein solution. The ratio of step1/step2 is also provided.

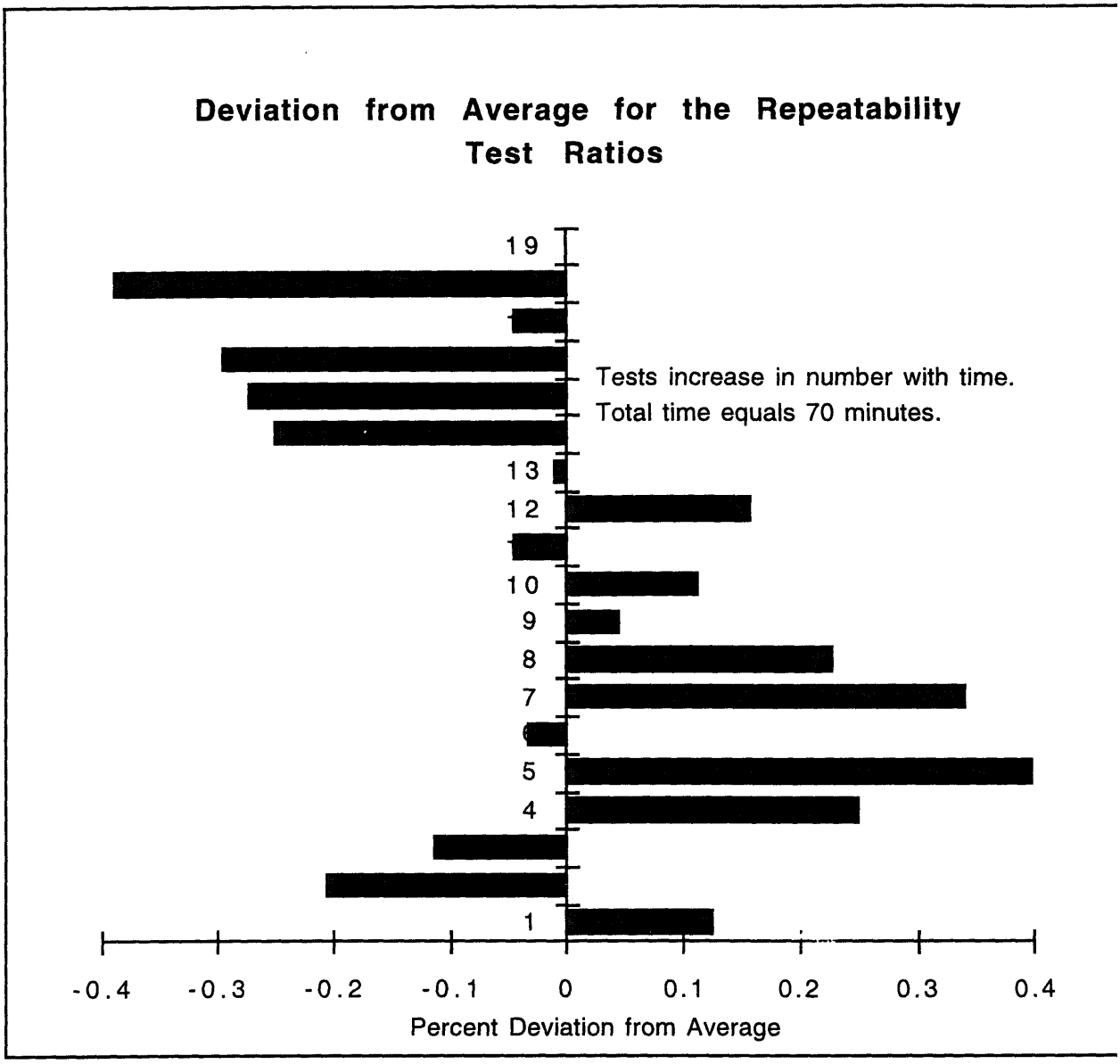

Figure 26. Deviation from average for the repeatability test ratios

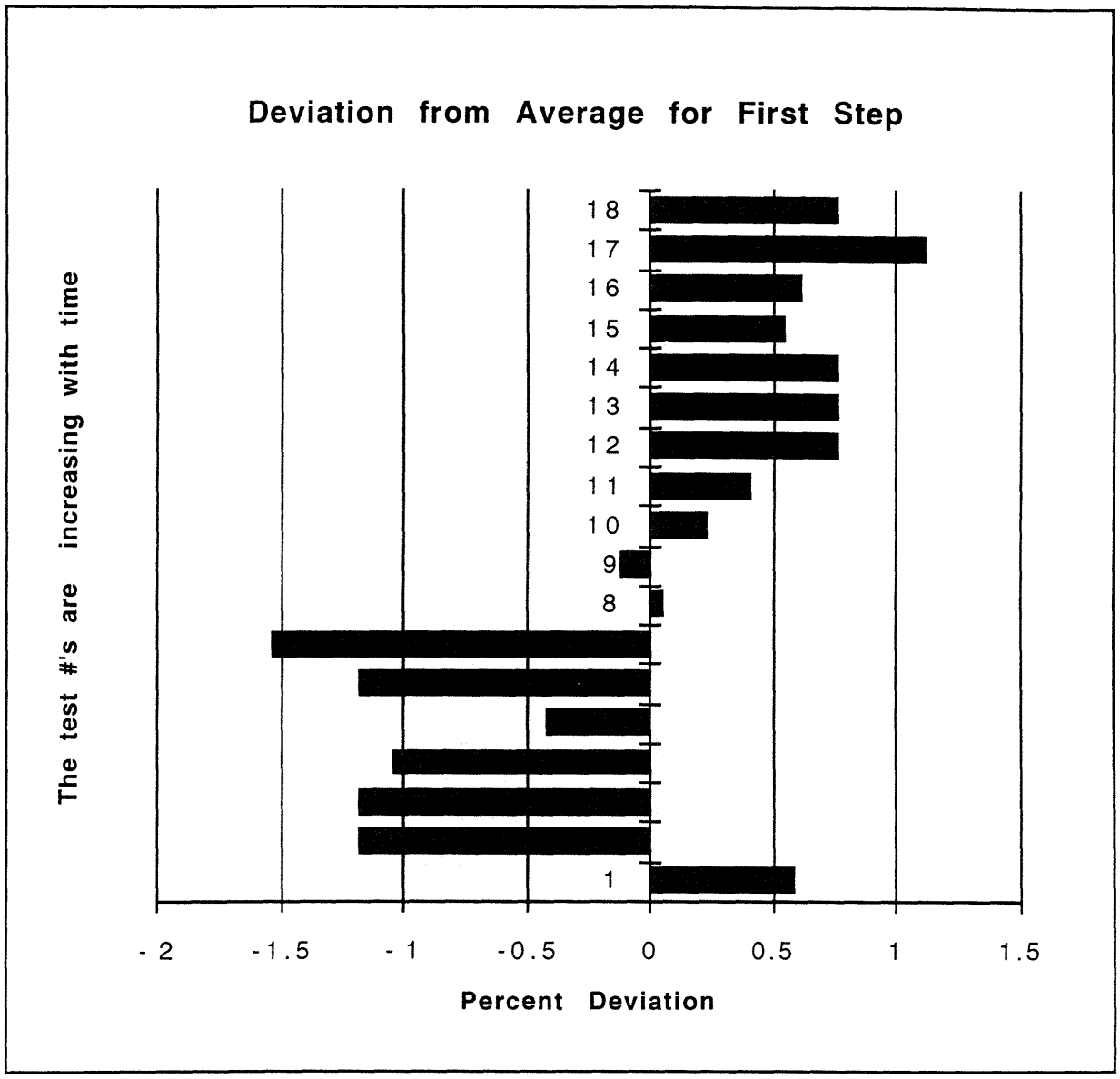

Figure 27. Percent error for measurements taken on the first step of the repeatability tests.

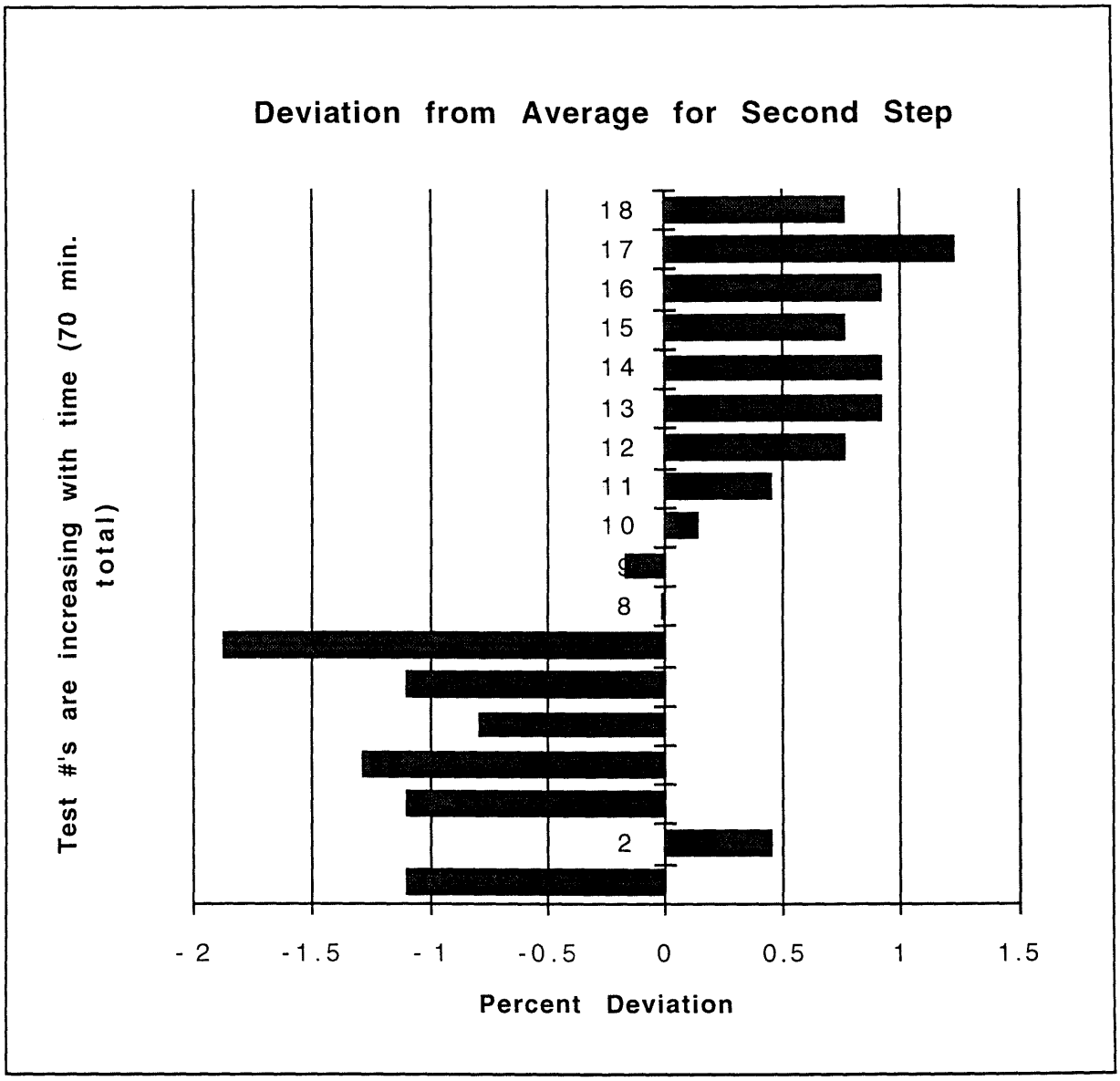

Figure 28. **Percent errors for measurements taken on the second step of the repeatability tests.**

This supports the concept that the correlation coefficient shifts as the system drifts with time, but this shift will be uniform for every point on any given measurement of a part. It is assumed that parts will be measured within 2 to 6 seconds.

4.5 SIMULATION OF PART MEASUREMENT

To simulate the measurement of a part, the third specimen holder was configured as a hemisphere. This hemisphere represents an axially-symmetric, complex product. The holder was then rotated through the scanning beam in 5 degree increments. The entire region constituted a 120 degree span. Each reading was taken over a seven second period with three minutes between each one. To prevent a bleaching of the dye, the signal was chopped during the test and a shutter was closed between tests. The signal was processed by smoothing it and removing values from the peaks formed by the chopping wheel. These values were then averaged to produce a final, scalar value for the reading. This process had a 98.6% confidence band stating that the final value obtained was within 1% of the true median of the data.

For comparison the hemisphere and holder were measured with a Coordinate Measuring Machine (CMM) with a resolution of .0005 inches. Figure 29 represents the data from the CMM, and Figure 30 and Table 7 display the data from three separate scans done with the LIF sensor. Figure 31 shows fluorescent intensity versus depth of solution with accompanying regression information. The statistical analysis yields an R^2 value of 71.0 for all data points and a value of 88.7 if the data are separated by region. It appears

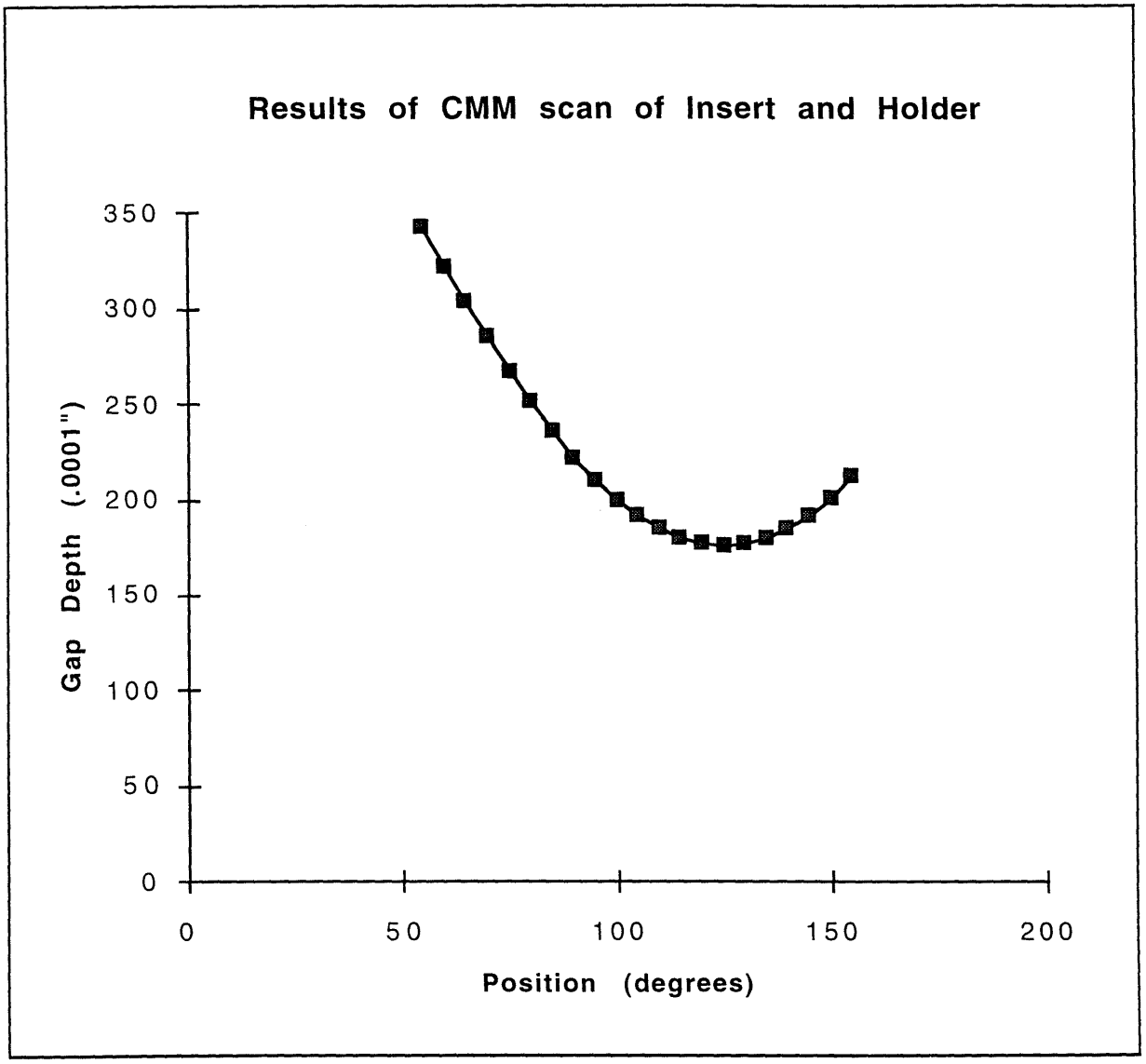

Figure 29. **Scatter plot representing the CMM data for the rotary specimen holder and insert.** Data depict the gap between the hemisphere and the holder wall for a horizontal cross-section across the middle of the hemisphere. This is also the depth of solution that will be present.

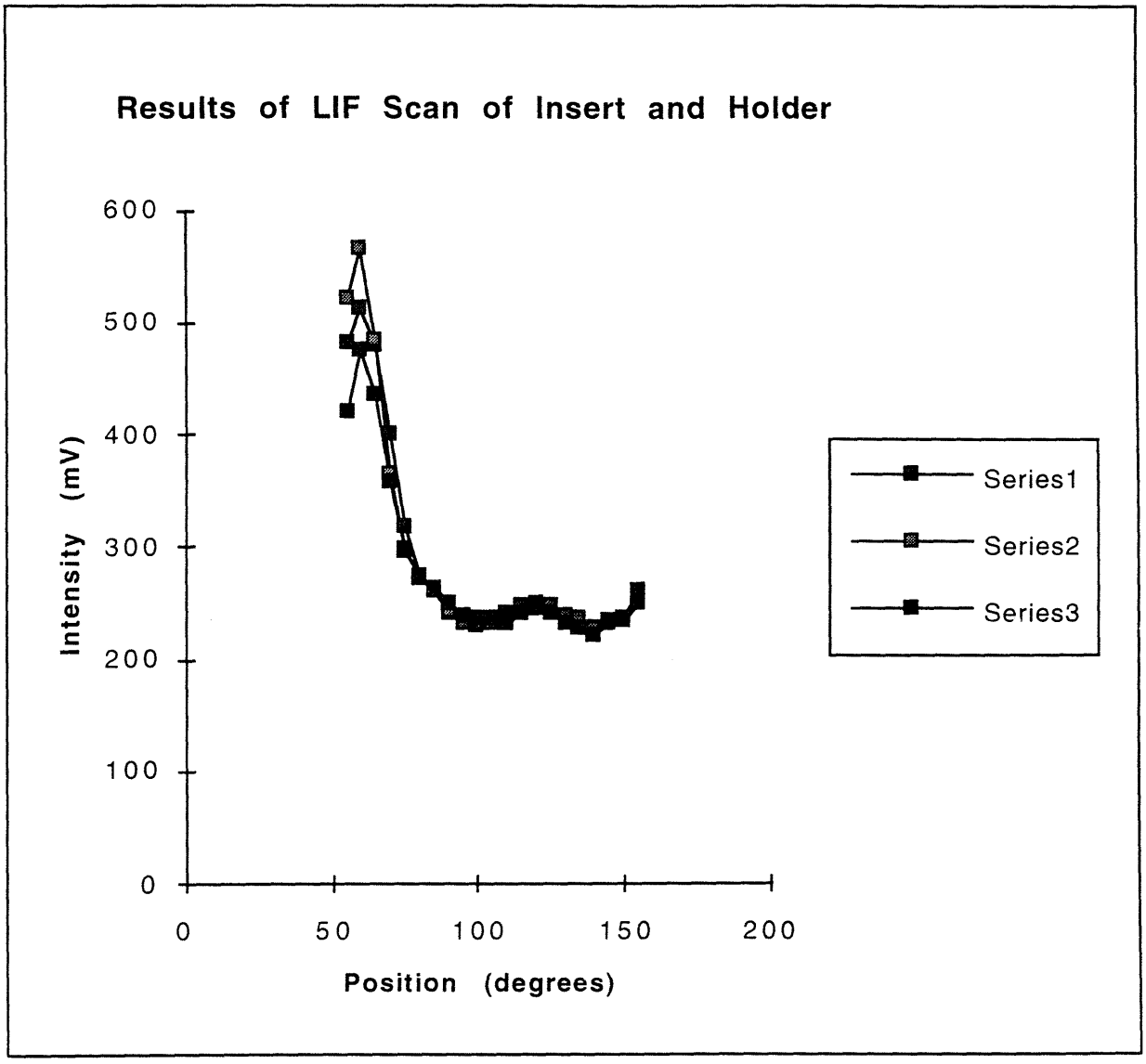

Figure 30. Scatter plot representing the LIF data for the rotary specimen holder and insert.
These data depict the intensity of the fluorescence emitted by the solution appearing in the gap between the hemisphere and the holder wall.

TABLE 7

Position (Degrees)	Depth of Solution (.0001")	run'1' (mV)	run'2' (mV)	run'3' (mV)
55	343	481	521	421
60	322	513	566	475
65	303	480	485	436
70	285	401	365	359
75	267	318	298	296
80	251	275	272	274
85	236	262	260	264
90	222	242	244	251
95	210	232	233	239
100	200	230	230	236
105	191	234	232	237
110	185	241	232	236
115	180	247	241	241
120	177	251	248	246
125	176	245	247	241
130	177	238	239	232
135	180	234	237	227
140	185	227	228	222
145	192	233	234	232
150	201	237	234	234
155	212	262	250	252

Table 7. Data from the CMM and LIF scans for the rotary insert and holder.

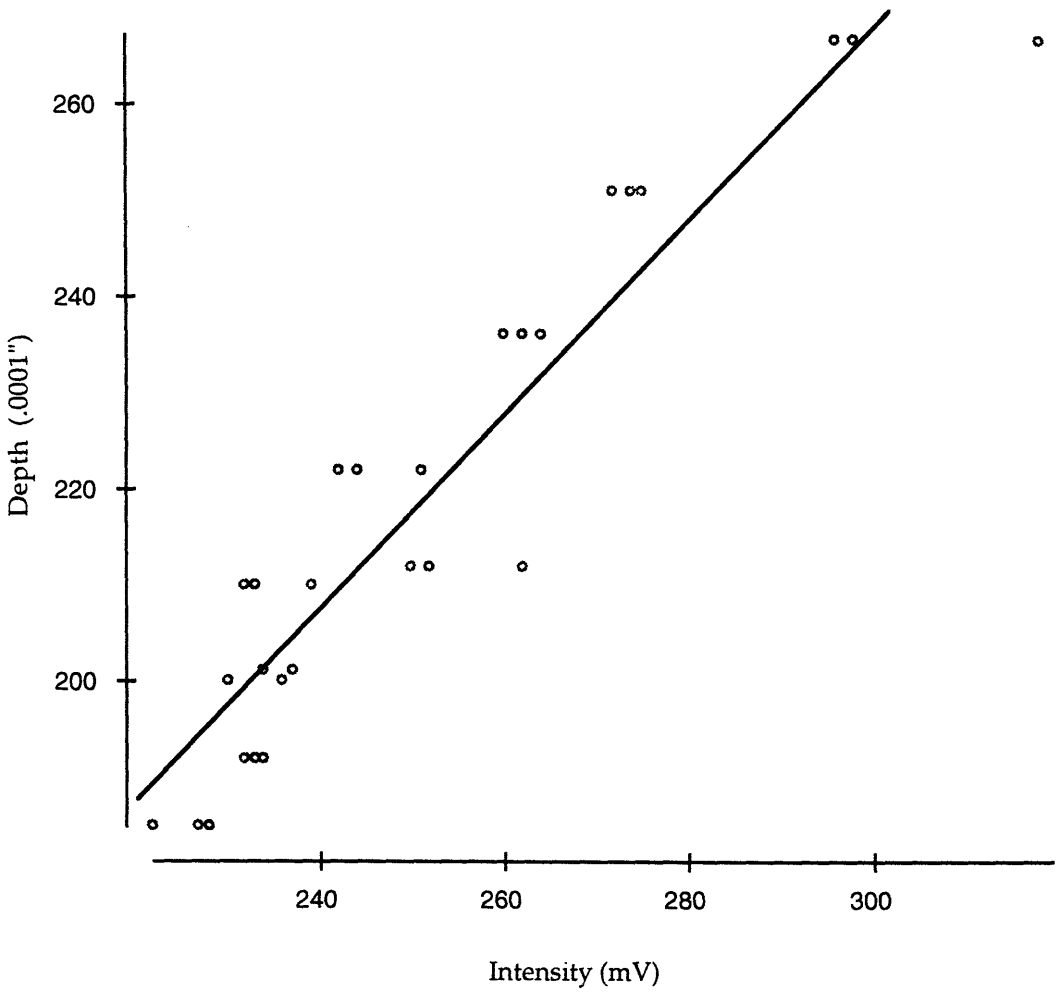

Dependent variable is: Depth
R squared = 88.7% R squared (adjusted) = 88.3%
s = 8.755 with 30 - 2 = 28 degrees of freedom

Source	Sum of Squares	df	Mean Square	F-ratio
Regression	16773.0	1	16773.0	219
Residual	2146.20	28	76.6502	

Variable	Coefficient	s.e. of Coeff	t-ratio	prob
Constant	-34.5317	17.12	-2.02	0.0534
Intensity	1.00839	0.0682	14.8	≤0.0001

Figure 31. Line fit and regression data for LIF scans vs. the CMM measurements.
The edge readings for the first four positions have been omitted since it is believed these points are affected by scattering.

that the curved surfaces provide unique reflectance or distortion characteristics at each point. This is explained by the fact that taking readings further to the side allows some solution excitation from the other side of the holder to be recorded. Transparent materials were selected for this holder to minimize reflectance and local heating problems. Production models will have to look at optimizing material selection for different types of products to be measured.

5. CONCLUSIONS AND FUTURE RECOMMENDATIONS

5.1 CONCLUSIONS

The goal of this research was to analyze the feasibility of using a LIF system as an on-line sensor. This goal was achieved by quantifying several key attributes. A summary of these results follows.

1. Signal to noise ratios were 5 to 10 with evidence that these could be increased to 50. There was also good success with processing these signals to achieve suitable resolutions.

2. Resolution levels of 0.3 mV, or 0.5%, were produced. The signal should be able to be boosted to 3 V while maintaining fraction of a mV resolution.

3. Accuracy and repeatability of the system remain at 5%. This is due primarily to presently unsolved errors of positioning and drift in the system. It seems reasonable to expect 1% accuracy if all recommendations are followed.

4. Linearity of the current system was represented by an R^2 value of 99 % This should improve as repeatability of the system increases. This should also improve with the higher precision specimen holders.

This summary of results indicates that an LIF based, on-line sensor is feasible; however, substantial work remains to increase the accuracy and robustness of the system to levels required of an on-line sensor. The following recommendations outline possible improvements.

5.2 RECOMMENDATIONS FOR FUTURE WORK

Although the results obtained from this prototype are promising, the system is not ready to be installed on a factory line. It has been optimized for the current design and requires fundamental improvements to achieve the performance levels required of a production model. These changes involve two distinct areas of the setup. The emitting and receiving optics need higher efficiency levels. Transmittance efficiencies should be improved by a factor of 20. The other key area is the specimen holder. The current holder simulating a part has to many inherent inaccuracies. The following recommendations should achieve the results necessary:

1. Changing to fiber optics would potentially increase the system efficiency by an order of 15. Fiber optics would also add robustness and flexibility making it feasible to put the system on an assembly line.

2. For the prototype, substituting a dichroic mirror for the beam splitter would give the necessary power increase. This would not, however, assist in the conversion to a line-ready instrument. For this reason it is recommended to simply make the transition to fiber optics.

3. Automating the positioning mechanism with an accurate servo-system and creating precision machined part holders would give several advantages:

a. It would reduce the positioning error component from 2.6% to potentially .1% if adequate care is taken.

b. It would make the operation "hands-off" thereby eliminating human error in taking data. This would also allow the system to be self-contained in a light-tight housing. This would eliminate the need for a dark room environment to conduct testing.

c. It would allow the scanning of parts to be completed in a matter of 2 to 6 seconds. This eliminates the potential for drift during tests.

4. Better Photomultiplier tubes can be purchased for higher costs. PMT housings can also be obtained that contain preamplifiers as integral parts. This, along with a better preamplifier power supply, would reduce some of the baseline noise in the system.

5. Linking the final signal to the power of the laser would eliminate inaccuracies due to laser drift. This would increase system repeatability by another 0.5%. This is made possible by having a digital voltmeter take readings from a banana jack provided in the laser housing. This signal is then incorporated in the signal processing.

6. Machining a custom lens spacer for the optics that focus the signal onto the PMT would allow for optimization. This is true because spacer tubes come in one inch increments (3.0" or 4.0") which does not allow for cleanly focusing the fluorescent signal through the final aperture in the reception optics. A custom spacer would increase the transmission efficiency of this subsystem by twofold.

It is believed that these recommendations would increase the performance of this sensor to a level where it could be effectively modified for on-line inspection. A detailed design and equipment list have been supplied in Appendix A providing the essential information needed to convert to fiber optics.

The preliminary results from this research are positive. The system has a resolution of 0.5 microns for 100 micron parts. Indications are that improvements suggested above will enable the system to have absolute measurement accuracies on the order of 1%. Also, the cycle-time constraint of 2 to 6 seconds appears to be no problem for this method. All of these factors suggest that this technology has great promise for on-line inspection of small, non-rigid parts.

REFERENCES

1.) Kalpakjian, J., Manufacturing Engineering and Technology, Addison-Wesley Publishing Company, Reading, MA, 1992.

2.) Hogg, R., Applied Statistics for Engineering and Physical Scientests, Macmilllan Publishing Company, New York, 1987.

3.) Shaw, B.T., Hoult, D.P., Wong, V.W., "Development of Engine Lubricant Film Thickness Diagnostics Using Fiber Optics and Laser Fluorescence.", Sloan Automotive Laboratory, Massachusetts Institute of Technology, 1992.

4.) Hoult, D.P., Takaguchi, M., "Calibration of the Laser Fluorescence Technique Compared with Quantum Theory.", Sloan Automotive Laboratory, Massachusetts Institute of Technology, 1990.

5.) Parker, C.A., Photoluminescence of Solutions, Elsevier Publishing Company, New York, 1968.

6.) Ebbing, D.D., General Chemistry, Houghton Mifflin Company, Boston, MA, 1987.

7.) Optics and Filters, Oriel Volume III," The Oriel Corporation, Strattford, CT, 1990.

8.) Ingles, E.N., "Instrumentation of a Diesel Engine for Oil Film Thickness Measurements using Fiber Optics and Laser Fluorescence," S.M. Thesis, Massachusetts Institute of Technology, Department of Mechanical Engineering, 1991.

9.) Light Sources, Monochromators & Spectographs, Detectors & Detection Systems, Fiber Optics, Oriel Volume II," The Oriel Corporation, Strattford, CT, 1990.

BIBLIOGRAPHY

1.) Blaker, J.W., Geometric Optics, The Matrix Theory, Marcel Dekker, Inc. New York, 1971.

2.) Fowles, G.R., Introduction to Modern Optics, Holt, Rinehart and Winston, Inc., New York, 1975.

3.) Guilbault, G.G., Fluorescence, Theory, Instrumentation, and Practice, Marcel Dekker, Inc., New York, 1967.

4.) Bowen, E.J., Luminescence in Chemistry, D. Van Nostrand Company LTD., London, 1968.

5.) Brown, M.A., McCann, H., and Thompson, D.M., "Characterization of the Oil Film Behavior Between the Liner and Piston of a Heavy-Duty Diesel Engine," Shell Research Ltd.

6.) Hoult, D.P., Lux, J.P., Wong, V.W., "Calibration of Laser Fluorescence Measurements of Lubricant Film Thickness in Engines," Massachusetts Institute of Technology, 1988.

7.) Bliven, M.D., "Oil Film Measurements for Various Piston Ring Configurations in a Production Diesel Engine," Massachusetts Institute of Technology, Department of Mechanical Engineering, 1990.

8.) Billian, S.A., "Advanced Laser Fluorescence Measurements of Lubricant Film Behavior in a Diesel Engine," Massachusetts Institute of Technology, Department of Mechanical Engineering, 1988.

9) Das, P., Lasers and Optical Engineering, Springer-Verlag, New York, 1991

10) Winburn, D.C., What Every Engineer Should Know about Lasers, M. Dekker, New York, 1985.

11.) Lux, J.P., "Lubricant Film Thickness Measurements in a Diesel Engine," S.M. Thesis, Massachusetts Institute of Technology, Department of Mechanical Engineering, 1989.

APPENDIX A: FIBER OPTIC DESIGN

A.1 OVERVIEW OF FIBER OPTICS

Fiber optic cables are commonly used to replace conventional lenses and mirrors thereby alleviating the alignment problems that are inherent to them. The fibers transmit light over distances with little power loss. They have the advantage of the different elements being unified and enclosed; this eliminates the potential for misalignment and contamination. Also, solutions to splitting and joining beams are simplified when using fiber optics. This stems from the ability to bundle individual fibers in different combinations. This feature allows for the combination of emission and reception optics in a single probe solving the positioning problems inherent in measuring small parts.

The actual fibers work by a "total internal reflection" principle. Each fiber has a core made from glass, fused silica, or light transmitting material. The core is then enclosed by a reflective material. This arrangement transmits light by bouncing it through the core over the length of the cable. This phenomenon also dictates that the light must enter and leave the cable within certain angles. Any light that hits the cable at an angle greater than this "acceptance cone" will not be transmitted. This principle is illustrated in Figures A1 and A2. The "acceptance" and "emergence" angles dictate the design of optics used to couple the fibers with other components.

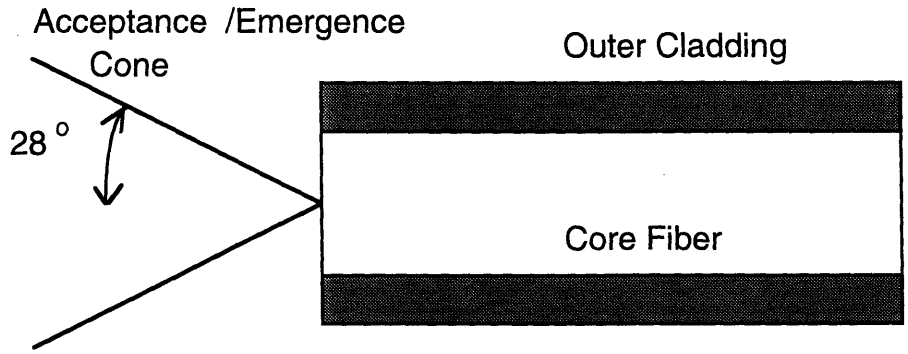

Figure A1. **Displays the acceptance/emergence cone for an optical fiber.**

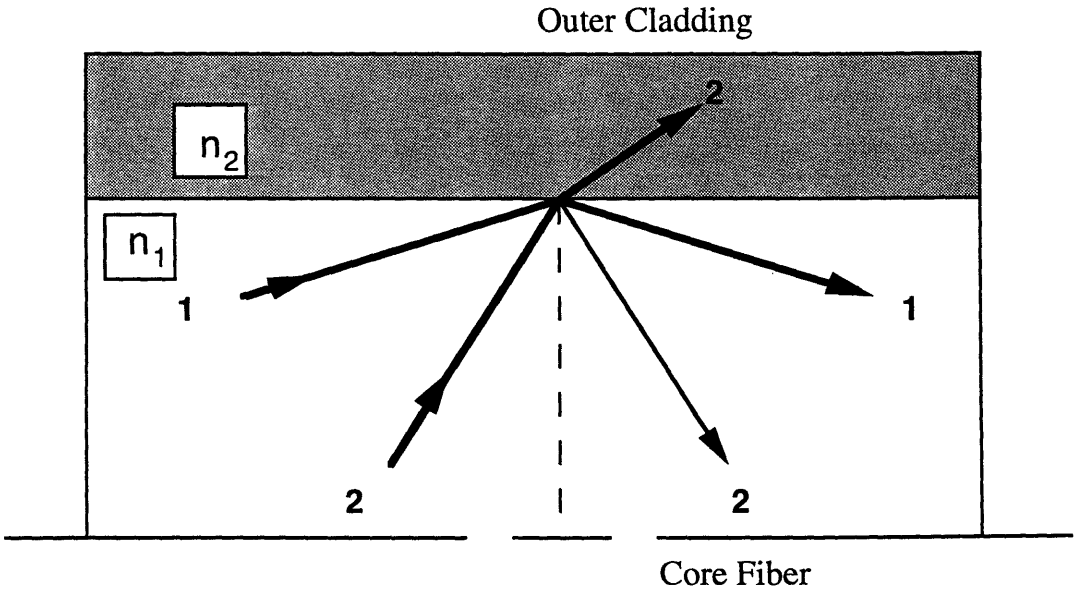

Figure A2. **Displays phenomena which determines the acceptance angle.**

Ray 1 is incident at an angle less than 28°, is completely reflected at the material interface, and is transmitted along the fiber. Ray 2 is incident at an angle greater than the acceptance angle, is refracted into the cladding material, and is not transmitted along the fiber. "n_1" and "n_2" represent two different refractive indices ($n_2 > n_1$).

A.2 RECOMMENDED DESIGN USING FIBER OPTICS

The design has four basic components. A coupler is used to focus the light from the laser into the fiber. The fiber is a bifurcated bundle meaning it has three ends, two individual and one common. A probe is used to focus light onto the specimen and then receive the fluorescent signal from it. And finally, optics transmit the fluorescence from the fiber onto the surface of the PMT. A schematic of the system appears in Figure A3. Table A1 lists the selected specific components.

Eccentric couplers are used to focus the laser beam onto the optical fiber. These couplers are sold as complete units and require little design consideration. One must be sure the coupler selected can accommodate the beam size of a particular laser. Also, couplers with standard SMA termination allow for easy connection of the optical fiber. The coupler chosen for this design is the General Fiber Optics, Inc. model # 85-22.

Ingles [8] conducted a study to determine the best material for the optical fiber selection. He found that a high grade fused silica material provided the best performance. Along with material selection, bundle configuration must be determined. This design makes use of a bifurcated clustering. This arrangement, shown in Figure A4, has a center core and several fibers surrounding it. The core and surrounding fibers each terminate at separate ends and then share one common end. This common end connects to the probe and allows the same optics to be used for emitting the laser light and receiving the fluorescent signal. The cable selected can be purchased from General Fiber Optics, Inc. as model # 2B16-50/100-2.5-SMA.

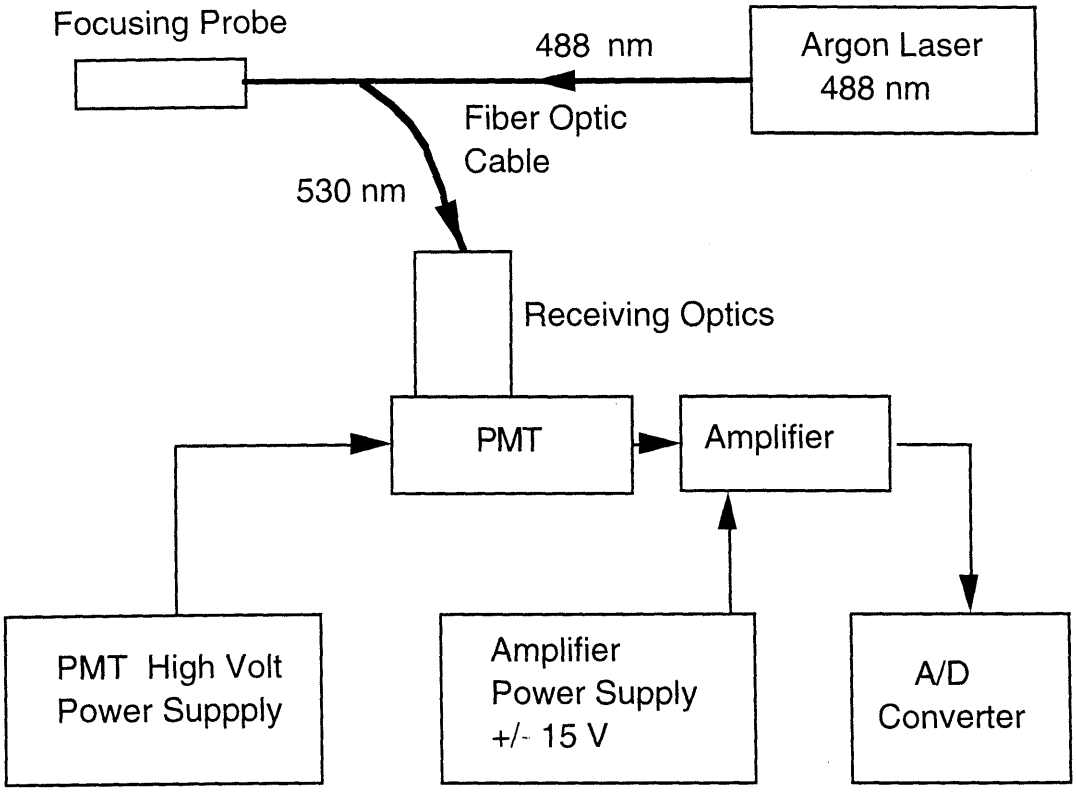

Figure A3. Schematic of fiber optic design.

TABLE A1

Equipment	Company Specifications
General	
Argon Ion Laser 20 mW	Omnichrome
Laser Power Supply	Omnichrome
Surge Supressor	Isobar 50F813 - 12 outlets
Optical Fibers and Coupler	
Eccentric Coupler	General Fiber Optics, #85-22
Bifurcated, Silica Optical Bundle (1m length)	General Fiber Optics, # 2B16-50/100-2.5-SMA
Optics	
Focusing Probe w/ Lens	Oriel #'s: 77646 & 41250
Male flange fiber bundle holder	Oriel # 77817
Lens and Filter Holders	Oriel # 7123 (5 x)
Collimating Lens	Oriel # 41330
Narrow Pass Filters	Oriel # 53874 (2x)
Focusing Lens	Oriel # 41390
Spacer Tube	Oriel # 7132
Aperture and Holder	Oriel # 49165 & 77660
Sensor Equipment	
Photo Multiplier Tube (PMT)	Hamamatsu # R446
PMT High Voltage Power Supply	Sorenson 1006-10
PMT Socket and Amplifier	Hamamatsu # C1053-01
PMT Housing	Custom built, fit Oriel flange & fit Hamamatsu socket

Table A1. Equipment specification for design of fiber optic LIF system.

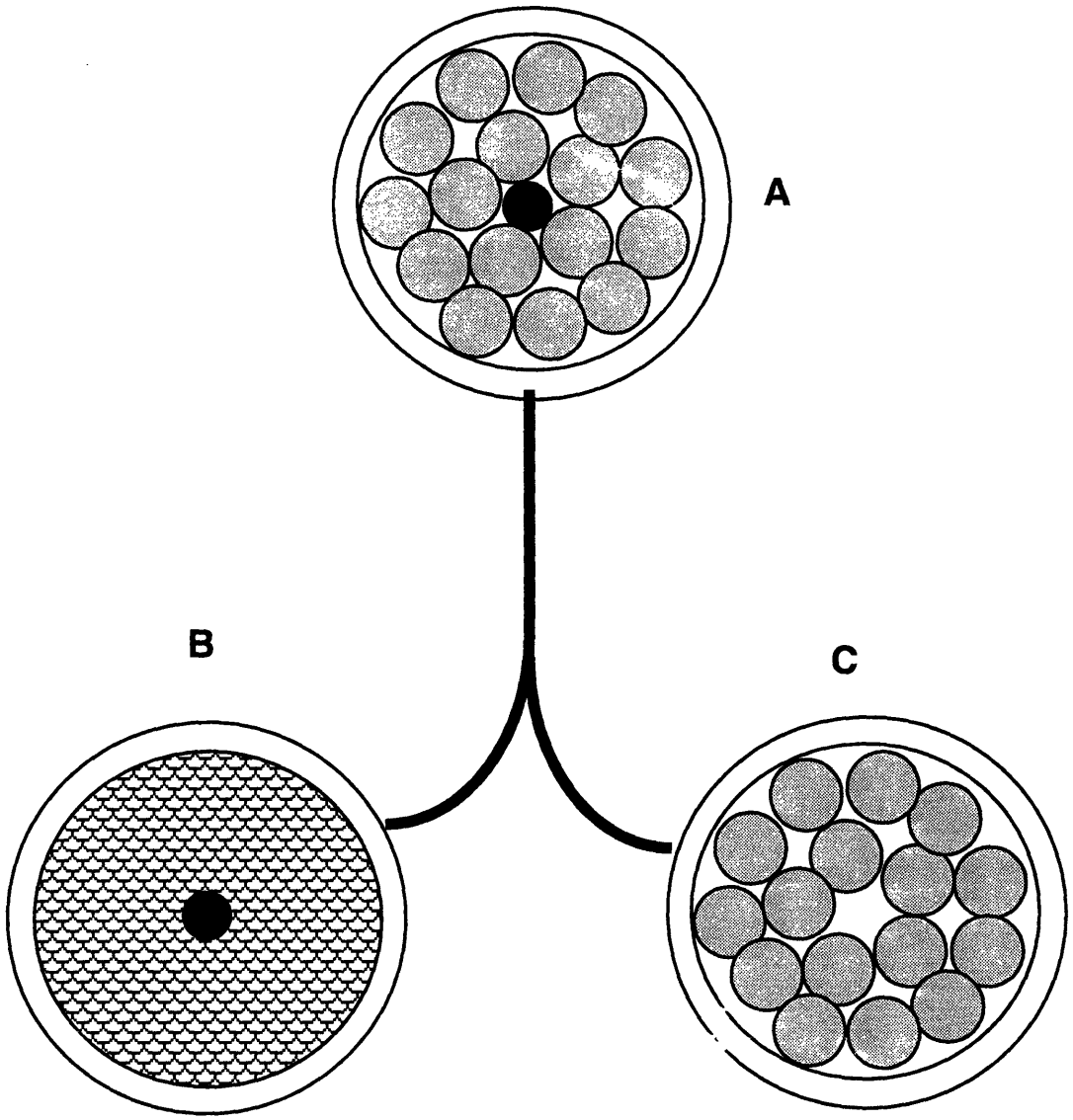

Figure A4. Bundle arrangement for the bifurcated cable. The cable has three ends. The laser is focused on end "B" which is a single, core fiber with á diameter of 50 microns. End "A" is the common end which goes to the focusing probe. The laser light emerges from the core fiber, and the fluorescence is received by the surrounding fibers. These fibers have diameters of 100 microns. End "C" emits the fluorescent signal through the receiving optics to the PMT.

The probe is also purchased as a standard unit. Oriel probe # 77646 has been chosen along with lens # 41250. The lenses used in this probe are fused silica. This probe and lens combination have a focal length of 38 mm. This probe will have to be integrated with future specimen holders which will require some customized machining and design for the probe positioner. The probe from Oriel is displayed in Figure A5.

The reception optics used to focus the signal on the PMT resemble the ones currently being used. A special holder is used to connect the SMA terminated fiber with the standard 1.5" lens holders used in the focusing assembly. Also, a different collimating lens has been selected to account for the emission angle of the optical bundle. The entire assembly can be found in Figure A6.

A.3 GENERAL COMMENTS

The incorporation of fiber optics will provide two main advantages:

1. They will provide the flexibility and robustness required to eventually install this system on-line in a manufacturing facility.

2. The bifurcated cables allow for a single probe to be used in emitting the laser light and receiving the fluorescent signal. This will solve positioning problems when designing the next specimen holder. It will also eliminate the need for a beam splitter which adds complexity and inefficiency to the system.

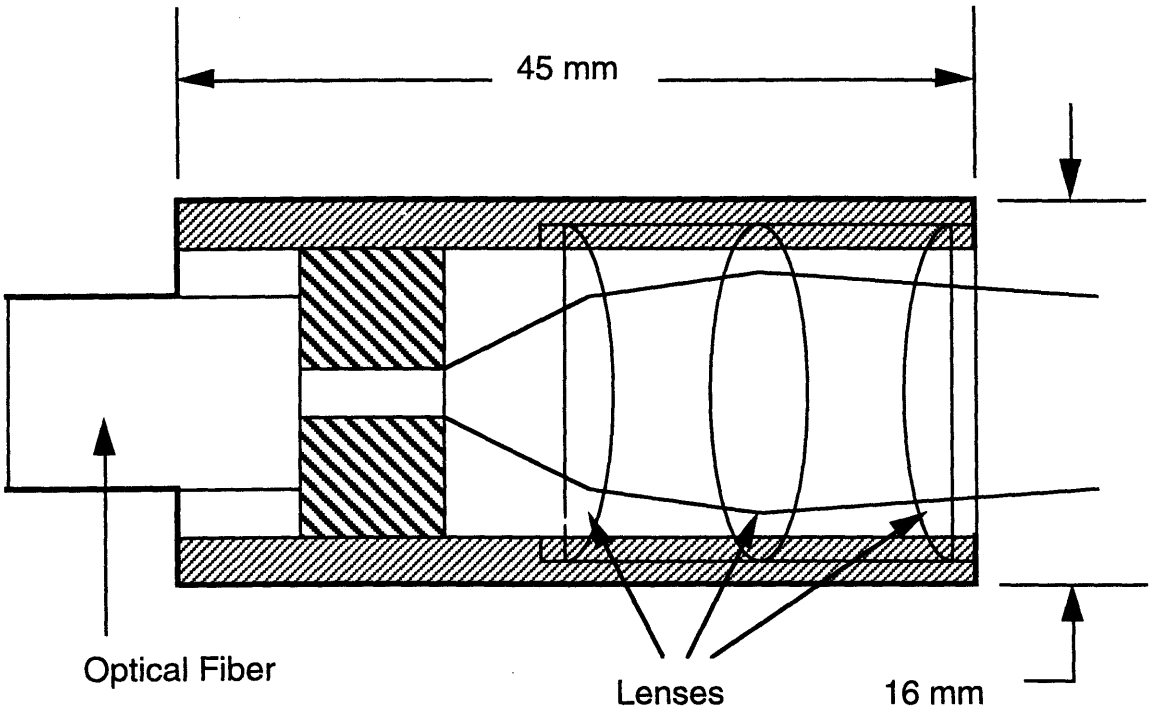

Figure A5. Focusing probe.
This probe can be purchased from Oriel, part #'s 77646 and 41250. The part #'s refer to the probe and the second focusing lens respectively. The optical fiber bundle attaches to the back of the probe using a standard SMA terminal.

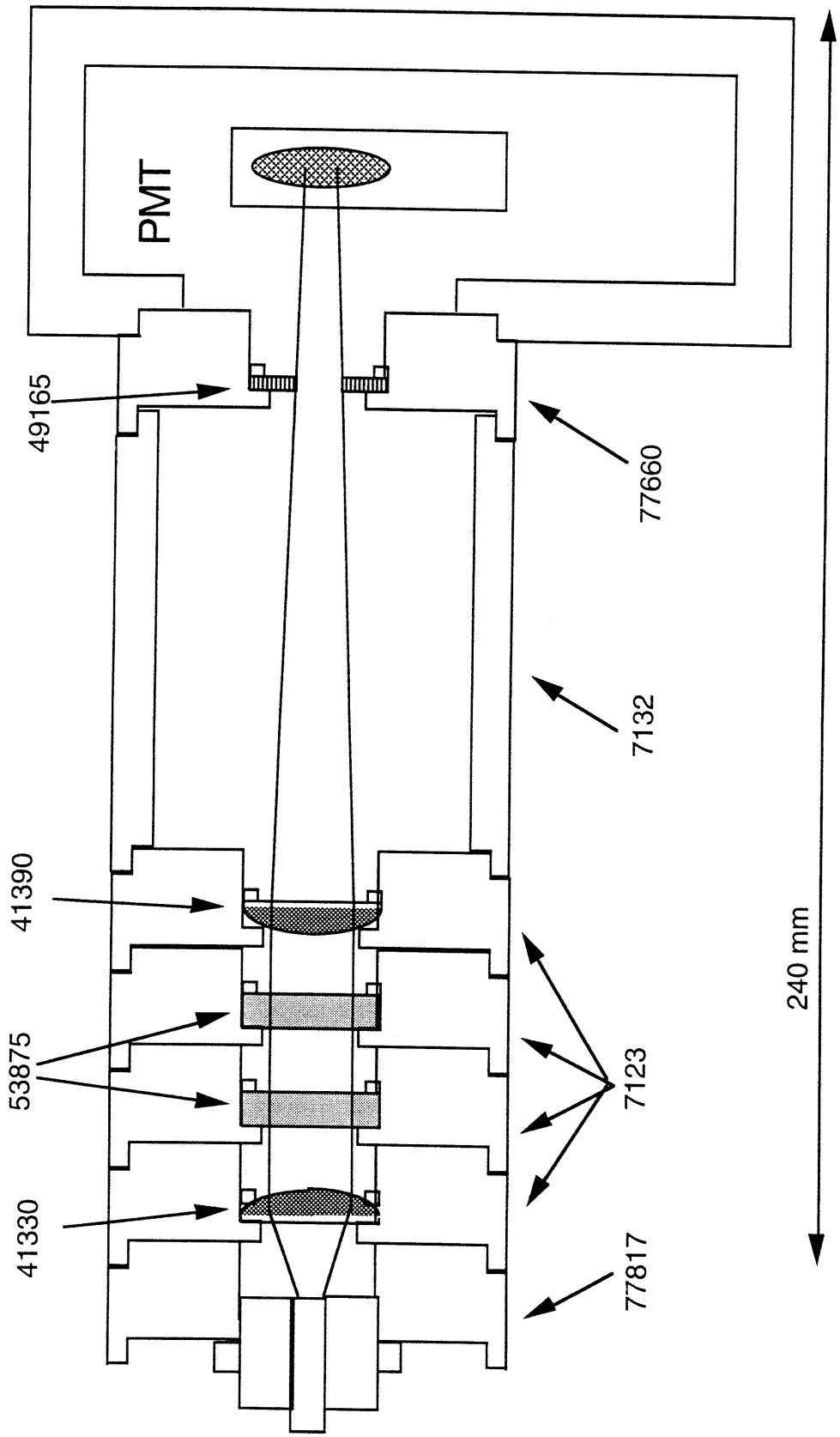

Figure A6. **The reception optics for the fiber optic design.**

APPENDIX B: OPTICAL ALIGNMENT

Aligning the optics is a simple process, but it requires care and patience. The following steps outline the procedure used for a typical system. Each setup will have unique features that may require special care.

1. The first step is to obtain all the components specified in the optical design. These parts should then be positioned roughly according to the specified focal lengths and calculations. This positioning includes bolting all the rails to the optical table and hand tightening all the lens and filter holders to the rails.

2. An alignment of the system is then performed sequentially. The divergent lens is adjusted vertically and horizontally until the laser beam is centered.

3. It is then noted where the beam strikes the second lens. It is probable that this alignment will not be correct. This is corrected using two adjustments. The second lens is moved horizontally and vertically to guarantee that the lenses are in line. One can then fine tune the pitch and yaw of the divergent lens to bend the beam onto the center of the second lens.

4. This procedure is then repeated for each lens in the setup. Placing a white piece of paper in the optical path is an easy technique used to check the beam entering or leaving any lens.

5. Separating the PMT housing from the lenses allows one to observe if the light is hitting the photo cathode. This is accomplished by again placing a piece of paper where the front of the PMT would be located. Care should be taken in observing the size of the focused beam on the paper. Referencing the technical data on the PMT will give the effective size of the photo cathode. All light should be falling within the described area.

6. This completes the rough alignment of the optics. The fine adjustment requires that the entire system be turned on and solution is placed in a specimen holder. A signal should now be observable using an oscilloscope or data acquisition system.

7. Each component is again adjusted in turn beginning with the diverging lens. The component should be rotated to maximize signal strength. By observing each piece in this manner, the system can be fine tuned to provide optimal performance.

8. This process should be completed by securing all bolts and finger screws. Positions of all the components should be recorded and markings should be placed on the mounts to give quick reference points.

APPENDIX C: TEST PROCEDURES

Three separate testing schemes were used in evaluating this system. The inspection of the step specimens to determine calibration coefficients used a non-chopped signal and evaluated each point sequentially. The dual tests used to prove the feasibility of calibration markings also used an unchopped signal but took pairs of tests on each scan. Finally, observations of the rotary holder made use of a chopped input and sequential observations of each point. These tests all shared a common preparation of the system and then varied in length of test and some other particulars.

C.1 GENERAL SETUP

1. Turn the equipment on two hours prior to any testing. This includes the laser power supply, the laser, the PMT power supply, and the preamplifier power supply.

2. The settings for these instruments should be observed. Any adjustments necessary should be made. The PMT power supply should be set at -850 Volts. The preamplifier is set to an amplification of 10^4 and is set on the "maximum" time constant position. A digital voltmeter can be used to confirm that the preamp power supply is producing a +/- 12 Volt signal.

3. After two hours have passed, the system will have stabilized. At this time a power meter should be used to confirm that the laser head is emitting a 20 mW signal. The light intensity at the specimen

should also be confirmed. Values of at least 0.5 mW for intensity reaching the specimen should be observed.

4. The actual testing that would now take place is unique to each different set. These details are outlined in the next three sections.

5. After the testing is complete, all components should be turned off except for the laser power supply. This will allow the cooling fan to continue operating. Approximately 3-5 minutes is sufficient to cool the laser at which time the power supply should be turned off.

6. At the end of a testing session, the specimen holder used is cleansed with distilled water. It is then dried and stored.

7. Double checking to be certain nothing has been left operating and that all covers have been replaced over the optics completes the testing procedure.

C.2 STEP TEST SPECIMENS

1. Filling the specimen with solution constitutes the first unique step for this procedure. It is assumed that the particular step specimen and dye concentration have already been selected.

2. A microscope slide is then placed over the specimen holder. This is done in such a manner that the excess fluid flows out from the center thereby preventing air bubbles.

3. It is next important to wipe off excess solution and inspect for any air bubbles that may have occurred.

4. Assuming that no air bubbles are found, the slide is clamped to the holder and the setup is wiped again to guarantee that no solution is on the outside of the holder and slide.

5. The specimen holder is then aligned and adjusted to the proper height. This step is done with the laser on. Observing the holder while sliding it through the different positions at this time will confirm that it is aligned properly.

7. At this time the lights are turned out and the "SuperScope™" software is loaded. A previously programmed instrument panel is used. An instrument panel is a program that has preset sampling rates and data processing programs. The data processing programs are detailed in Appendix D.

8. Hitting a button marked "Acquire" activates the data acquisition sequence. This sequence is as follows: the program waits 2 seconds and beeps, it then waits one second and begins acquiring data for 3 seconds, and it then signals that it is finished by beeping.

9. The operator opens the shutter after the first beep. He then waits approximately 4 seconds until he hears the second beep. This will signify that the computer has finished taking data points. At this time the operator should move the specimen holder so that the laser

beam falls in the middle of the next step. He can then close the shutter. It should be remembered that the operator should where optical safety glasses during this operation. These glasses are specific to the 488 Argon Laser. Also, a penlight or flashlight can be used to assist in seeing to make adjustments since the room lights are off during the testing.

10. The operator must now wait three minutes before taking the next sampling. During this time, hitting the button marked "calculate" will initiate the data processing which takes approximately 1 second. After this a note should be made of the specimen position. This is done in an on-screen journal where the results of the data processing have already been transferred automatically.

11. After waiting three minutes, the operator can begin another scan by hitting the "Acquire" button. Steps 8 to 10 are now repeated.

12. Sampling of an entire step specimen should be completed by saving and printing a copy of the journal that holds the test results.

13. The system should then be shut down and the specimen holder cleansed. A quick check of the data should be made to be sure no problems have occurred during the testing.

C.3 REPEATABILITY TESTING

1. The repeatability testing uses steps 1 through 8 of the step specimen routine.

2. The acquiring of data follows a different pattern and uses a separate instrument panel designed for this test. Hitting "Acquire" in this program will initiate this sequence.

   2.1 The computer will beep acknowledging that a program has been initiated.

   2.2 It will then wait 2 seconds and beep again. This is the cue for the operator to remove the shutter from the system.

   2.3 The sampling period is 6 seconds long. This allows a 2.75 second sample to be taken on the first point. The operator then has 0.5 second to move the holder to a second position. A 2.75 second sample is then taken of this position. Physical stops allow the repositioning to be done in one tenth of a second. This provides a margin of error on the timing of moving the holder.

   2.4 After the 6 second sampling period occurs, the computer will beep signifying that the program has finished. The operator replaces the shutter at this time and returns the specimen holder to the first position.

3. The operator now has three minutes before the next test. This time allows him to hit the "compute" which initiates the data analysis. The results of this analysis are transferred automatically to the on screen journal.

4. Once all tests have been taken, in approximately 90 minutes, the results in the journal can be saved and printed.

5. The equipment can then be shut down, and the specimen holder can be cleaned.

C.4 ROTARY TESTING

1. The insert is first placed into the specimen holder. Figures of these parts have been provided. A steel pin locks the location of the insert with respect to the holder.

2. Solution is then dripped in the holder from the top. This is done using an eye dropper. Approximately 3 ml of solution are required. Care should be taken in observing that no air bubbles form.

3. The holder is then placed in the rotary table. A flat on the stem correlates in position to a finger screw on the rotary table. Marks on the holder and table are used to assure alignment. A customized spacer determines the height of the holder.

4. Once alignment has been completed, the lights are turned off, and the rotary "SuperScope™" program can be loaded.

5. With the shutter closed the rotary table is turned to the appropriate position. The base of the table is indexed every degree to assist in this positioning.

6. The "Acquire" button is then touched on the computer screen initiating the sampling program. There is a two second delay built in to allow for the removal of the shutter. The sampling period is then 7 seconds. The wave will appear on the screen denoting that the scan is complete. At this time the shutter is replace.

7. The data processing is then conducted by running the calculation scheme which is detailed in Appendix D. This requires 1 second.

8. The position of the rotary table is noted in the journal with the results which have been automatically placed there.

9. The holder is then moved to the next position. A time interval of 1 minute should pass before taking the next test. This assures that no bleaching is occurring. This time can be shorter than the previous two test schemes because the laser beam is being chopped allowing only 3% exposure time per revolution.

10. After completion of the testing, all equipment is turned off and the specimen holder and insert are cleaned. The results journal is saved and printed. A quick inspection guarantees that nothing abnormal has occurred during the testing.

APPENDIX D: DATA PROCESSING

D.1 DATA PROCESSING

Three distinct programs have been written to process the data from each series of tests: the step tests, the repeatability tests, and the tests using the rotary holder and the hemisphere specimen. Each step in this processing is described for the different series. Figures are provided to assist in the explanation of the operation and to give examples of how the raw and finished data appear on screen.

D.2 STEP TEST

1. An unchopped signal is recorded for 1.5 seconds. Figure D1 shows an example of this and how the results appear after the computations are finished. Figure D2 shows the same wave on a different time scale allowing more detail to be seen.

2. The first data processing step is to average the signal over a 10 point span. This effectively gives an average signal for a 200 ms time period. A smoothed signal compared with a signal in raw form is shown in Figure D3.

3. The program then averages all points on the signal. This reduces the wave to a scalar value which is transferred to an on-screen journal. This journal can latter be loaded directly into a spreadsheet for further analysis.

4. The minimum and maximum values, the standard deviation for all the points, and the time are also noted and placed into the journal.

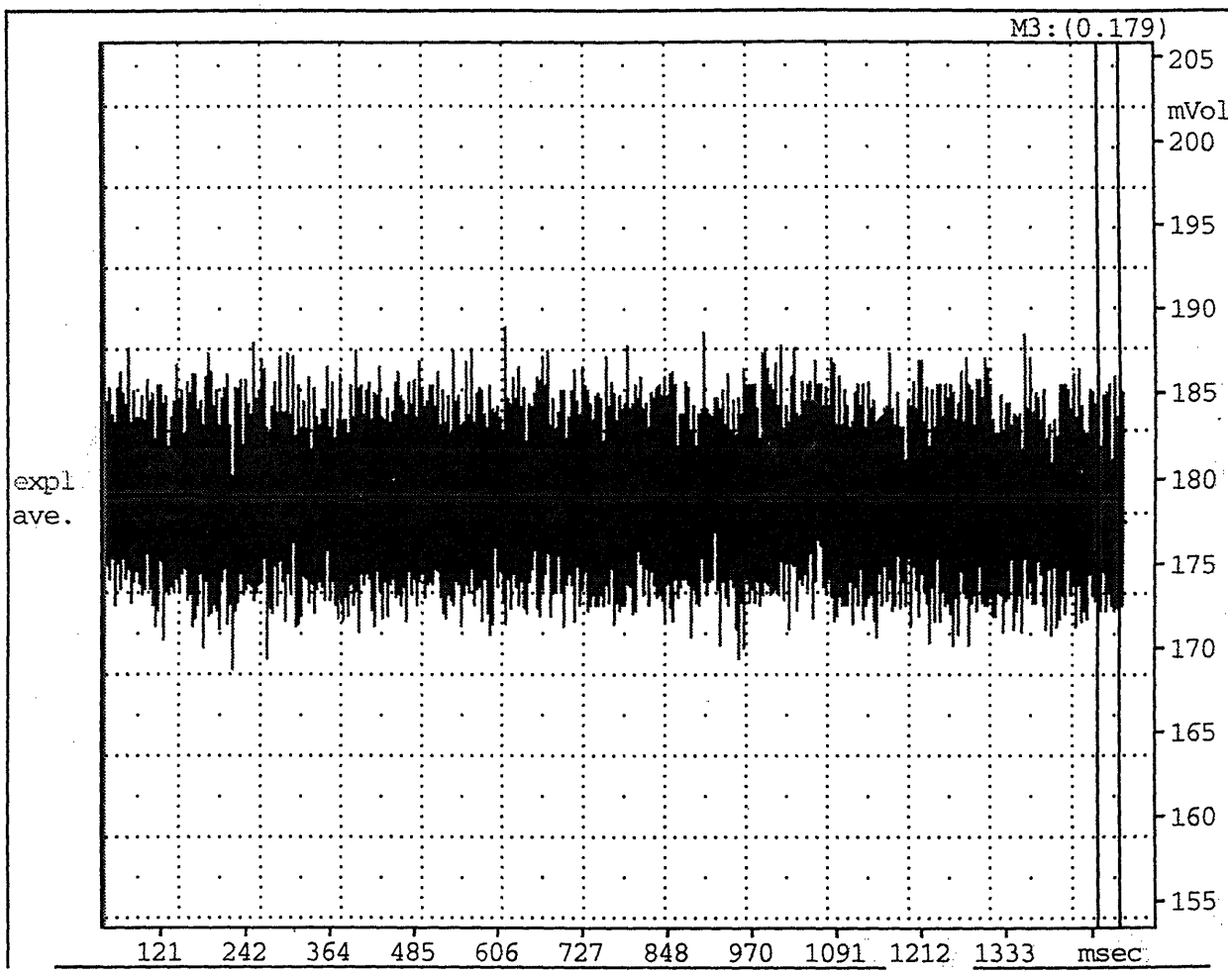

RESULTS

ave.pk value Volt	Seg1 avg Volt	Seg1 min Volt	Seg1 max Volt	Seg1 std dev Volt	Time
0.17886	0.17884	0.171	0.188	2.46e-3	13:28:22

Figure D1. Example of a signal taken from the step tests.

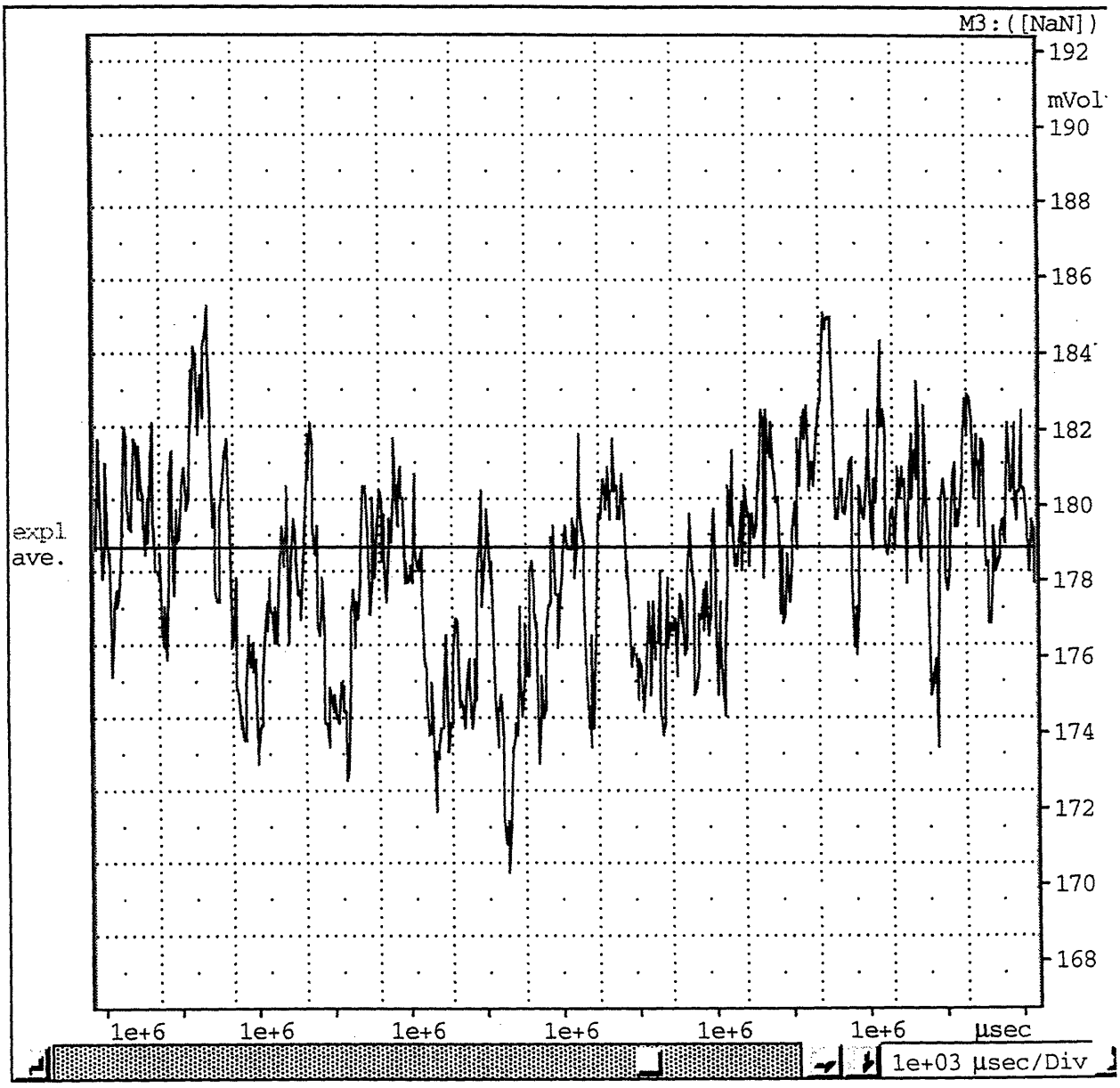

Figure D2. **Basic wave with the time scale adjusted to show more detail.**

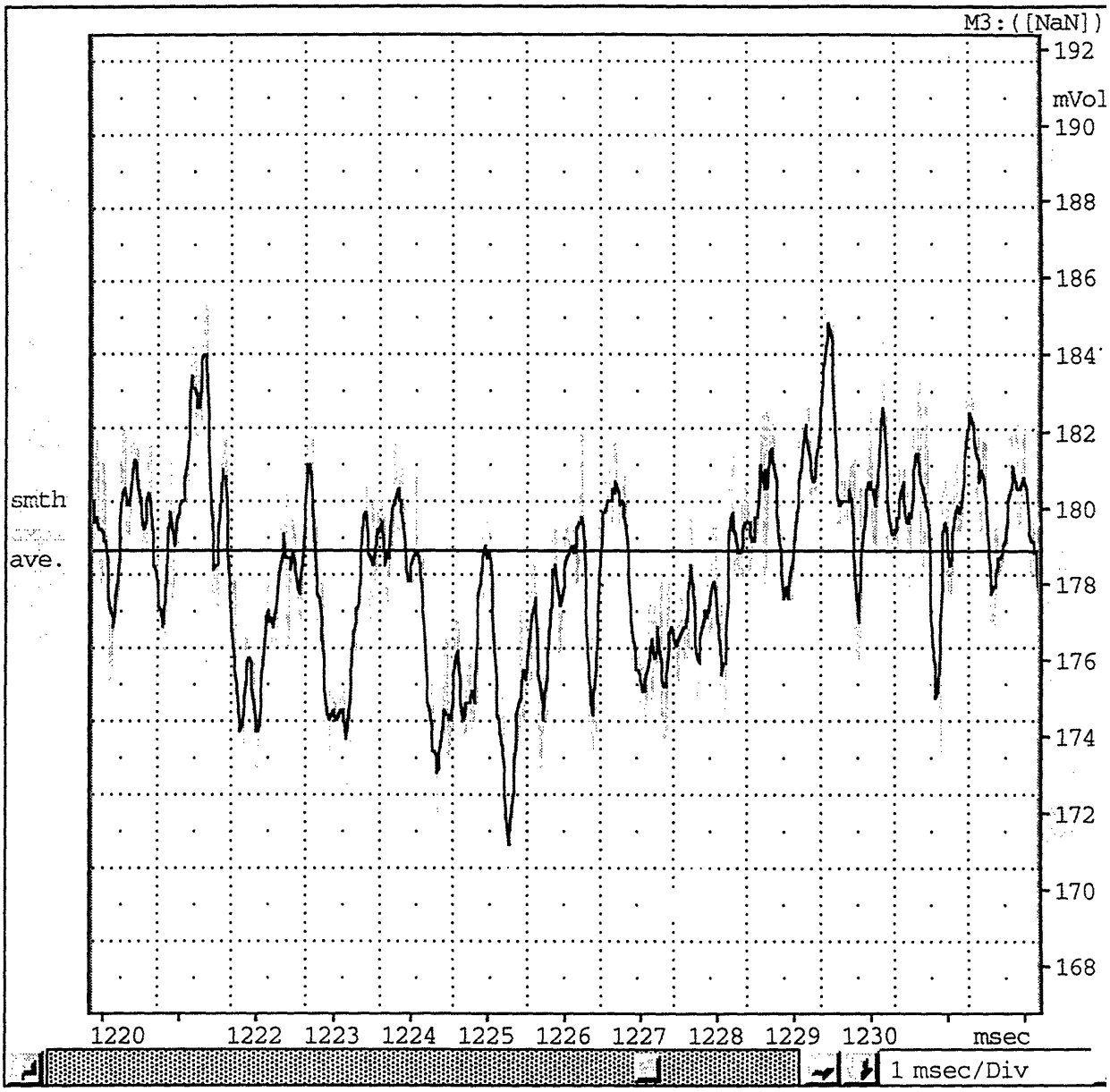

Figure D3. Smoothed version of the original signal.
The smoothing occurs over a 10 point (200 ms) span.

This concludes the data processing of the step specimen data. This method provides micro volt resolution assuming that the dominant noise is random and can be averaged out over 75,000 data points.

D.3 REPEATABILITY TEST

1. An unchopped signal is recorded for 6 seconds. Figure D4 shows an example of this and how the results appear after the computations are finished. Figure D5 gives an enlarged view of the signal that is obtained. It displays the noise range of the signal.

2. This scan is then broken into three regions. The first 2.75 seconds constitute the signal from the first step. The next 0.5 seconds allow for the transition between the two steps. The final 2.75 seconds account for the data used from the second step.

3. A running averages of the first and second sections are taken and the final values of these averages are transferred to a journal.

4. These values are then computed as a ratio and this value is placed next to the averages in the journal. Next to this ratio the time of day is noted.

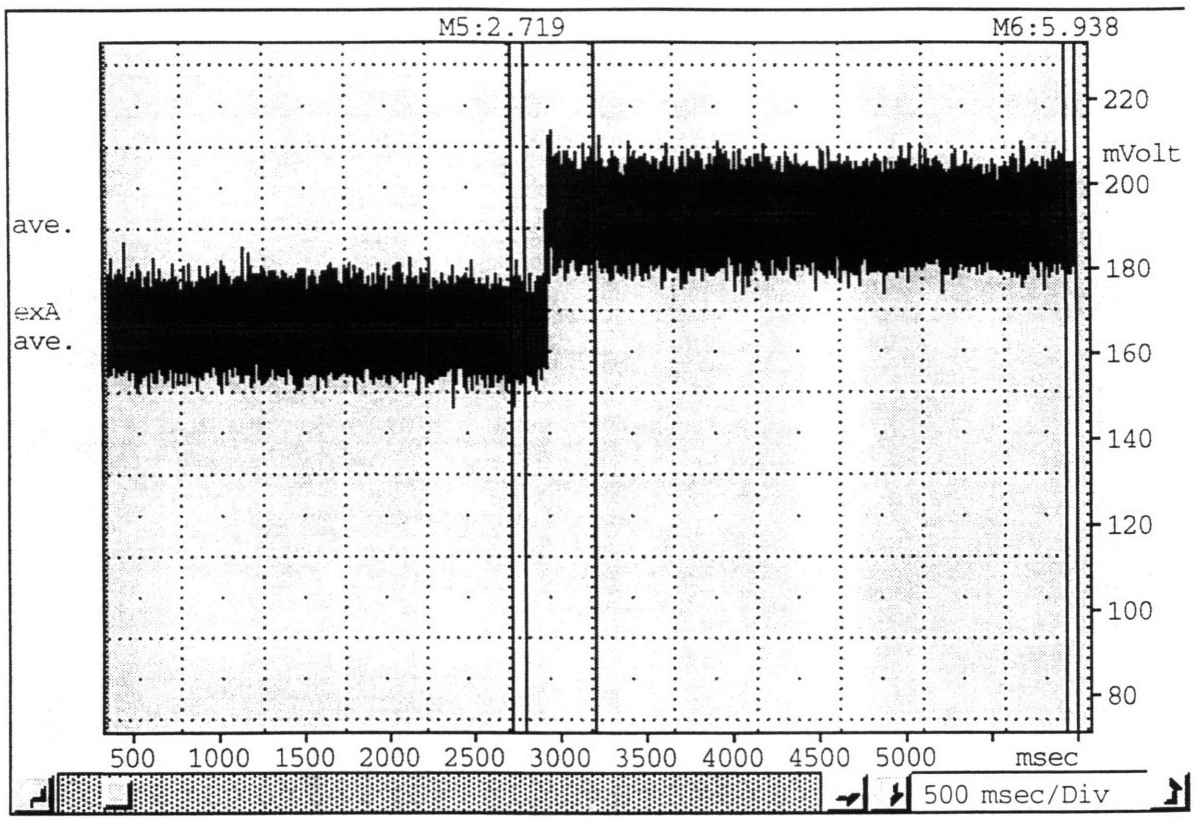

RESULTS

ave.pk value Volt	ave.pk2 value Volt	Ratio	Time
0.16607	0.19212	0.8644374	13:53:04

Seg1 avg Volt	Seg1 min Volt	Seg1 max Volt	Seg1 std dev Volt
0.16605	0.150	0.180	4.15e-3

Seg2 avg Volt	Seg2 min Volt	Seg2 max Volt	Seg2 std dev Volt
0.19212	0.116	0.204	3.90e-3

Figure D4. Example of a signal taken from the repeatability testing.

The results appear in the above format when they are placed automatically in an on-screen journal.

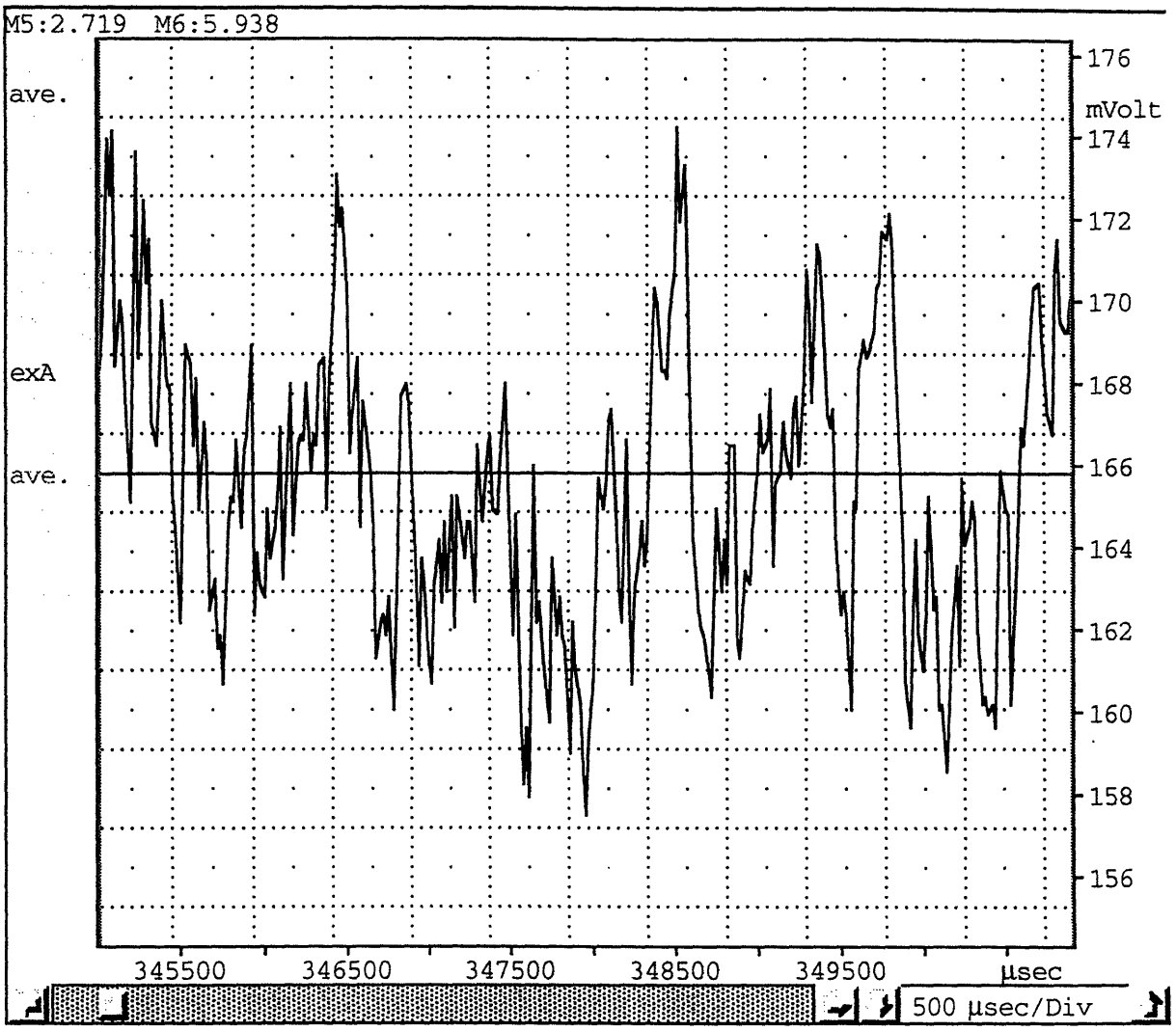

Figure D5. Enlarged view of the wave shown in Figure D4.

5. A series of statistical analysis are then performed on the signal. An average of all points in the segment is then taken and transferred to the journal. This serves as a check against the running average. Minimum and maximum values and standard deviation are also transferred to the journal.

6. The final journal of results can then be transferred to a spreadsheet where the information is further analyzed.

D.4 SIMULATION OF PART INSPECTION

1. A chopped signal is acquired for 7 seconds. Figure D6 shows clearly the signal appearing in the form of short peaks and long valleys. Figure D7 displays only one peak making it easier to see the shape. A closer look at only the peak tip can be seen in Figure D8.

2, The signal is first smoothed over 10 points. This reduces the impact of any outlying points. The result of this smoothing is shown in Figure D9

3. Analysis is then performed on each peak in the signal. The maximum value is determined for each wave. These points are then put together to form a signal that essentially skips across the peaks. This gives a continuous signal that can be further analyzed. Figure D10 depicts this "peak" signal.

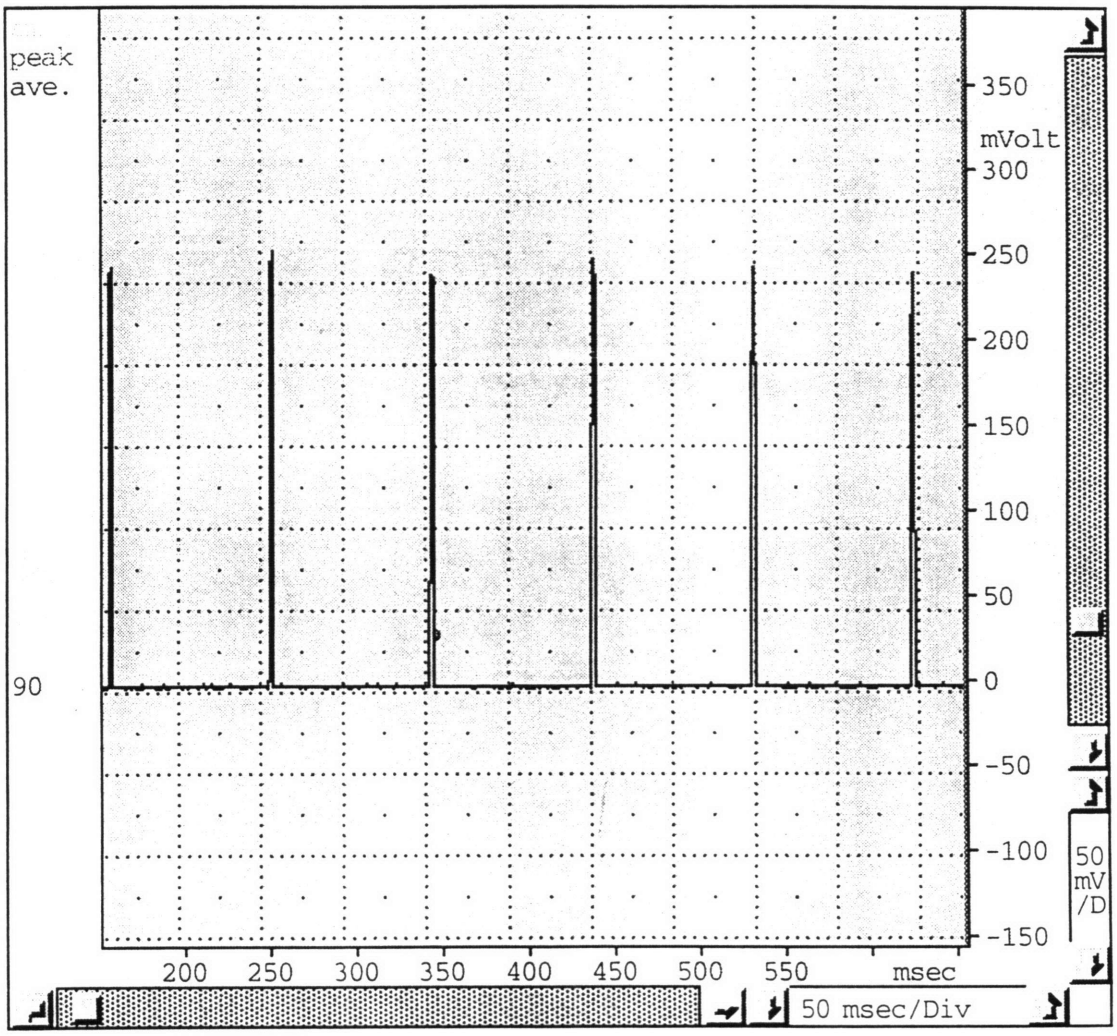

Figure D6. **Section of a chopped signal.**

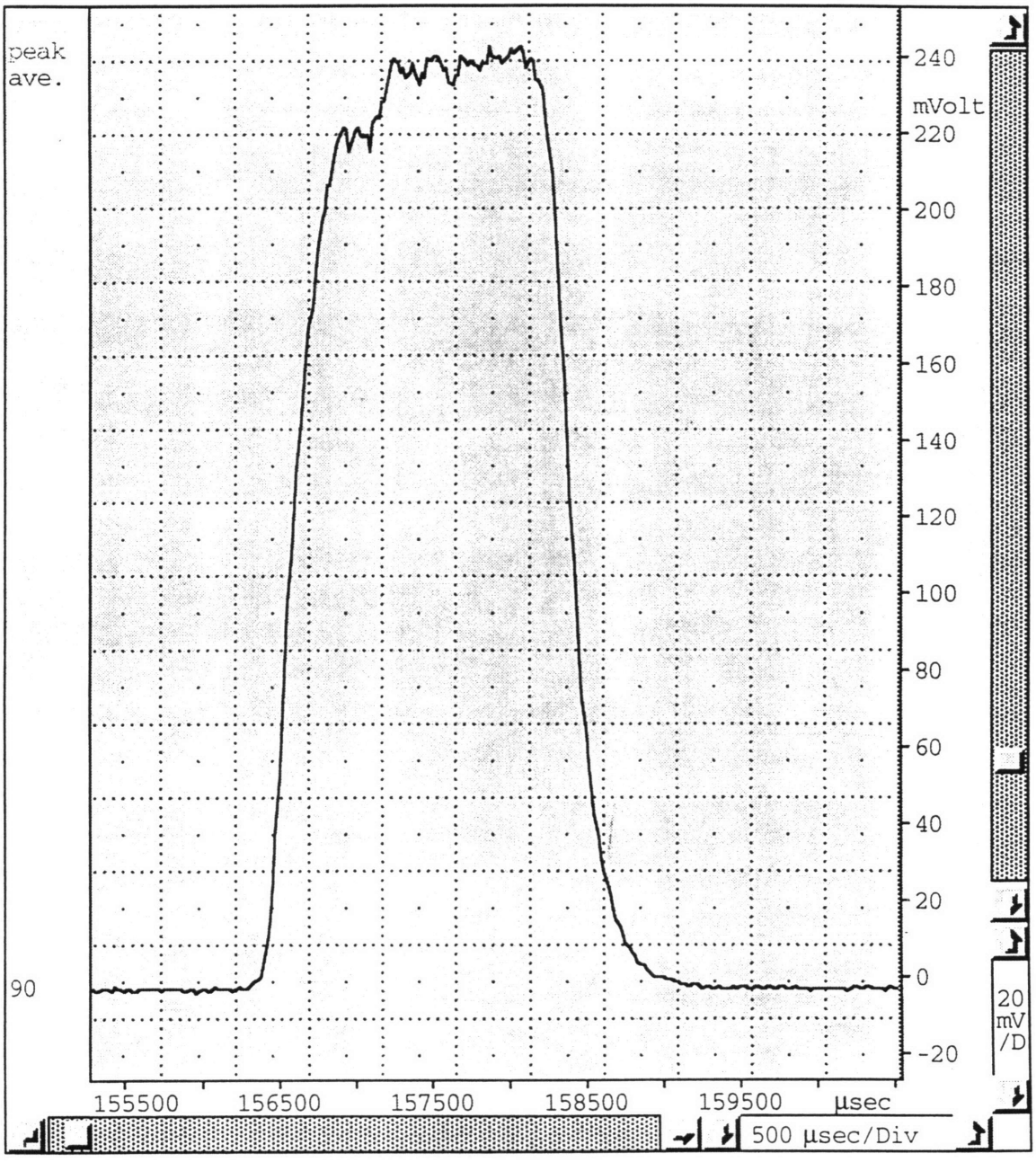

Figure D7. Enlarged view of a single peak.

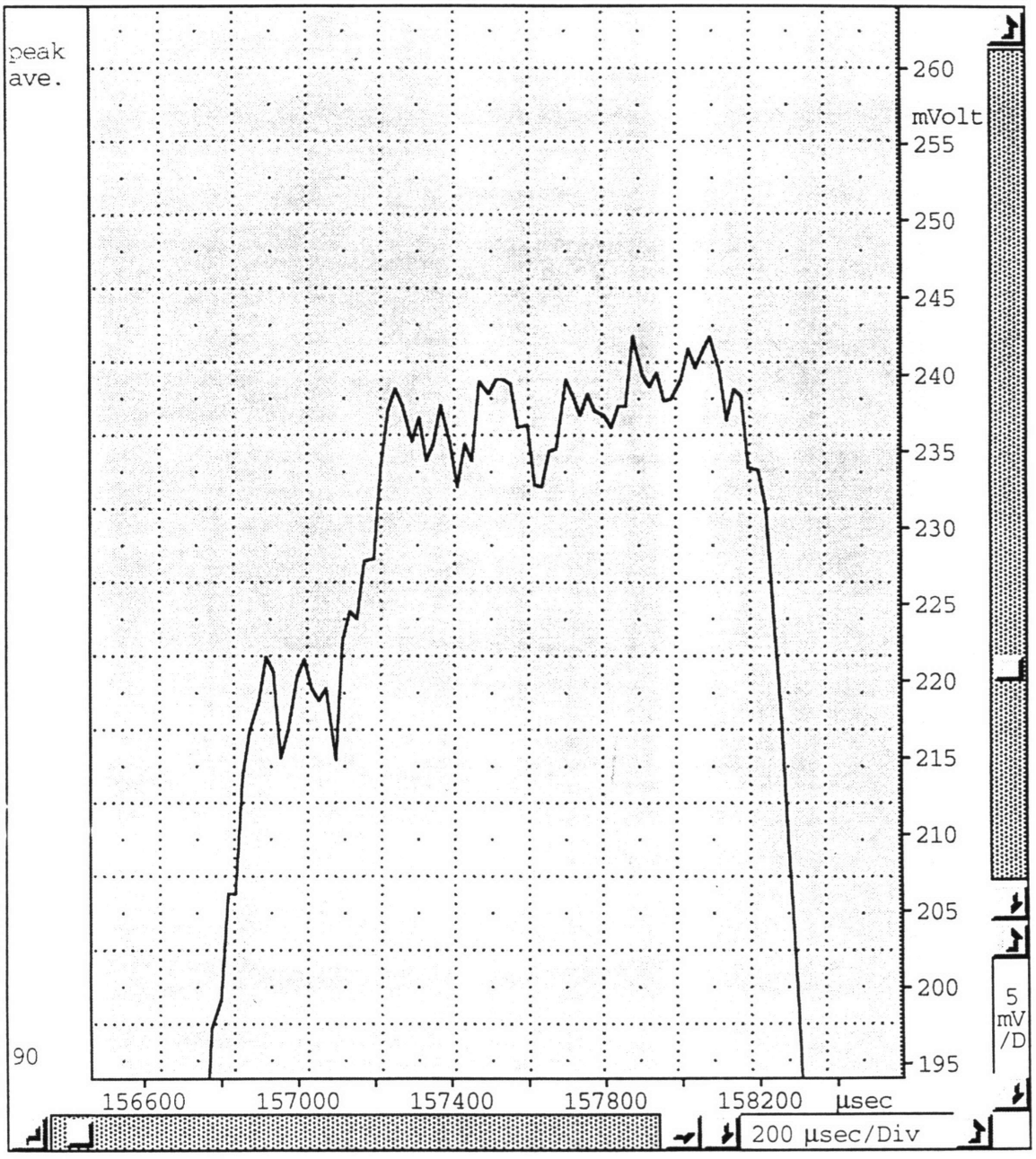

Figure D8. Closer look at the tip of the peak shown in D7.

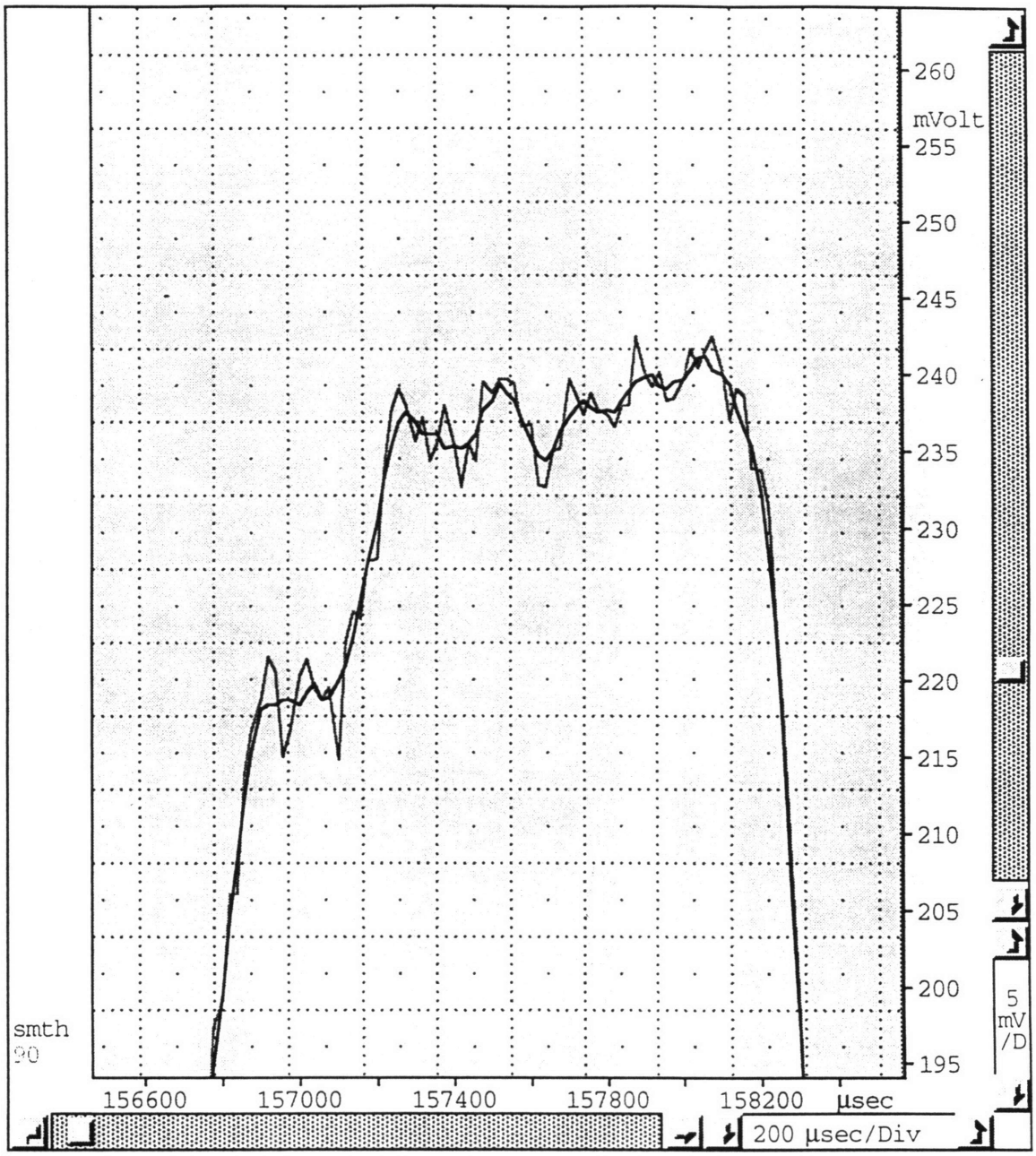

Figure D9. **Smoothed version of original peak.**
The darker line is the smoothed signal. The lighter line is the original signal.

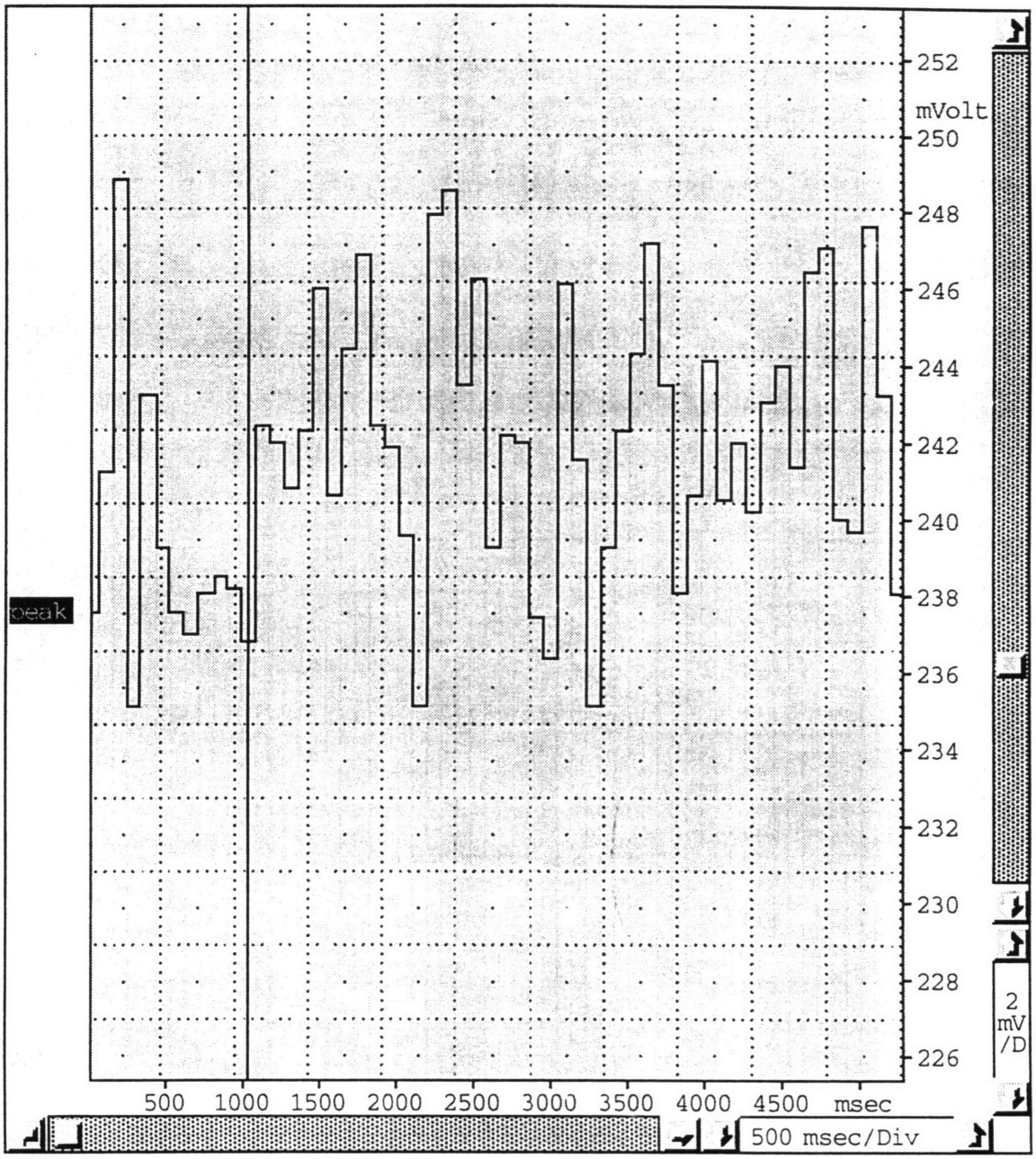

Figure D10. **"Peak" signal that occurs when the maximum values are taken from each peak.**

4. These peak values are then averaged over the course of the run. The final result of this averaging, shown in Figure D11, is transferred to an on-screen journal. Approximately 85 peaks appear in a 7 second sampling.

5. From this journal the information can be transferred to a spreadsheet for further analysis.

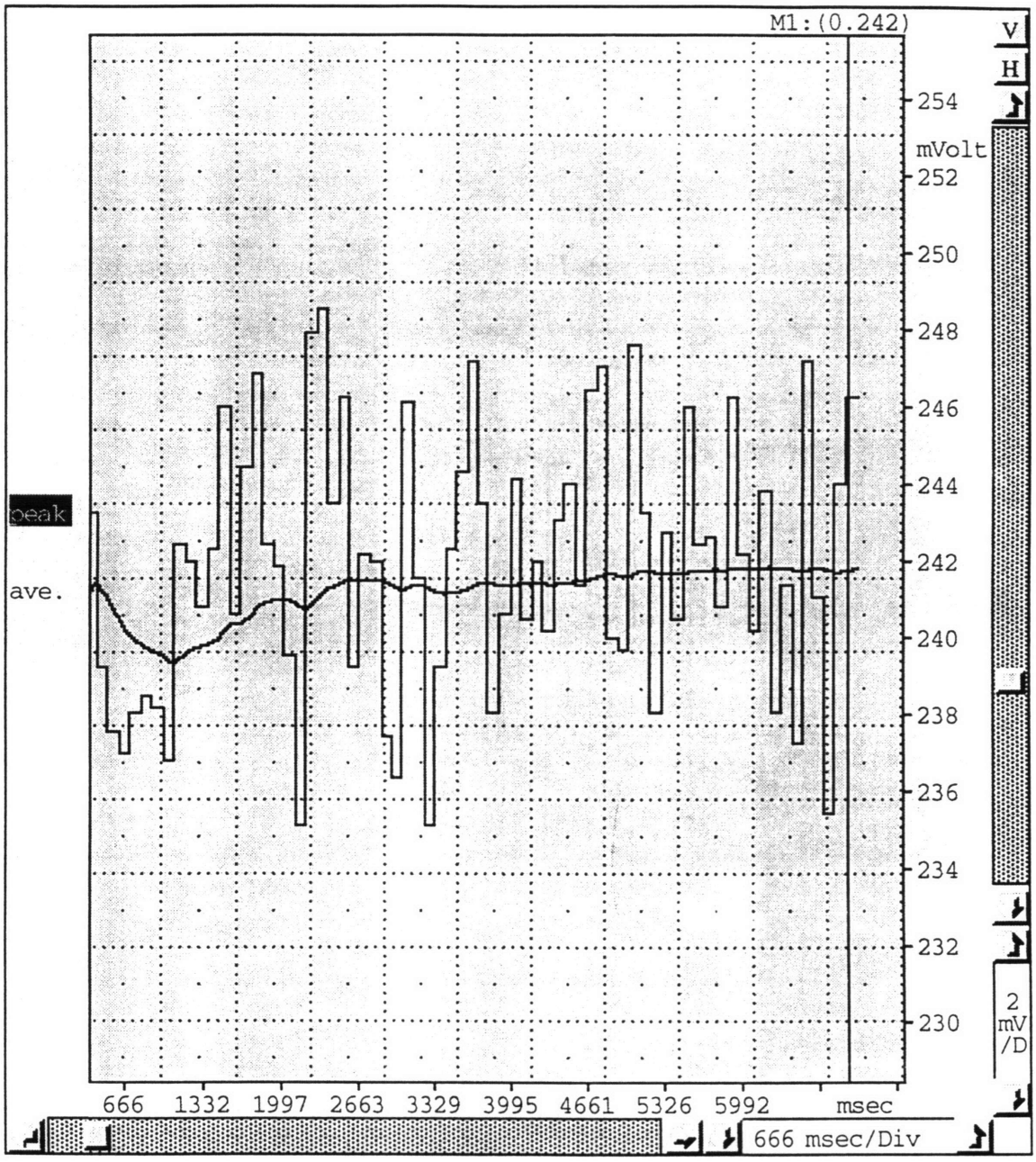

Figure D11. A running average of the peak values.
The final value of this average is transferred to the on-screen journal.

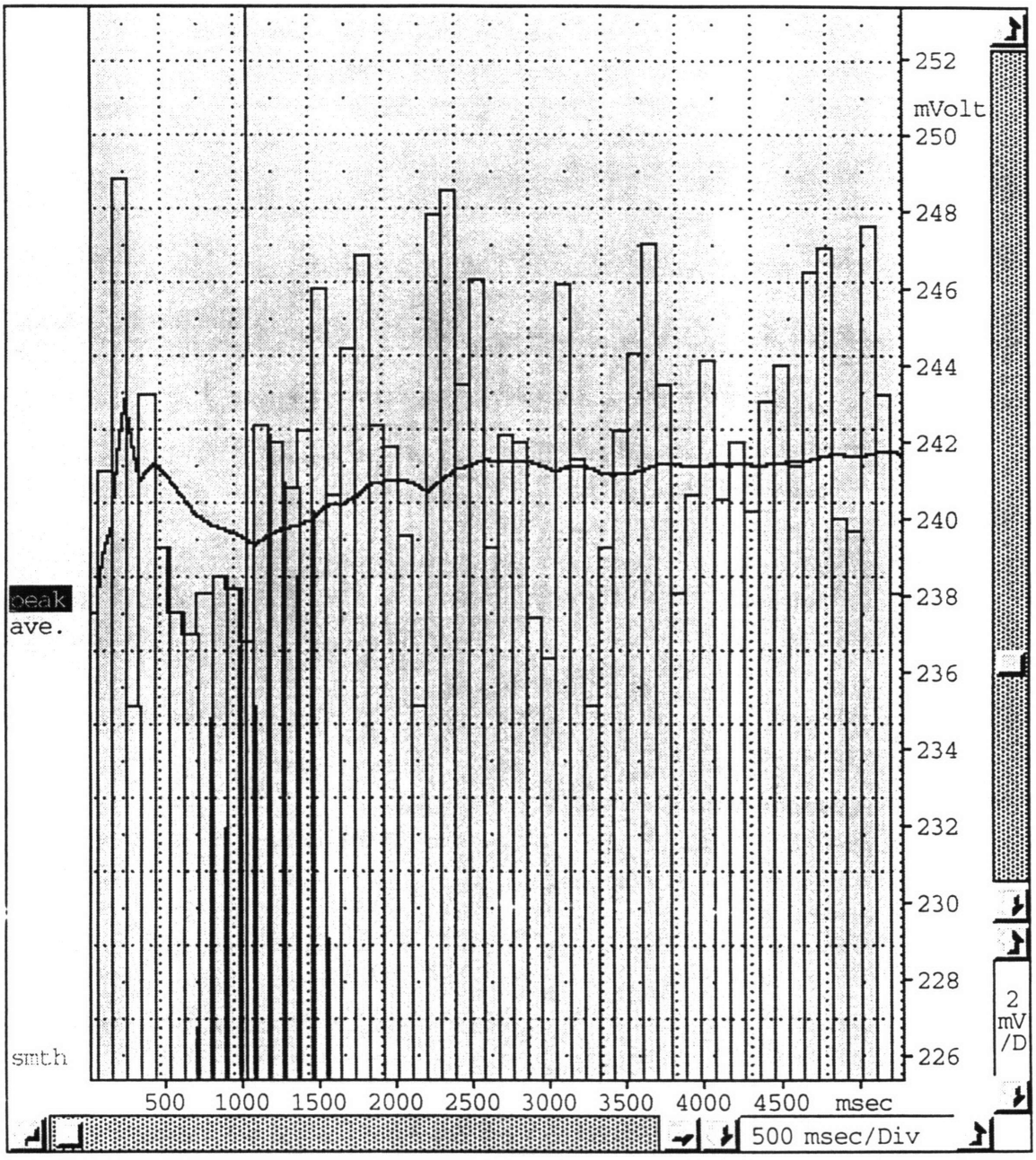

Figure D12. Typical display seen as a signal is acquired and the data is processed.

4958-10